8-4-2014

Characterization of Flavin-containing Monooxygenase-3 (FMO3) as a Novel Genetic Determinant of Acetaminophen (APAP) Induced Hepatotoxicity

Swetha Rudraiah
University of Connecticut - Storrs, swetha.rudraiah@uconn.edu

Characterization of Flavin-containing Monooxygenase-3 (FMO3) as a Novel Genetic Determinant of Acetaminophen (APAP) Induced Hepatotoxicity

Swetha Rudraiah, Ph.D.

University of Connecticut, 2014

Mice pretreated with a mild toxic dose of acetaminophen (APAP) acquire resistance to a second, higher APAP dose. This phenomenon is termed APAP autoprotection and the exact mechanism by which such resistance develops is not clearly known. Given the prevalence of APAP-hepatotoxicity and the human health impact of this potentially hepatotoxic agent, a further understanding of the mechanism(s) involved in such protection are of considerable significance and could lead to new modalities of treatment of acute drug-induced liver injury. The work presented in this thesis investigates *FMO3* gene expression during APAP-induced liver injury as well as the functional significance of *FMO3* over-expression during APAP-induced liver injury. Furthermore, *FMO3* gene regulation during oxidative stress conditions is also examined.

Acetaminophen treatment resulted in up-regulation of liver Fmo3 protein in male mice. Female mice express higher liver *Fmo3* than males and are highly resistant to APAP hepatotoxicity. Inhibition of Fmo3, by methimazole, renders female mice susceptible to APAP-induced liver injury. These findings are suggestive of a protective function for Fmo3. In addition to

APAP, ANIT and BDL also increase *Fmo3* gene expression in mice. Because these hepatotoxicants also induce oxidative stress, we also investigated the potential role of the oxidative stress sensor and transcription factor, NRF2, in *FMO3* gene regulation. Both *in vivo* and *in vitro* results show that transcriptional regulation of *FMO3* might not involve the NRF2-KEAP1 regulatory pathway.

Human liver can adapt to APAP-induced hepatotoxicity similar to our APAP autoprotection mouse model. The last part of this dissertation examined *FMO3* gene induction in a human hepatoma cell line, HepaRG. APAP induced *FMO3* gene expression in HepaRG cells, and over-expression of *FMO3* protects cells against APAP-induced cytotoxicity. The unexpected observation of a faster differentiation phenotype in HepaRG cells over-expressing *FMO3* suggests that *FMO3* may play an important role in cellular differentiation.

Collectively, data presented in this thesis provide evidence for *Fmo3* as a novel genetic determinant of APAP-induced liver injury. Furthermore, this thesis describes a novel protective function for *FMO3*. Findings from HepaRG cells suggest that *FMO3* over-expression in response to APAP may be a driving force for differentiation in regenerating hepatocytes.

Characterization of Flavin-containing Monooxygenase-3 (FMO3) as a Novel Genetic Determinant of Acetaminophen (APAP) Induced Hepatotoxicity

Swetha Rudraiah

B.V.Sc. & A.H., University of Agricultural Sciences, India, 2004

M.V.Sc., Karnataka Veterinary, Animal and Fisheries Sciences University, India, 2006

A Dissertation

Submitted in Partial Fulfillment of the

Requirements for the Degree of Doctor of Philosophy

at the

University of Connecticut

2014

APPROVAL PAGE

Doctor of Philosophy Dissertation

Characterization of Flavin-containing Monooxygenase-3 (FMO3) as a Novel Genetic Determinant of Acetaminophen (APAP) Induced Hepatotoxicity

Presented by

Swetha Rudraiah

Major Advisor: _____
José E. Manautou, Ph.D.

Associate Advisor: _____
Ronald N. Hines, Ph.D.

Associate Advisor: _____
Urs A. Boelsterli, Ph.D.

Associate Advisor: _____
Richard S. Bruno, Ph.D.

University of Connecticut

2014

DEDICATION

To everyone who taught me, guided me, and inspired me.

ACKNOWLEDGEMENTS

I would first and foremost like to thank my major advisor, Dr. José Manautou. Dr. Manautou has been an excellent mentor and has provided me invaluable guidance, continued advice and critical discussions that have allowed me to grow both professionally and personally. I would also like to thank my committee members Drs. Ronald Hines, Urs Boelsterli and Richard Bruno for their scientific inputs during the completion of my graduate degree. My special thanks to Dr. Hines for his willingness to help and answer my questions even before being a part of my thesis committee. Thank you for your guidance throughout.

Many thanks to other faculty at the University of Connecticut School of Pharmacy for their assistance and advise during this research. Thanks to our collaborators Drs. Angela Slitt, Lauren Aleksunes, and Sarah Campion for providing samples and for insightful scientific discussions. My special thanks to Dr. Carolina Ghanem for the inspiration and friendship. I am very grateful for the support and friendship of the other members of our lab, both past and present, Xinsheng Gu, Amy Bataille, Ron Scialis, Dan Ferreira, Phil Rohrer, and Meeghan O'Connor. Also, thanks to fellow graduate students and postdocs including Bindu, Igor, Supriya, Joe, Greg, Kyle, Vince, Janine, Ritvik, Chad, Stephanie, Lai and Erica for making my stay here at UCONN memorable. I am grateful for the assistance provided by staff at the Department of Pharmaceutical Sciences especially Mark Armati and Leslie

Lebel, Denise Long at the histology laboratory, and all the hardworking staff in the animal care facility.

I would also like to acknowledge the financial support of the National Institutes of Health Grant (DK069557) and the UCONN School of Pharmacy Department of Pharmaceutical Sciences without which none of this would have been possible. Thanks to the Society of Toxicology Mechanisms Specialty Section, for recognizing this work through Carl C. Smith Graduate Student Award.

Lastly, I would like to extend my sincere thanks to my parents for instilling in me the values of hard work, perseverance, and good education. Their unconditional love, sacrifices, continued support, encouragement and constant pride in my accomplishments have led me so far. Thanks to my sister Shylaja and brother Omprakash, for always being there for me and for believing in me. Thanks to my extended family for all the motivation. To my husband, Sangamesh, thanks for the daily support and love and for this I will always be grateful. Finally, to my daughter, Gauri, your smile and cuteness have immensely helped me cheer, especially on some of those gloomy days. I am very fortunate to have you all in my life.

TABLE OF CONTENTS

LIST OF FIGURES

LIST OF TABLES

LIST OF ABBREVIATIONS

AhR	Aryl hydrocarbon Receptor
ALF	Acute Liver Failure
AlOH	Allyl Alcohol
ALT	Alanine amino Transferase
ANIT	Alpha-Naphthylisothiocyanate
APAP	Acetyl-para-aminophenol, Acetaminophen
ARE	Antioxidant Response Element
BA	Bile Acids
BaP	Benzo(a)pyrene
BDL	Bile Duct Ligation
BSEP/Bsep	Bile salt export pump
CCl_4	Carbon tetrachloride
C/EBPβ	CCAAT enhancer-binding protein β
CRE	Causal Reasoning Engine
CYP	Cytochrome P450
DMEM	Dulbecco's Modified Eagle's Medium
DTNB	5,5'-dithiobis(2-nitrobenzoate)
DTT	dithiothreitol
FMO3/Fmo3	Flavin-containing MonoOxygenase-3
FXR	Farnesoid X Receptor
FXRE	Farnesoid X Receptor-response Element
GCLC/Gclc	Glutamate Cysteine Ligase Catalytic subunit
GSH	Glutathione
GST/Gst	Glutathione S-Transferase
HIF-1α	Hypoxia-Inducible Factor-1α
HMOX1/Hmox1	Heme oxygenase-1
HNF1α	Hepatocyte Nuclear Factor 1α
Hsp	Heat shock protein
I3C	Indole-3-Carbinol

JNK	c-Jun N-terminal Kinase
KEAP1/Keap1	Kelch-like ECH-Associated Protein 1
LDH	Lactate dehydrogenase
LUC	Luciferase
3MC	3-Methylcholanthrene
MDR/Mdr	Multidrug Resistance protein
MMI	Methimazole
MPT	Membrane Permeability Transition
MRP/Mrp	Multidrug Resistance-associated Protein
NAPQI	N-Acetyl-*p*-benzoquinone Imine
NFE2L2/NRF2	Nuclear Factor (Erythroid-derived 2)-Like 2
NF-κB	Nuclear Factor kappa-light-chain-enhancer of activated B cells
NF-Y	Nuclear Factor-Y
NQO1/Nqo1	NAD(P)H:Quinone Oxidoreductase-1
Nrf2KO	Nrf2 Knockout
NTCP	Sodium Taurocholate-Cotransporting Polypeptide
OATP	Organic Anion Transporter Polypeptide
OxyR	Oxygen Response
Pbx_2	Pre-B-cell leukemia factor 2
PG	Propylene Glycol
Pgp	P-glycoprotein
PMSF	Phenylmethylsulfonylfluoride
PXR	Pregnane X Receptor
ROS	Reactive Oxygen Species
SoxRS	Superoxide Response
tBHP	tert-Butyl Hydroperoxide
tBHQ	tert-Butyl Hydroquinone
TCDD	2,3,7,8-Tetrachlorodibenzo-p-dioxin
TMA	Trimethylamine
TNB	Nitro-5-thiobenzoate

TNFα	Tissue Necrosis Factor α
TP53	Tumor Protein-53
UGT1A1	UDP glucuronosyltransferase 1 family, polypeptide A1
USF1	Upstream Stimulatory Factor 1
YY1	Yin yang 1

CHAPTER 1

Review of Literature

1.1 Liver Function and Structure

The structure and function of the liver is well understood. The description that follows is adapted from Casarett and Doull's Toxicology: The Basic Science of Poison (Klaassen, 2008), Guyton and Hall: Textbook of Medical Physiology (Hall, 2011), and Wheater's Functional Histology (Young, Lowe, Stevens and Heath, 2006).

***Liver Function*.** The liver's strategic location between the gastrointestinal tract and the rest of the body helps to serve as a checkpoint for substances arriving in portal veins. The liver has multiple functions involving nutrient homeostasis (processing of carbohydrates, amino acids and lipids); storage of glycogen, vitamins and iron; filtration of particulates like bacterial endotoxins; protein synthesis including albumin, clotting factors and transport proteins; bioactivation and detoxification of xenobiotics; and synthesis and secretion of bile and cholesterol. Importantly, the liver is the main organ where xenobiotics and endogenous compounds are metabolized into more polar, water-soluble derivatives that can be easily excreted into urine and/or bile.

Structural Organization of the Liver. The liver is the largest visceral organ, as well as the largest gland in the body, representing 2.5 % of total body weight. Blood flow into the liver sinusoids comes from the hepatic portal vein

(60-70 %) and hepatic artery (30-40 %). The liver is therefore unusual in having both arterial and venous blood supplies as well as a separate venous drainage. The liver consists of various cell types: hepatocytes (parenchymal cells), sinusoidal lining cells (endothelial cells, Kupffer cells, Ito cells and pit cells), hematopoietic cells, nerve cells, and blood and lymphatic vessel cells. Hepatocytes are the main functional cells in the liver. The majority of cells lining the hepatic sinusoids are endothelial cells that are fenestrated and have contractile and metabolic functions. Kupffer cells, which are resident macrophages that form part of the monocyte-macrophage defense system, phagocytize particles, detoxify endotoxin, secrete mediators of inflammation, process antigens, and catabolize lipids and glycoproteins. Ito cells have dual functions of vitamin A storage and production of extracellular matrix and collagen. Lastly, pit cells are liver-specific natural killer (NK) cells that reside mostly near portal veins.

The liver is structurally organized into polygon-shaped lobules surrounded by connective tissue (Figure 1.1). Each lobule consists of a central vein. Cords of hepatocytes and the intervening sinusoids extend radially between the central vein and the periphery of the lobule. At the corners of the lobule are the portal triads that are made up of a hepatic arteriole, portal vein and bile duct. This lobular organization is most easily appreciated in sections of pig liver. In human liver, lobules are not as well defined by connective tissue although they still contain a central vein and are surrounded by portal triads. Blood entering the portal tract via the portal vein

and hepatic artery mixes as it enters the sinusoids, percolates along the cords of hepatocytes and eventually flows into central veins, and exits the liver via the hepatic vein. The lobule is thus divided into three regions known as centrilobular, midzonal, and periportal. Even though the structural unit of the liver can be considered as a conceptually simple hepatic lobule, the physiology of the liver is more precisely represented by a unit structure known as the hepatic acinus. The acinus is a roughly berry-shaped liver parenchymal unit centered on the portal tract (comprising the terminal branches of the portal vein and hepatic artery). The acinus is divided into zone 1, 2, and 3. Zone 1 is closest to the portal tract (similar to the periportal area) and receives blood rich in oxygen (9-13 %) and nutrients, while Zone 3 abuts the central vein (coincides with the centrilobular region) and receives the least oxygen (4-5 %). Zone 2 is intermediate between Zone 1 and Zone 3 and coincides with the midzonal region.

In addition to the gradient in oxygen concentrations along the hepatic sinus, there are gradients in blood bile acid concentrations and heterogeneities in protein levels within hepatocytes that generate gradients of metabolic functions. For example, mitochondria-rich Zone 1 has high levels of oxidative enzymes (fatty acid oxidation), gluconeogenesis and ammonia detoxification to urea. Hepatocytes in Zone 3 contain high levels of esterases and low levels of oxidative enzymes. Gradients of enzymes involved in the bioactivation and detoxification of xenobiotics is seen along the acinus. For example, greater amounts of cytochrome P450 proteins (CYP), particularly

CYP2E1, are higher in Zone 3, and glutathione (GSH) levels are higher in Zone 1. Hepatocytes in different zones exhibit differences in sensitivity to chemical toxicity, which are dictated by zonal gradients in GSH, nutrients, oxygen, and bioactivation enzymes.

Cords of hepatocytes are arranged radially around the central vein with bile canaliculi between adjacent hepatocytes. The canaliculi are separated from the intercellular space between hepatocytes by tight junctions that are permeable to water, electrolytes, and some small organic cations. These tight junctions are impermeable to anions such as bile acids (BA), glutathione, and bilirubin-diglucuronide resulting in their high concentrations in bile. Canaliculi form channels between hepatocytes that connect to a series of ducts in the liver. The large extrahepatic bile ducts merge into the common bile duct. Bile is modified and stored in the gall bladder before it is released into the duodenum. It is important to note that several species including rats do not have gall bladders.

1.2 Hepatic Metabolizing Systems. The liver is the main organ where a majority of the xenobiotics are metabolized and eventually excreted. Blood from the stomach and the intestine carrying ingested nutrients along with drugs and environmental toxicants flow into the portal vein and then through the liver before entering the systemic circulation. Hence, the liver is exposed to high concentrations of these absorbed compounds. The goal of hepatic metabolism is to eliminate endogenous intermediates and exogenous chemicals by making it more polar and readily excreted through urine. The

mammalian liver is equipped with enzyme systems that perform this function. During the past six decades, a large body of knowledge has accumulated documenting the role of xenobiotic-metabolizing enzyme systems in the mediation of the toxic effects of drugs, environmental pollutants, and some endogenous compounds. Here, some of these enzyme systems are briefly discussed.

Conceptually, the drug metabolizing enzymes involved in xenobiotic-metabolism or -biotransformation fall into three groups: Phase I, Phase II, and Phase III reactions. Phase I metabolism involves enzymes that catalyze hydrolysis, reduction, or oxidation reactions by introducing functional groups such as -OH, $-NH_2$, -SH, or -COOH. Phase I metabolism usually results in a small increase in water solubility. One of the most important enzyme systems involved in Phase I metabolism is the microsomal CYP superfamily, which to date includes fifty-seven identified enzymes in humans. Other Phase I enzymes include flavin-containing monooxygenases (microsomal), carboxylesterases, epoxide hydrolases, etc.

Phase II conjugation reactions require cofactors (except acetylation and methylation reactions) that react with functional groups that are either already present on the molecule or are introduced/exposed during Phase I metabolism. The Phase II drug metabolizing enzymes catalyze the coupling of endogenous small molecules to xenobiotics that usually result in large increases in water solubility so that they are more readily excreted. Phase two enzymes include members of the UDP-glucuronysltransferase (microsomal),

sulfotransferase (cytosolic), and GSH transferase (cytosolic, microsomal and mitochondrial).

Phase III reactions result in the cellular efflux of polar xenobiotics by membrane-bound transporters to either blood or bile. For the purposes of this thesis, only three members of the ABCC transport family will be discussed: multidrug resistance-associated proteins (Mrp) 2, 3, and 4. Mrp2 is predominantly expressed at the hepatocyte canalicular membrane and is responsible for the efflux of chemicals and metabolites into bile. Substrates for Mrp2 include glucuronide and GSH conjugates. Mrp 3 and 4, on the other hand, are basolateral efflux transporters that transport metabolites into the blood. Transporters commonly exhibit broad and overlapping substrate specificities.

The result of xenobiotic biotransformation is typically a reduction in lipophilicity and toxicity. However, in some cases, metabolism can produce reactive intermediates that can result in an enhancement of toxicity. Some of these intermediate metabolites covalently bind to cellular macromolecules (proteins and lipids) resulting in oxidative stress and eventually cellular death. Examples of xenobiotic activation by CYP enzymes include acetaminophen (APAP), carbon tetrachloride, benzene, and benzo[a]pyrene.

1.3 APAP Hepatotoxicity

Incidence. Acetaminophen, currently one of the most commonly used analgesic and antipyretic agents in the U.S. and Great Britain, was first

described more than a century ago. However, APAP-poisoning and APAP-hepatotoxicity was first recognized in Great Britain (Davidson & Eastham, 1966) and later in the U.S. (McJunkin et al., 1976). APAP usage increased after aspirin was implicated in over 80 % of Reye's syndrome cases in children. As APAP usage increased, the incidence of APAP-induced hepatotoxicity also increased. In a retrospective study from 1994 to 1996, APAP-induced hepatotoxicity comprised 20 % of acute liver failure (ALF) cases in the U.S. (Schiodt et al., 1999). These numbers increased over time and by the early 2000s nearly 50 % of ALF cases were due to APAP. Even though this fraction has remained fairly constant over the past decade, it is still a very prominent leading cause of acute liver failure accounting for more that 50 % of all acute liver failure cases from all etiologies (Larson et al., 2005; W. M. Lee, 2010). The potential for drug-related morbidity and mortality, and the popularity of this drug, make it a significant human health problem.

***Metabolism*.** Upon administration of a therapeutic dose of APAP, a majority of the parent compound (~90 %) undergoes Phase II metabolism in the liver by glucuronidation and sulfation, and the metabolites (APAP-GLUC and APAP-SUL) are safely excreted in urine or bile (Nelson, 1990). A small portion of APAP (5-15 %) undergoes Phase I metabolism by several members of the CYP superfamily including CYP2E1, 1A2, and 3A4. This reaction results in the formation of a reactive metabolite, N-acetyl-p-benzoquinone imine (NAPQI), which by GSH conjugation is effluxed out into

the bile (Mitchell et al., 1973; Mitchell et al., 1973; Zaher et al., 1998). The GSH conjugate can further undergo cleavage to form a cysteine conjugate (APAP-CYS) and subsequent acetylation to the mercapturic acid conjugate (APAP-NAC). However, during APAP overdose, the Phase II pathways are saturated and a large fraction of the drug undergoes metabolism by CYP enzymes, generating more NAPQI. Once GSH stores are depleted, unconjugated NAPQI can then exert it's cytotoxic effect by causing oxidative stress, covalent binding to thiol groups on macromolecules and/or lipid peroxidation and mitochondrial dysfunction. (Cohen et al., 1997; Jaeschke & Bajt, 2006; Patten et al., 1993).

Phase III metabolism of APAP includes transport of APAP-metabolites into bile or urine for excretion and there is an overlap in metabolite transport between transporters. While Mrp2 is responsible for the excretion of APAP-GLUC conjugate into bile (Chen et al., 2003), Mrp3 is involved in the efflux of APAP-GLUC into plasma. Mrp3 has a higher affinity for APAP-GLUC compared to Mrp2 (Manautou et al., 2005). Mrp4 and the Breast cancer resistance protein (Bcrp) are responsible for the transport of APAP-SUL conjugate into plasma and bile, respectively (Zamek-Gliszczynski et al., 2005; Zamek-Gliszczynski et al., 2006).

***Protein Covalent Binding in APAP-Induced Cell Injury*.** As previously mentioned, the CYP oxidative metabolite of APAP, NAPQI, is responsible for cytotoxic effects of APAP. The earliest effect of NAPQI generation is profound depletion of hepatocellular GSH (Mitchell et al., 1973). Once hepatocellular

GSH levels are depleted, NAPQI reacts with thiol groups of protein leading to protein adducts (Jollow et al., 1973; Potter et al., 1973). Using radioactively labeled APAP, studies demonstrated that APAP binds irreversibly to hepatic proteins in multiple subcellular compartments, including nucleus, mitochondria, endoplasmic reticulum, and cytosol (Jollow et al., 1973; Potter et al., 1973). Immunohistochemical studies further identified some of these covalently modified proteins that are implicated in APAP-induced liver injury (Cohen et al., 1997). Studies also demonstrated that APAP could inhibit mitochondrial respiration and increase mitochondrial oxidative stress by modifying mitochondrial proteins (Jaeschke, 1990; Meyers et al., 1988). Although the covalent binding of proteins and APAP hepatotoxicity occur concurrently, APAP-bound proteins are detectable in mice given non-toxic doses of APAP. Conversely, antioxidant treatment that prevents APAP hepatotoxicity does not alter covalent protein binding. These data suggest that covalent binding is required but not sufficient for APAP-induced hepatotoxicity.

Mechanism of Oxidative Stress Mediated Liver Pathophysiology. Reactive Oxygen Species (ROS) are produced during metabolism. Under normal physiological conditions, these pro-oxidants are detoxified by cellular antioxidant systems. When the balance between pro-oxidants and antioxidants is disturbed, in favor of ROS generation to the cell's capacity to detoxify them, a state of oxidative stress ensues. During APAP overdose, there is a significant elevation of GSH disulphide (GSSG) in cellular as well as

mitochondrial compartments of hepatocytes (Jaeschke, 1990; Jaeschke et al., 2012). Studies show that oxidative stress is an initiating event in APAP hepatotoxicity (Bajt et al., 2004; Jaeschke, 2003). Mitochondrial dysfunction generates superoxide that reacts with nitric oxide to form a potent oxidant and nitrating species, peroxynitrite. Immunohistochemical analysis shows formation of lipid peroxide and nitrotyrosine adducts in liver during APAP overdose. The oxidative stress caused by ROS and nitrogen species increases intracellular calcium levels resulting in the opening of mitochondrial membrane permeability transition (MPT) pores (Jaeschke & Bajt, 2006). ROS also activates JNK MAPKinase pathway. Activated c-Jun N-terminal Kinase (JNK) inactivates anti-apoptotic proteins Bcl-2 and Bcl-xL by phosphorylation. The resulting increase in pro-apoptotic proteins results in an increase in permeability of the mitochondrial membrane and triggers the release of cytochrome C from mitrochondria to cytosol (El-Hassan et al., 2003; Ghosh et al., 2010). This combination ultimately results in reduction of cellular adenosine-tri-phosphate (ATP) and necrosis of the liver.

Transporter Expression During APAP-induced Liver Injury. Rodent models are extensively used to investigate the mechanisms of APAP-induced hepatotoxicity and the effect of APAP on hepatic transport protein expression. Mrp2 and P-glycoprotein (Pgp) protein expression increases during APAP-induced liver injury in rat livers. This increased expression resulted in increased biliary elimination of substrates such as dinitrophenyl- S-glutathione, oxidized glutathione, and digoxin. While the first two are

substrates for Mrp2, the latter is a substrate for Pgp (Ghanem et al., 2004). A comprehensive analysis of transporter expression performed previously in our lab shows that APAP at toxic doses in mice increased expression of basolateral (*Mrp3*, *Mrp4*) and canalicular (*Mrp2*) efflux transporters. Simultaneously, APAP also decreased expression of basolateral uptake transporters such as organic anion transporter polypeptide *(Oatp)1a1* and *1b2* and sodium taurocholate-cotransporting polypeptide (*Ntcp*) (Aleksunes et al., 2006; Campion et al., 2008). Additionally, it was also shown that the increased *Mrp3* and *Mrp4* expression was localized to hepatocytes surrounding the central vein, the region where APAP-induced damage is localized (Aleksunes et al., 2006). Increases in hepatic efflux transporter expression (MRP2, BCRP, MRP4 and MRP5) are also evidenced in human liver samples obtained during liver transplantation after APAP overdose (Barnes et al., 2007). APAP-GLUC is a substrate for Mrp3 (Manautou et al., 2005; Slitt et al., 2003) and its altered expression due to toxic APAP pre-treatment in rats alters the elimination of APAP-GLUC from bile to urine (Ghanem et al., 2005). Although the impact of hepatic transport protein induction during APAP hepatotoxicity is not clearly known, Aleksunes et al. have demonstrated that in a mouse model of resistance to APAP-induced hepatotoxicity termed “APAP autoprotection”, there is a significant induction of the Mrp4 protein (Aleksunes et al., 2008). *Mrp4* induction is localized to the hepatocytes surrounding the central vein where proliferation following a mildly toxic dose of APAP is confined. Further, colchicine (antimitotic agent)

treatment blocked the hepatocelluar proliferation around the central vein as well as induction of the Mrp4 protein, thus supporting the role of *Mrp4* in protection from APAP hepatotoxicity (Aleksunes et al., 2008).

1.4 Liver Injury Models and Mechanisms of Hepatotoxicity

Allyl Alcohol Hepatotoxicity

Mechanism of Allyl Alcohol-induced Liver Injury. Allyl alcohol (AlOH) is an unsaturated alcohol used in the production of food flavoring agents, fire retardants, organic chemicals, drugs, plastics, pesticides, and herbicides. Exposure to AlOH occurs primarily in industries where AlOH is produced or used. Since exposure to AlOH is limited, it does not pose a significant health problem in humans. Today, AlOH serves as a useful experimental tool for studying chemical-induced periportal hepatic necrosis (Reid, 1972). AlOH is metabolized in the liver by alcohol dehydrogenase to its reactive metabolite, acrolein (Badr, 1991). Humans are exposed to acrolein through cigarette smoke, automobile exhaust, and oil burning. Acrolein is detoxified by aldehyde dehydrogenase to acrylic acid or conjugated to glutathione. The glutathione adducts can potentially be converted by CYP enzymes to glycidaldehyde, a mutagen & carcinogen that produces oxidative stress and lipid peroxidation in periportal hepatocytes. Glycidaldehyde also binds covalently to cellular macromolecules leading to hepatocellular injury and death (Burcham & Fontaine, 2001; Ohno et al., 1985). While some studies suggest that alkylation of cellular proteins by acrolein is the initiating event in

hepatotoxicity, some studies also suggest that AlOH-induced hepatotoxicity is mediated by lipid peroxidation. The exact mechanisms of AlOH-induced hepatotoxicity are not clearly known. However, it is believed that the periportal necrosis induced by AlOH targets is due to high oxygen tension in these regions, which allows for increased superoxide anion formation and lipid peroxidation (Badr, 1991).

Transporter Expression During AlOH-induced Liver Injury. Our laboratory has demonstrated that AlOH treatment decreases expression of uptake transporters *Oatp1a1* and *1b2* and *Ntcp* in mice. The reduction is accompanied by increases in efflux transporters *Mrp1, 2, 4* and *5* (Campion et al., 2009). In this study, kupffer cell depletion enhanced AlOH-induced hepatotoxicity, while there were no changes in hepatic transporter expression (Campion et al., 2009).

Alpha-naphthylisothiocyanate Hepatotoxicity

Mechanism of Alpha-Naphthylisothiocyanate-induced Liver Injury. Alpha-naphthylisothiocyanate (ANIT) is a hepatotoxicant used to model intrahepatic cholestasis in rodents. It produces intrahepatic cholestasis dose dependently (Capizzo & Roberts, 1971). Following oral administration, ANIT reaches the liver through the portal vein. In the hepatocytes, ANIT is conjugated with glutathione and transported into bile by the canalicular efflux transporter, Mrp2. Upon crossing the canalicular membrane, the ANIT-GSH conjugate dissociates, yielding free GSH and ANIT in the bile. ANIT

selectively causes damage to the bile duct epithelial cells leading to cholestasis (Dietrich et al., 2001).

Transporter Expression During ANIT-induced Liver Injury. In mice, ANIT decreases the expression of uptake transporters *Ntcp, Oatp1a1*, and *Oatp1b2,* and increases expression of efflux transporter *Mrp3*, Organic solute transporter β (*Ostβ*), Multidrug resistance protein 2 (*Mdr2*), *Mrp2* and ATPase, aminophospholipid transporter, class I, type 8B, member 1 (*Atp8b1*) (Cui et al., 2009). Nuclear receptors, farnesoid X receptor (FXR) and pregnane X receptor (PXR) regulate expression of hepatic uptake transporters, basolateral, as well as canalicular transporters during ANIT treatment. Nuclear receptor FXR regulates the canalicular and basolateral transporters bile salt export pump (*Bsep*), *Mdr2, Mrp2, Atp8b1,* and *Ostβ,* while PXR regulates *Mrp2* (Cui et al., 2009). While *Mrp3* expression in response to ANIT treatment is regulated by oxidative stress responsive transcription factor Nrf2 alone, Bsep mRNA expression is regulated by both Nrf2 and FXR (Cui et al., 2009; Tanaka et al., 2009).

Biliary Obstruction Cholestasis

Mechanism of Bile Duct Ligation-induced Liver Injury. Obstructive cholestasis is a complex disease characterized by decreased or impaired bile flow resulting in increased biliary pressure, impaired excretion or accumulation of bile salts and various other organic anions within hepatocytes, oxidative stress and subsequent activation of proinflammatory

cytokines. Common bile-duct ligation (BDL) is used to model extrahepatic obstructive cholestasis in rodents. After BDL, the liver accumulates BAs and other compounds such as bilirubin and bilirubin-glucuronide leading to liver injury. Eventually, bile acid levels increase in liver, plasma, and urine.

Transporter Expression During BDL-induced Liver Injury. Transporters transport BAs both from blood into liver and from liver into bile. Ntcp and Oatps (Oatp1a1, 1a4 and 1b2) transport BAs into the liver, while transporters such as Mrp2 and Bsep transport BAs out of the liver into bile, and Mrp3, Mrp4 and Ostα/β transport BAs from liver into blood. BDL decreases expression of hepatic uptake transporters such as Ntcp and Oatp1a1 and the reduction corresponds to lower uptake of taurocholate in rat hepatocytes (Gartung et al., 1996; Geier et al., 2005). In mice similar to rats, BDL decreases expression of uptake transporters *Ntcp, Oatp1a1,* and *1b2* as well as increases expression of efflux transporters *Mrp1, 3, 4,* and *5* (Slitt et al., 2007). It is suggested that a decrease in uptake transporters is an adaptive mechanism that will extract less BA from blood into liver thus reducing BA levels in the hepatocytes. Similarly, up-regulation of efflux transporters during BDL decrease BA levels in hepatocytes by enhancing clearance of bile acids into the blood and urine.

Carbon Tetrachloride Hepatotoxicity

Mechanism of Carbon Tetrachloride-induced Liver Injury. Carbon tetrachloride (CCl_4), a non-polar solvent, was used for industrial and home

use as a cleaning agent, degreasing agent, fire extinguisher, etc. Exposure to CCl_4 results in severe hepatotoxicity or nephrotoxicity, hence it is banned or severely restricted from usage. Currently, CCl_4 is used as a model hepatotoxicant to study the mechanisms of liver injury such as fatty degeneration, fibrosis, hepatocellular death, and carcinogenicity (Weber et al., 2003). In the liver, CCl_4 is bioactivated into tricholoromethyl radical ($^{\cdot}CCl_3$) by Cyp (Cyp2e1, Cyp2b1 and Cyp2b2) dependent systems (Gruebele et al., 1996). This $^{\cdot}CCl_3$ radical readily reacts with oxygen to form a more reactive free radical, trichloromethylperoxyl radical ($CCl_3OO^{\cdot}$). Free radicals generated can also bind covalently to Cyp2e1 resulting in suicide inhibition. The toxic effect mediated by $CCl3OO^{\cdot}$ includes oxidation of membrane polyunsaturated fatty acids resulting in lipid peroxidation. $CCl3OO^{\cdot}$ can also covalently bind to microsomal proteins, nucleic acids, and lipids resulting in generation of superoxide and hydroxyl radicals (Tom et al., 1984). Lipid peroxidation alters membrane permeability of cellular and subcellular structures resulting in loss of cellular calcium and uncoupling of oxidative phosphorylation leading to cellular degeneration and necrosis. The antioxidant defense machinery is also affected following exposure to this toxin.

Transporter Expression During CCl_4-induced Liver Injury. Similar to drug metabolizing enzymes, transporters exhibit zonal distribution patterns. In rats, basal expressions of Mdr mRNA and protein levels are higher in zone 1 and lowest in zone 3. Following exposure to CCl_4, *Mdr1b* and *Mdr2* expression increases in zone 1 and gradually extends to zone 3 (Nakatsukasa et al.,

1993). Expression of some basolateral transporters such as Oatp1, 4, and Ntcp decreases in rats exposed to CCl_4 (Geier et al., 2002). Blockage of TNFα signaling using the inhibitor etanercept inhibits CCl_4-induced downregulation of Oatp1a1, Oatp1a4, and Ntcp mRNA supporting the concept that proinflammatory cytokines are one of the key regulators of organic anion transporters (Geier et al., 2003). Previous work in our laboratory reported a simultaneous increase in expression of sinusoidal efflux (Mrp1 and Mrp4) and canalicular transport proteins (Mrp2) as well as a decrease in expression of Ntcp and Mrp3 proteins in mice in response to CCl_4 treatment (Aleksunes et al., 2006). This coordinated induction of efflux transport proteins and reduction of uptake carriers suggests an adaptive response by the liver for elimination of xenobiotics and oxidative stress products that are generated during CCl_4-induced liver injury.

1.5 Nrf2 Signaling Pathway

Oxidative stress is a steady-state level of oxidative damage in a cell, tissue, or organ caused by reactive oxygen species (ROS). ROS are transiently formed during the normal course of cellular metabolism, and elevated levels damage cellular macromolecules including proteins, lipids, mitochondrial, and nuclear DNA. Cells possess defense systems that protect against oxidative stress. In prokaryotes, the transcription factors oxygen response (OxyR) and superoxide response (SoxRS) sense the redox status of the cell and during oxidative stress induce expression of defensive genes (Zheng & Storz, 2000). Eukaryotic cells have similar mechanisms to protect

against oxidative stress. Nuclear factor (erythroid-derived 2)-like 2 (Nrf2 or NFE2L2), heat shock protein (Hsp) activator protein 1 and nuclear factor kappa-light-chain-enhancer of activated B cells (NF-κB) promote cell survival, whereas activation of JNK, p38 kinase, and tumor protein-53 (TP53) lead to cell cycle arrest and apoptosis.

Nrf2 belongs to the cap 'n' collar family of transcription factors that share a conserved basic region-leucine zipper (bZIP) structure. Nrf2 was identified during a screen for proteins that bind to the control region of the β-globin gene (Moi et al., 1994). Unlike p45-NF-E2 that is expressed only in blood cells such as megakaryocyte, erythroid, and mast cells, Nrf2 is present in a wide variety of tissues including liver, lung, intestine, and kidney.

Negative Regulation of Nrf2 Mediated by Keap1. Under basal conditions, Nrf2 is largely bound to the cytoskeletal anchoring protein Kelch-like ECH-associated protein 1 (Keap1), also known as cytosolic Nrf2 inhibitor (INrf2) in the cytoplasm. Keap1 exists as a dimer and retains Nrf2 in the cytoplasm. Serine 104 of Keap1 is required for dimerization of Keap1, and mutations in serine 104 leads to disruption of the Keap1 dimer and release of Nrf2 (Zipper & Mulcahy, 2002). Amino acid sequence and domain structure-function analyses show that Keap1 has broad-complex, tramtrack, bric-a-brac (BTB) / poxvirus, zinc finger (POZ) domain, Kelch domain also known as the double glycine repeat (DGR) domain, N-terminal region (NTR), Intervening region, and C-terminal region (CTR) (Figure 1.2). The BTB/POZ domain serves as an adapter for the cullin 3/ring box 1(cul3/Rbx1) E3 ubiquitin ligase complex and

promotes ubiquitination of Nrf2 (Kaspar et al., 2009). On the other hand, the DGR/Kelch domain binds to actin, allowing the scaffolding of Keap1 to the actin cytoskeleton, which plays an important role in Nrf2 retention in the cytosol. Thus, Keap1 is responsible not only for sequestering Nrf2, but also for its normal proteosomal targeting and degradation.

Cytoplasmic Retention of Nrf2. Two nuclear export signals in the leucine zipper and transactivation domains of Nrf2 are responsible for cytoplasmic localization of Nrf2. One of these nuclear export signals is redox sensitive and can be disabled in the presence of ROS allowing Nrf2 to translocate into the nucleus (Aleksunes & Manautou, 2007). Evidence also suggests that phosphorylation of Nrf2 is important for dissociation of Nrf2 from Keap1. More recently, it has been demonstrated that phosphorylation and dephosphorylation of tyrosine 141 in Keap1 regulate its stability and degradation, respectively. It is also shown that modification of critical cysteines (Cys 151, Cys 273, and Cys 288) in Keap1 lead to a change in the conformation of the BTB domain by means of perturbing the homodimerization site, disrupting Neh2 ubiquitination and causing ubiquitination of Keap1 (Kaspar et al., 2009). The switch of ubiquitination from Nrf2 to Keap1 leads to Nrf2 nuclear accumulation.

Antioxidant Response Element and Nrf2. Ubiquitination of Keap1 occurs in response to a variety of stimuli. Following ubiquitination of Keap1, Nrf2 is released that translocates into the nucleus. The nuclear localization signal in the basic region of Nrf2 stimulates its nuclear translocation. The basic region

is also responsible for DNA binding, and the acidic region of Nrf2 is required for transcriptional activation (Jaiswal, 2004). In the nucleus, Nrf2 binds to the GTGACA***GC core sequence of antioxidant response element (ARE) (Rushmore et al., 1991) and regulates ARE-mediated antioxidant gene expression (Figure 1.3). ARE-mediated transcriptional activation requires heterodimerization of Nrf2 with other bZIP proteins, including Jun (c-Jun, Jun-D, and Jun-B) and small Maf (MafG, MafK, and MafF) proteins.

The aforementioned Keap1:Nrf2 regulatory pathway is generally thought to dictate subcellular localization of Nrf2 and activity. However, questions regarding how Nrf2 maintains constitutive transcription of drug metabolizing enzymes have prompted researchers to put forth alternative models of Nrf2 signaling. One hypothesis includes the constitutive targeting of *de novo* Nrf2 protein to the nucleus. In this model, there is continuous shuttling of Keap1/cul3/Rbx1 complex into the nucleus, and this nuclear import is mediated by Prothymosin- α (Niture & Jaiswal, 2009). This complex inside the nucleus exchanges prothymosin-α with Nrf2 resulting in degradation of Nrf2 (Kaspar et al., 2009).

Other regulatory mediators of Nrf2 include Bach1, which is a transcription repressor. Bach1 heterodimerizes with small Maf proteins in the absence of cellular stress and represses gene expression. In the presence of oxidative stress, Bach1 is released from the Maf proteins and is replaced by Nrf2. The activation of a delayed mechanism involving glycogen synthase kinase 3β (GSK3β) controls the switching off of gene transcription by Nrf2

activation. GSK3β is a serine/threonine kinase that phosphorylates Fyn (a tyrosine kinase) leading to nuclear localization of Fyn. Fyn phosphorylates Nrf2 resulting in nuclear export of Nrf2, binding with Keap1, and degradation of Nrf2 (Kaspar et al., 2009).

Activation of Nrf2-Keap1 Regulatory Pathway in Liver Injury Models

Nrf2 and APAP-induced Hepatotoxicity. Nrf2 knockout mice are more susceptible to APAP-induced liver injury compared to their wild-type counterparts (Chan et al., 2001; Enomoto et al., 2001). This susceptibility of Nrf2 knockout mice to APAP hepatoxicity is attributed to altered phase1 and phase 2 metabolism of APAP in the liver, where Nrf2 knockout livers exhibit lower Ugt1a6 activity, which is a detoxification pathway for APAP (Enomoto et al., 2001). It is also demonstrated that Nrf2 knockout mice have an 85 % lower Nqo1 activity compared to wild-type mice (Reisman et al., 2009). On the other hand, mice with Keap1 deficient livers exhibit resistance to APAP-induced hepatotoxicity compared to Nrf2 knockout mice as well as their wild-type counterparts (Okawa et al., 2006; Reisman et al., 2009). Higher nuclear accumulation of Nrf2 in Keap1 knockout livers markedly enhances the constitutive expression of genes regulated by Nrf2 such as NAD(P)H:quinone oxidoreductase-1 (*Nqo1*) (about 415 % compared to wild-type), glutathione S-transferase (*Gst*), and glutamate cysteine ligase catalytic subunit (*Gclc*) (Okawa et al., 2006; Reisman et al., 2009).

A low toxic APAP dose causes nuclear accumulation of Nrf2 in CD-1 mouse livers (Goldring et al., 2004). Nrf2 nuclear translocation in these mice is accompanied by increased expression of Nrf2 dependent genes such as heme oxygenase-1 (*Hmox1*) and *Gclc.* Similar studies confirmed the induction of Nrf2 dependent genes *Nqo1* and *Hmox1* in liver (Aleksunes et al., 2005; Aleksunes et al., 2006; Bauer et al., 2000; Chiu et al., 2002). *NQO1* induction is also reported in human liver samples obtained from patients during transplantation following APAP overdose (Aleksunes et al., 2006). Taken together, Nrf2 not only regulates expression of enzymes that metabolize APAP, but also alters the detoxification mechanism involved during APAP-induced hepatotoxicity.

Nrf2 and AlOH-induced Hepatotoxicity. Liu et al. have demonstrated the Nrf2 role in protection against AlOH-induced liver injury using Nrf2-null, Keap1-knockdown (Keap1-KD), and Keap1-hepatocyte knockout (Keap1-HKO) mice called "graded Nrf2 activation" model (Liu et al., 2013). While there was lower plasma ALT activity in Keap1-HKO mice following AlOH treatment, plasma ALT activity was not detectable in Keap1-KD mice. Furthermore, Nrf2-null mice showed increased plasma ALT activity compared to wild-type controls. Collectively, it can be concluded from this study that Nrf2 activation confers moderate protection against AlOH-induced hepatotoxicity in mice (Liu et al., 2013).

***Nrf2 and ANIT-induced hepatotoxicity*.** ANIT causes intrahepatic cholestasis and activates Nrf2 (Tanaka et al., 2009). This is evidenced by

Nrf2 translocation and Nqo1 mRNA and protein induction. Surprisingly, the authors did not see any difference in degree of liver injury in both wild-type and Nrf2-null mice following ANIT treatment. This response was attributed to compensatory alteration in Shp and Hnf1α signaling in Nrf2 knockout mice. Activation of Nrf2 by oltipraz in Nrf2 knockout mice protected against ANIT-induced liver injury (Tanaka et al., 2009).

***Nrf2 and BDL-induced Hepatotoxicity*.** Cholestasis resulting from BDL increased *Nqo1* gene expression in mouse liver, and this increase is Nrf2-dependent (Aleksunes et al., 2006). Consistent with this, Yamamoto's group showed that Nrf2 activation protects against BDL-induced liver injury in Keap1-knockout mice, an animal model for Nrf2-activation (Okada et al., 2009). In spite of the lack of *Nqo1* induction in Nrf2 knockout mice liver, BDL in Nrf2 knockout mice did not result in significant elevations of ALT activity (Aleksunes et al., 2006; Weerachayaphorn et al., 2012). This discrepancy is attributed to the adaptive compensatory changes involving nuclear transcription factors, including Fxr, Shp, Pxr, efflux bile acid transporters, altered GSH levels, and bile flow rates in Nrf2 knockout mice (Weerachayaphorn et al., 2012). These multiple adaptations lessen the susceptibility of Nrf2 knockout mice to BDL-induced liver injury. While the levels of various isoforms of Gst's, Gclc, and Gclm increase from day 1 to day 7 after BDL (Aleksunes et al., 2006; Yang et al., 2009), this transient increase is followed by a fall to below baseline by day 14 that persists up to day 28 (Yang et al., 2009). This lack of expression of GSH synthetic enzymes during

the later stages of cholestasis was shown to be due to the fall in Nrf2 nuclear binding activity to ARE (Yang et al., 2009). Collectively, these studies demonstrate the influence of Nrf2 on the regulation of bile acid homeostasis in the liver as well as protection against BDL-induced liver injury.

Nrf2 and CCl_4-induced Hepatotoxicity. CCl_4 treatment results in induction of oxidative stress (*Ho-1*) and detoxification (*Nqo1*) genes at 6 h and 24 h, respectively (Aleksunes et al., 2005). A later report by Randle et al. demonstrated that CCl_4 administration results in Nrf2 nuclear translocation at 1 h, while severe hepatic necrosis was evident 24 h later (Randle et al., 2008). As expected, in this study Nrf2 nuclear translocation was accompanied by induction of *Hmox1* 24 h after CCl_4 administration (Randle et al., 2008). The Nrf2 role in CCl_4-induced liver injury is further supported by the CCl_4 study in Nrf2-null mice (Liu et al., 2013). In this study, Nrf2-null mice are more susceptible to CCl_4-induced hepatotoxicity compared to Keap1-KD or Keap1-HKO mice. The Nrf2-mediated protection is attributed to induction of antioxidant genes, suppression of inflammatory responses, and attenuation of oxidative stress in the livers (Liu et al., 2013).

1.6 APAP Autoprotection

An experimental approach to modulate APAP hepatotoxicity in rodents is through auto/heteroprotection. Autoprotection is resistance to toxicant re-exposure following acute, mild injury with the same toxicant, whereas in heteroprotection, the initial toxicant used is different from the second.

Mehendale and his colleagues first demonstrated autoprotection in rats in the early 1990's with carbon tetrachloride (CCl_4) (Thakore & Mehendale, 1991). Previous studies conducted in our laboratory have demonstrated both auto/heteroprotection in mice and that pre-treatment with various chemicals reduce the severity of APAP toxicity in mice (Aleksunes et al., 2008; Manautou et al., 1994). For instance, Manautou et al. show that peroxisome proliferators such as clofibrate at subtoxic doses protect rodents from APAP toxicity (APAP heteroprotection) (Manautou et al., 1994). Alternatively, APAP at a mild toxic dose protects mice against hepatotoxicity from higher doses of APAP (APAP autoprotection) (Aleksunes et al., 2008). This model of APAP autoprotection was used to investigate the role of hepatobiliary drug transporters during the development of resistance to APAP hepatotoxicity. In this study, an increased expression of the sinusoidal efflux transporter Mrp4 is evidenced in the hepatocytes localized to centrilobular areas where compensatory hepatocellular proliferation following pre-treatment with mildly toxic doses of APAP is confined. The protection occurs independently of changes in bioactivation or detoxification of APAP.

The phenomenon of autoprotection is also seen in patients who are repeatedly exposed to supratherapeutic doses of APAP. Shayiq et al., while describing the incremental dose model of APAP autoprotection in mice, introduced a clinical case where a physician addicted to prescription pain medication reported tolerance to the combination product (containing opiod and APAP) (Shayiq et al., 1999). The physician claimed to have consumed

200 tablets per day in the later stages of his addiction (about 65 g APAP) with no apparent liver damage. Another later study demonstrated a similar phenomenon, where healthy adults given 4 g APAP per day over a period of 14 days showed elevations in plasma ALT activity around day 7 to 8 that decreased by day 14 (Watkins et al., 2006). This shows an adaptation to hepatocyte injury during repeated exposure to APAP. These clinical evidence supports evaluation of mechanisms underlying APAP autoprotection.

Gene Expression Profiling in APAP Autoprotection Model

The utility of gene array analysis to address mechanistic toxicology questions has been demonstrated in our lab (Moffit et al., 2007). Even though our previous study demonstrated the role of the drug transporter Mrp4 in APAP autoprotection (Aleksunes et al., 2008), a gene array analysis was performed to identify any other differentially expressed genes resulting from APAP pre-treatment that might also contribute to the development of resistance to APAP hepatotoxicity upon re-exposure to this toxicant. A gene array analysis revealed statistically significant genes unique to the APAP autoprotection mouse model (mice pretreated and re-exposed to APAP) and further analysis of these genes using the causal reasoning engine (CRE) provided insights into the signaling pathways involving autoprotection (O'Connor et al., 2014). Out of several noteworthy genes that were identified to be differentially expressed in APAP autoprotected mice, Fmo3 was one of them.

1.7 Flavin-containing Monooxygenase-3

Flavin-containing monooxygenase (FMO) is one of the major microsomal monooxygenase enzyme systems located in the membrane of the endoplasmic reticulum. Mammalian FMO is an NADPH-dependent and oxygen-dependent microsomal FAD-containing enzyme system that functions as a nitrogen, sulfur, and phosphorus oxygenase (Rettie & Fisher, 1999).

Discovery of FMO Enzymes. Miller and his co-workers in the 1960's reported that liver microsomes contained enzymes that catalyzed the NADPH- and O_2-dependent oxidation of butter yellow and a number of other azo dyes (Miller et al., 1960). Later, Ziegler studied the nature of enzymes catalyzing the mixed function oxidation reactions. N-oxidation of N, N-dimethylaniline was selected as a model reaction to characterize enzymes in liver microsomes and a high activity was observed in microsomes isolated from pig liver. The Ziegler lab further purified the enzyme that catalysed the NADPH- and O_2-dependent N-oxidation of N, N-dimethylaniline in 1972 from pig liver (Ziegler & Mitchell, 1972). This enzyme was called "mixed-function amine N-oxidase" or "Ziegler's enzyme" until 1979. Shortly after the isolation of the enzyme from pig liver, Jollow and Cook demonstrated that it catalyzed oxygenation of a wide range of xenobiotics that had no common structural features (Ziegler et al., 1971; Ziegler & Poulsen, 1998). The list includes inorganic and organic compounds and some of these compounds contain functional groups bearing sulfur or selenium instead of nitrogen. Since the

name “mixed-function amine N-oxidase” was restrictive, the enzyme was given the name flavin-containing monooxygenase, abbreviated as FMO.

Biochemical Properties Unique to FMOs.

Thermal Stability and NADPH. With the exception of FMO2, placement of microsomes in an argon environment at 55°C for 1 min in the absence of NADPH decreases FMO activity by 85 % or more, while CYP activity is reduced by 15 % or less (Cashman, 1999). NADPH stabilizes FMO activity (Cashman, 1999).

Effect of Detergent. The FMO activity increases at Triton X-100 concentrations between 0.05-0.5 %. At concentrations above 0.5 %, the enzyme activity decreases (Brunelle et al., 1997). Sodium cholate and fatty acid at a low concentration inhibit FMO1 and FMO3, while sodium cholate at a high concentation (1 %) does not inhibit FMO2 function (Krueger & Williams, 2005).

Effect of pH. The optimal pH for animal and human FMO-mediated N- and S-oxygenation is generally equal to or above pH 9.0. On the other hand, maximum CYP activity is seen at pH 7.4 (Cashman, 1999).

Formation of a Relatively Stable Hydroperoxyflavoprotein Intermediate. Among the flavoproteins that exist, FMO is distinct in its ability to form a relatively stable hydroperoxyflavin intermediate. This is because the protein environment of the FMO and the presence of NADPH protect the hydroperoxy species from decomposing, reacting with apoprotein or disproportionating into

reactive oxygen species. Thus, it does not expose the cell to the untoward effects of oxidative stress. However, in the absence of NADPH, peroxyflavin can decompose to hydrogen peroxide resulting in significant loss of enzyme activity (Cashman, 1999).

Metabolite Prediction. Barring steric constraints, the metabolite produced by an FMO of a particular substrate can be predicted based on the oxidation product produced from the treatment of substrate with alkyl hydroperoxides or peracids (Cashman, 1999).

Approaches to Distinguish Between FMO- and CYP-mediated Metabolism.

The similarities and differences between the FMO and CYP enzymes are summarized in Table 1.1. FMO and CYP have overlapping substrate-specificity. There are a number of *in vitro* approaches to distinguish CYP activity from that of FMO.

Thermal Inactivation. Heating the enzyme up to 50°C for 1 min in the absence of NADPH results in the loss of 85 % of FMO activity, while retaining 85 % of CYP activity (Cashman, 2005).

pH of Incubation Mixture and Detergents. Performing microsomal incubations at pH 8.4 to 9.4 generally abrogates CYP activity (Cashman, 2005). The presence of high concentrations of Emulgent 911 also abrogates CYP activity (Cashman, 2005). Thus, solubilization of microsomes using

detergents at elevated pH is another approach to selectively examine FMO activity (Cashman, 1999).

NADPH and Enzyme-mediated Reactions. FMO-dependent reactions are initiated by the addition of substrate to a previously pre-equilibrated microsomal preparation containing NADPH, while CYP-dependent reactions are initiated by the addition of NADPH (Cashman, 1999).

Metal Ions. FMO is relatively sensitive to metal ions, thus incubations should be carried out in the absence of $MgCl_2$ and in the presence of a chelating agent (Cashman, 1999).

Inactivation of prosthetic group. While CYPs can be inactivated via saturation of heme prosthetic group by carbon monoxide, FMOs are unaffected by carbon monoxide (Krueger & Williams, 2005).

Inhibitors.

- Chemical inhibitors: FMO inhibitors include methimazole (MMI), thiourea and indole-3-carbinol (I3C), whereas CYP inhibitors include N-benzylimidazole, aminobenzotriazole, and proadifen hydrochloride (SKF-525).
- Immunological inhibitors: Antibodies directed against FMOs and NADPH-P450 reductase.

Molecular Biology Tools. Recombinant FMO and CYP enzymes.

The Potential of Chemical Inhibitors in vivo and Knockout Mouse Lines. In rodents, pretreatment with MMI or I3C has been demonstrated to block FMO-mediated conversion of various compounds (Nace et al., 1997). MMI is not a specific inhibitor, and inhibits thyroid peroxidase along with FMO. The reactive intermediate of MMI metabolism, sulfenic acid, also inhibits CYP activity. On the contrary, I3C induces CYP enzymes (Katchamart & Williams, 2001). These problems associated with FMO-inhibitor usage for evaluating the FMO role in drug metabolism *in vivo* can be overcome by use of engineered knockout mouse lines. To date, only one Fmo knockout mouse line has been produced and this knockout mouse line lacks genes encoding *Fmo1, Fmo2,* and *Fmo4*. Because the expression of *Fmo3* in male mouse liver is switched off during development, male mice are essentially void of the Fmo3 protein. In the absence of functional Fmo3 protein in normal male mice, there has been no need for developing a knockout model (Hernandez et al., 2009; Shephard & Phillips, 2010).

The Mechanism of Catalysis. FMO and CYP both require NADPH and O_2 as cofactors for its catalytic activity. The mechanism of reactions catalysed by FMO is different from that of the CYP-mediated metabolism. In CYP-mediated metabolism, the first step is the addition of substrate to the enzyme, and electron transfer follows this from the flavoprotein NADPH-CYP reductase to the substrate-bound CYP. The catalytic cycle of FMO is shown in Figure 1.4. In contrast to CYP, the first step in FMO-mediated metabolism is reduction of the FAD by NADPH. This step is followed by the formation of a relatively

stable intermediate, C4α-hydroperoxyflavin, by the addition of a molecular oxygen to the reduced FAD. Therefore, when substrate is accepted by FMO, the enzyme is in an active form (i.e. a cocked gun) ready to effect oxygenations. CYP forms an unstable ferrous-O_2 complex that is capable of decomposing to generate superoxide anion or hydrogen peroxide. Oxygenation by FMO proceeds through an attack of the nitrogen atom (or any other nucleophilic heteroatom) on the terminal hydroperoxyflavin oxygen atom to produce the N-oxygenated substrate and the hydroxyflavo enzyme species. Thus, one atom of molecular oxygen is transferred to the substrate and the second to form water. The rate-limiting step of the catalytic cycle is thought to be the breakdown of the FADOH pseudobase or the release of NADP+. As this occurs after the substrate transformation, substrate binding has no influence on Vmax (Cashman, 1999; Cashman, 2005).

FMO Ontogeny and Tissue Specificity in the Mouse and Humans. FMO enzymes exhibit tissue-, species-, gender- and age-specificity in expression. FMOs are expressed in the liver, lung, kidney, intestine, and brain. For the purpose of this thesis, *FMO* expression in mouse liver will be discussed in comparison to human liver. Cherrington et al. examined hepatic *Fmo1, Fmo3,* and *Fmo5* ontogeny in CD-1 mouse liver by western blotting and this was quantified in a review by Hines (Cherrington et al., 1998; Hines, 2006). Hepatic Fmo3 is undetectable at day 2 after birth in both male and female mice. By day 14 after birth, the Fmo3 protein is detectable in both sexes and is approximately about 50 % of adult female levels. On day 42 (young adult

age), there is a gender-dependent dimorphism apparent, where male mice express undetectable levels and female mice express very high levels of hepatic Fmo3. This is consistent with other reports that show gender-dependent dimorphism with respect to liver Fmo3 levels in B6C3F1 mice (Ripp et al., 1999) as well as 129/SV mice (Janmohamed et al., 2004). Fmo5 on the other hand is expressed at very low levels in the fetus at gestation day 17, and by day 2, the levels are at adult values. Unlike Fmo3, no gender-dependent dimorphism is seen with Fmo5. Fmo1 is detectable on gestation day 15, and by day 17 of gestation, the levels reach adult values. By young adult age, a gender-dependent dimorphism in liver Fmo1 expression is evident, where male mice express detectable but lower Fmo1 compared to females (Cherrington et al., 1998; Hines, 2006). Janmohamed et al. reported tissue specificity and ontogeny of liver FMO mRNA levels in the 129/SV mouse strain, measured by RNase protection assay and *in situ* hybridization (Janmohamed et al., 2004). In this study, it was demonstrated that *Fmo5* expression in female mouse liver is about 2- to 3-fold higher than *Fmo3*, which in turn is 2-fold higher than *Fmo1*. On the contrary, hepatic *Fmo3* is expressed at undetectable levels in adult male mice. Little or no *Fmo2* and *Fmo4* expression is seen in both sexes (Janmohamed et al., 2004). There is a gradient for FMO expression in liver where *Fmo1* and *Fmo5* show a decreasing concentration gradient from central vein to periportal areas. Conversely, Fmo3 mRNA in female liver is localized to the periportal region. Consistent with this, our results from immunohistochemical staining for the

Fmo3 protein in female C57BL/6J mice livers also show a similar staining pattern (Rudraiah et al., 2014).

FMO1 is the predominant FMO in fetal human liver, whereas FMO3 is predominant in adults (Koukouritaki et al., 2002). Dolphin et al. provided the first evidence of a developmental switch from FMO1 to FMO3 in human liver (Dolphin et al., 1996). Although this study was the first to suggest a hepatic FMO developmental switch in humans, Koukouritaki et al. demonstrated a detailed ontogeny in FMO enzyme expression, and also that the FMO1 and FMO3 are independently regulated during development (Koukouritaki et al., 2002).

FMO Substrates Specificity. Different FMO enzymes exhibit broad and overlapping substrate specificity. This property is in part attributed to the formation of C4α-hydroperoxyflavin intermediate in the absence of the substrate. Substrate specificity is determined more by access to the activated flavin as opposed to specific binding at the active site (Hines, 2006; Poulsen & Ziegler, 1995).

FMO1, 2, and 3 oxygenate a wide variety of nucleophilic tertiary and secondary amines as well as sulfur-containing compounds compared to FMO4 and FMO5. FMO5 has restricted substrate-specificity because it does not form a stable intermediate (Ziegler, 2002). The substrate-specificity of FMO5 is poorly defined, although is apparently distinct from FMO3. Because of their limited substrate specificity and low expression levels in most tissues

in humans, FMO4 and FMO5 currently are not thought to play an important role in drug metabolism (Krueger & Williams, 2005).

In general, structural requirements for FMO substrates are as follows (Krueger & Williams, 2005):

- Any compound that contains a soft nucleophile and that is accessible to the C4α-hydroperoxyflavin intermediate can be a substrate.
- Compounds containing a single positive charge are excellent substrates (e.g., cationic tertiary amines).
- Negatively charged compounds are poor substrates with a few exceptions, such as sulindac sulfide and lipoic acid.
- Zwitterions and compounds with more than one positive charge are typically not substrates.

Few examples for FMO substrates are presented in Table 1.2.

Transcriptional Regulation of FMO. Mammalian FMOs were considered non-inducible by xenobiotics (Cashman & Zhang, 2002; Krueger & Williams, 2005). Thus, the transcriptional regulation of FMO involving stress activated transcription factors or a receptor that binds ligand and interacts with DNA was not studied as other forms of regulation. However, recent studies by Celius et al. show that activation of the Aryl hydrocarbon (Ah) receptor by 2,3,7,8-tetrachlorodibenzo-p-dioxin (TCDD) induces Fmo3 mRNA in mice, with marginal changes in protein levels (Celius et al., 2008; Celius et al., 2010). Authors also show that the Fmo3 mRNA up-regulation by 3-

methylcholanthrene (3MC) and benzo(a)pyrene (BaP) but not TCDD in Hepa-1 cells is mediated by p53 and its binding to a p53-response element in the promoter region of Fmo3 (Celius et al., 2010).

The hormonal effects on FMO activity have been described. Adult female mice livers exhibit higher Fmo3 activity compared to male mice. Gender-related differences in mouse liver Fmo3 activity are shown to be due primarily to testosterone-dependent repression of the enzyme in male mice (Duffel et al., 1981). Rat liver FMO is positively regulated by testosterone and repressed by estradiol (Cashman & Williams, 1990; Cashman & Zhang, 2006; Lemoine et al., 1991). Diurnal cortisol secretion also regulates FMO activity in female mice (Dixit & Roche, 1984). In pregnant rabbits, plasma concentration of progesterone and corticosterone is shown to regulate lung Fmo2 mRNA and protein levels at day 15 and 28-31 (Hines et al., 1994). In cultured rat hepatocytes, lipopolysaccharide and proinflammatory cytokines treatment decreased FMO1 mRNA levels via a cGMP-independent destabilizing effect of nitric oxide rather than decreased transcription (Ryu et al., 2004).

In humans, Lou and Hines demonstrated that hepatocyte nuclear factor (HNF) 1α and HNF4α positively regulate, while Yin yang (YY1) negatively regulate *FMO1* expression (Luo & Hines, 2001). An upstream SNP was also identified within the conserved core binding sequence for the YY1. Transient expression assays showed that this SNP in YY1 could account for two- to three-fold loss of FMO1 promoter activity, and genotype analysis showed individuals of Caucasian, African, and Hispanic descent had 11 %, 13

% and 30 % frequency, respectively (Hines et al., 2003). Klick and Hines also demonstrated that binding of transcription factors such as nuclear factor-Y (NF-Y), upstream stimulatory factor 1 (USF1), YYI and an unidentified GC box to the regulatory domains upstream of the transcription start site are important for constitutive *FMO3* transcription regulation (Klick & Hines, 2007). The pre-B-cell leukemia factor 2 (Pbx_2) as a heterodimer with an unidentified homeobox (Hox) isoform contributes to *FMO3* developmental- and tissue-specific regulation (Klick & Hines, 2007). A later study by the same group identified another element, CCAAT enhancer-binding protein β (C/EBPβ), as being more distal to the transcription start site and this is shown to be important for *FMO3* developmental expression pattern (Klick et al., 2008). Shimuzu et al. reported that HNF-4 and NF-Y could play crucial roles in modulating the activity of the *FMO3* expression in the Japanese population (Shimizu et al., 2008).

Post-transcriptional Regulation of FMO. Post-transcriptional regulation of FMO is not well understood. For example, not much is known about enhancement of FMO mRNA stability or mechanisms regulating the stability of FMO mRNA transcripts. Recent reports by Celius et al. showed an increase in miRNA following TCDD treatment in C57BL/6J mice livers (Celius et al., 2008). *In silico* analysis further predicted binding sites on mouse Fmo3 mRNA for the up-regulated miRNAs (mmu-miR203 and mmu-148a). The authors concluded that a modest increase in FMO catalytic activity evidenced

following TCDD treatment, in spite of a large increase in Fmo3 mRNA, is due to targeted degradation of mRNAs by miRNAs (Celius et al., 2008).

FMOs have a consensus sequence for N-glycosylation, and mass spectrometry studies have shown that FMO1 is selectively N-glycosylated at Asn 120 (Korsmeyer et al., 1998). The highly conserved nature of this site suggests that this region could be important in a structural or functional role in enzyme action, but cDNA expression of FMOs in bacterial expression systems show that enzyme activity does not require N-glycosylation (Cashman & Zhang, 2006).

Physiological functions of FMO. The function of FMO is described previously and is involved in the oxygenation of endogenous compounds and xenobiotics. The importance of mammalian FMO in xenobiotic metabolism is known, while its physiological role has not yet been identified, except for TMA N-oxygenation. Trimethylamine (TMA) is an odorous compound formed by gut bacteria and is responsible for a fish odor. In humans, a mutation in the *FMO3* results in failure to efficiently N-oxygenate TMA, leading to a genetic disease known as trimethylaminuria.

FMO is involved in oxygenation of sulphur-containing endogenous substrates such as cysteamine (reduced form) to cystamine (disulfide form) (Poulsen, 1981). Although the physiological role of cysteamine S-oxygenation by Fmo3 is not clear, in the 1970s, Ziegler and Poulsen suggested a role for FMO in protein disulphide bond formation through

oxidation of cysteamine. It was also proposed that oxygenation of cysteamine may be a significant source of disulphide, maintaining the cellular thiol:disulphide potential in a cell (Ziegler et al., 1979). Further, Suh and Robertus showed that yeast FMO serves as a modulator of cellular thiols and maintains optimum redox potential within the endoplasmic reticulum, allowing for proper folding of disulfide bond- containing proteins (Suh & Robertus, 2002).

The cytoprotective functions of Fmo3 and its possible involvement in APAP autoprotection are summarized below. However, this is entirely speculative at this point. The relationship between cellular thiol:disulphide ratios and the regulation of metabolic reactions has been recognized for a long time (Barron, 1953). Oxygenation of cysteamine during APAP hepatotoxicity may serve to help control the overall thiol:disulphide redox state of the cell, which in turn may modulate cellular metabolism and/or activate signal transduction pathways leading to altered susceptibility to APAP (or protection). It is also possible that oxygenation of cysteamine to cystamine by Fmo3 and transport out of the cell may represent a detoxication mechanism or protective function, since cysteamine is toxic to cells at concentrations as low as 39 μM through the transition metal-dependent formation of hydrogen peroxide (Jeitner & Lawrence, 2001).

1.8 Summary

The project described in this thesis originated from a gene array analysis on the APAP autoprotected mice livers performed previously. One of the differentially expressed genes identified during analysis is Fmo3. For a long time, Fmo3 was considered non-inducible by xenobiotics. Thus, the mechanism(s) underlying Fmo3 gene induction by a xenobiotic is not well studied. Apart from its role in drug metabolism and fish odor syndrome, the physiological functions of Fmo3 are not currently known. The goal of this project was to investigate the mechanistic role of Fmo3 gene expression during APAP-induced hepatotoxicity. The results presented in this dissertation show Fmo3 mRNA and protein induction during APAP hepatotoxicity in mice. To verify that Fmo3 gene induction is not model-specific, Fmo3 gene expression in other mouse models of hepatic injury was also investigated. Since a common event for all hepatotoxicants tested is oxidative stress, the oxidative stress transcription factor Nrf2 role in FMO3 gene expression was examined. Similar to APAP autoprotection mouse model, human liver acquires resistance to supratherapeutic doses of APAP. HepaRG cells were employed to evaluate whether APAP-induced cytotoxicity induces FMO3 gene expression. The functional significance of FMO3 over-expression during APAP hepatotoxicity was also evaluated both *in vivo* and *in vitro*.

In conclusion, this thesis clearly demonstrates *Fmo3* as a genetic determinant of APAP toxicity. Although many hepatotoxicants that result in oxidative stress induces *Fmo3* gene expression, both *in vitro* and *in vivo*

studies demonstrate that FMO3 gene expression does not involve activation of the NRF2-KEAP1 regulatory pathway. Results from human cell line studies show that FMO3 over-expression alters susceptibility to APAP-induced hepatotoxicity and that FMO3 may play an important role in cellular differentiation. The cellular differentiation phenotype appears to be important because the only gene altered in this cell line is FMO3 and differentiation is happening in the absence of multiple gene expression changes that would result in response to APAP (as in the autoprotection mouse model). With the recent advancements showing a relationship between FMO3 gene expression in humans, and the risk of atherosclerosis as well as ischemic stroke, a complete understanding of the FMO3 over-expression function appear to be important. This work not only emphasizes FMO3's novel protective function, but also its unexplored facets of function.

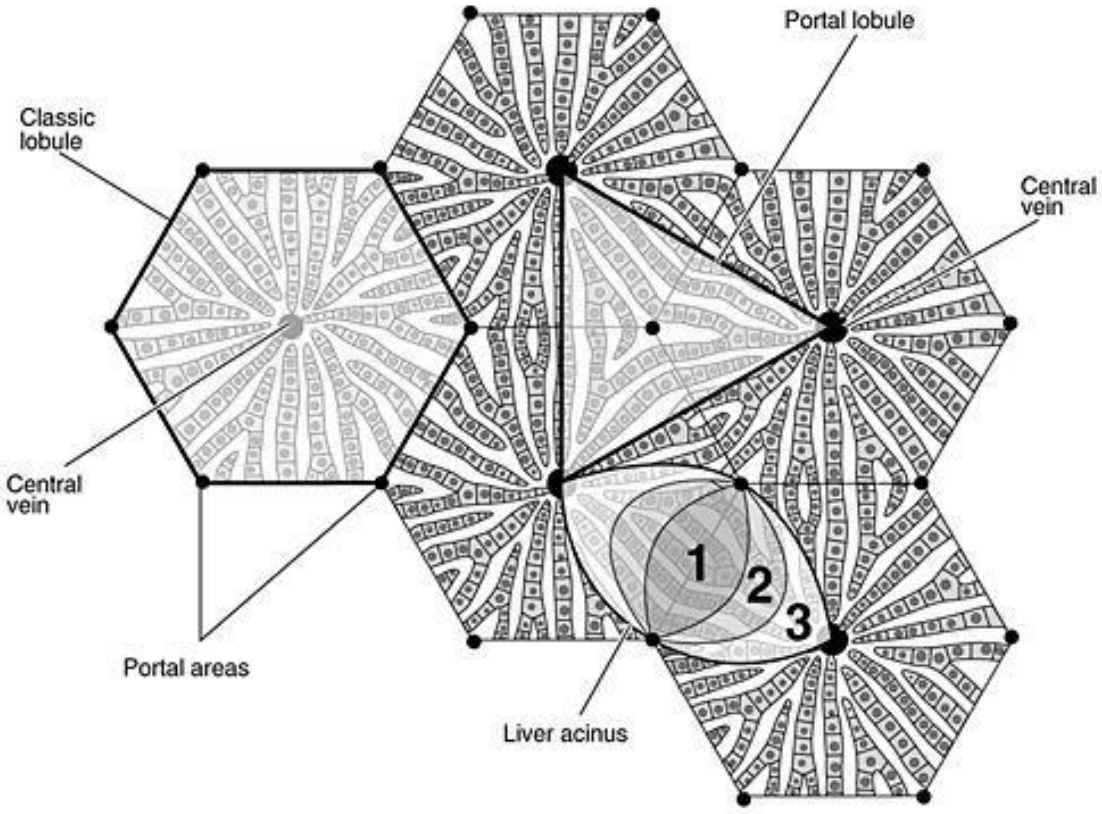

Figure 1.1. Scheme showing structural organization of the liver lobule.

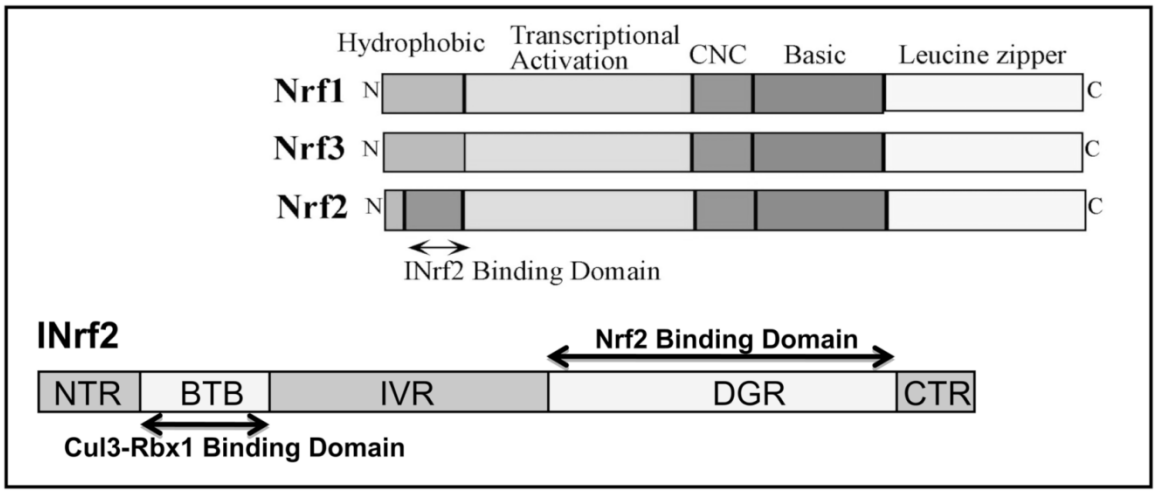

Figure 1.2. Schematic drawing of various domains of Nrf (Nrf1, Nrf2, Nrf3) and Keap1/INrf2 (Kaspar et al., 2009).

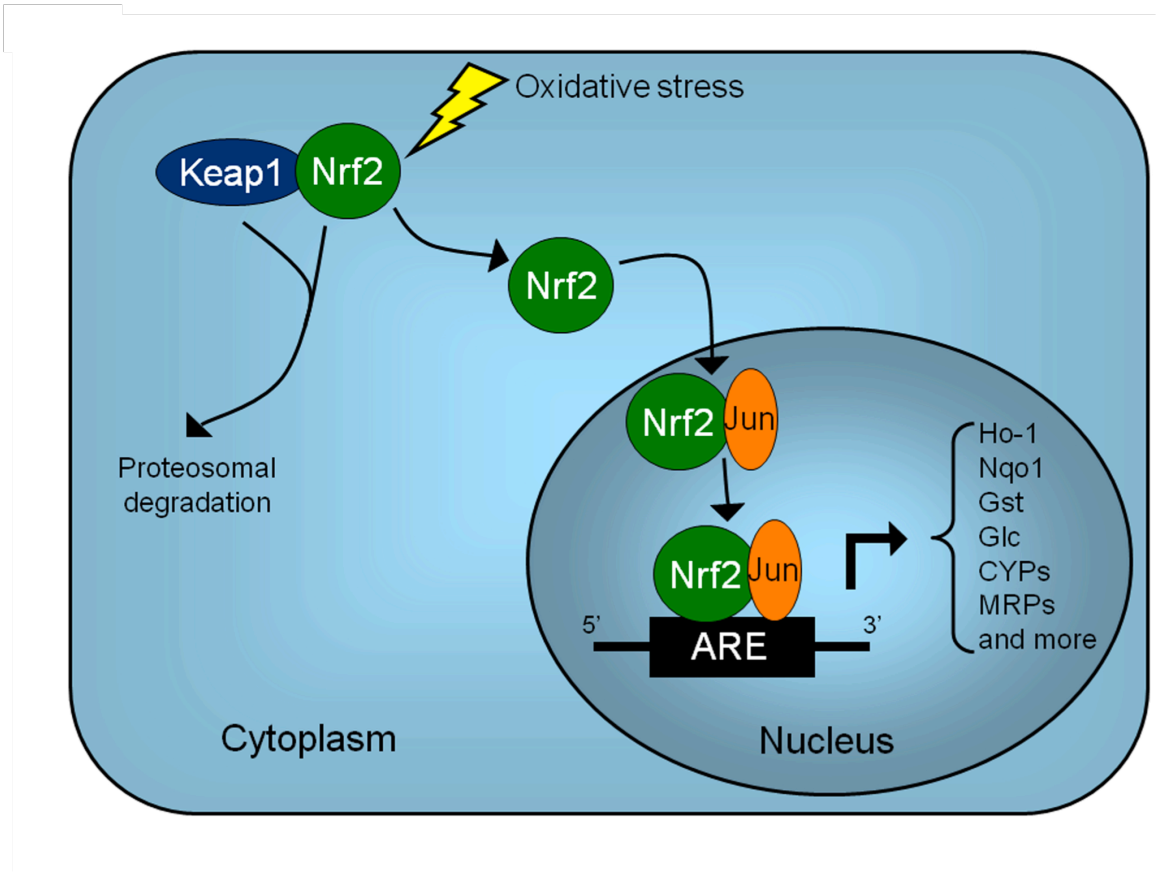

Figure 1.3. A schematic representation of Nrf2-mediated gene transcription (Bataille & Manautou, 2012).

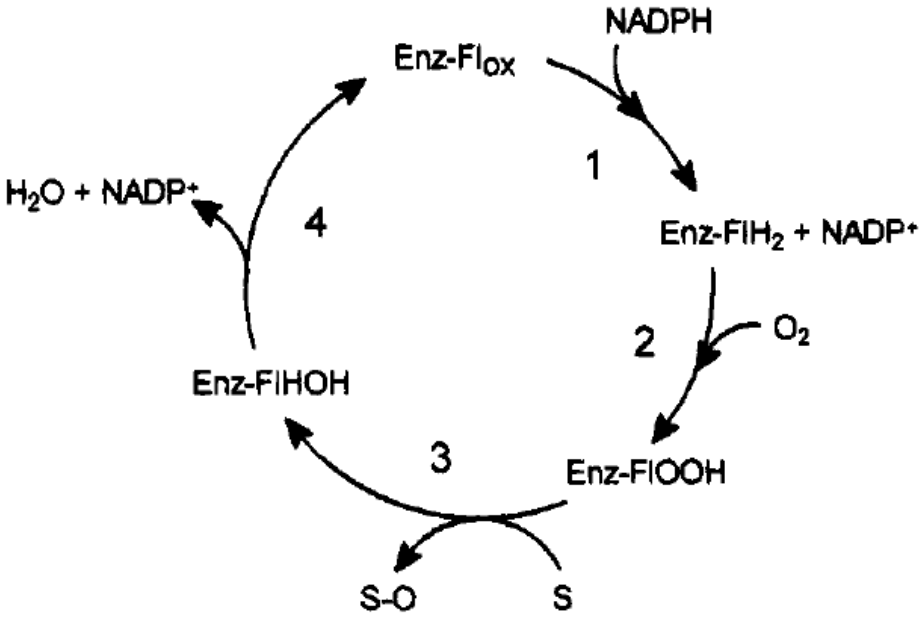

Figure 1.4. A schematic representation of catalytic cycle of FMO. S: Substrate, S-O: Oxygenated substrate, Enz(Flox): Oxidized flavoprotein, Enz(FlH2): Enzyme in reduced form, Enz(FlOOH): C4α-hydroperoxyflavin of FAD, Enz(FlHOH): Hydroxyflavin of FAD (Cashman, 1995).

Table 1.1 Similarities and differences between the FMO and CYP (Cashman, 2005; Hodgson et al., 1999).

	FMO	**CYP**
Co-substrates	NADPH, O_2	NADPH, O_2
Coupled enzymes	None	NADPH-P450 reductase Cytochrome b_5 *
Cellular location	Microsomes	Microsomes, mitochondria
Xenobiotic inducers	AhR activators (TCDD)** (Celius et al., 2008 and 2010).	Many, e.g. Phenobarbital, TCDD
Inhibitors	Competitive substrates, only	Competitive substrates and mechanism based inhibitors, e.g.SKF525A, piperonyl butoxide
Isoforms	Few, only 11 known currently. FMO6 to FMO11 are pseudogenes in humans (Hines, 2006).	Many, over 3000 known currently
Substrates	Some inorganics, organic compounds with N, S, Se, P heteroatoms	Organic compounds with and without N, S, Se, P heteroatoms
Oxygenation	FMO oxygenates compounds via a two-electron mechanism	Oxidizes compounds via a sequential one-electron processes
Toxicity of metabolites	Usually non-toxic	Greater prevalence for generation of toxic metabolite

* Cytochrome b_5 is required only for some CYP isoforms and for some substrates

** Activation of the Aryl hydrocarbon receptor (AhR) induces Fmo3 mRNA in mice, but with marginal changes in protein levels.

Table 1.2 Substrates for FMO. Taken from (Hodgson et al., 1995; Krueger & Williams, 2005; Ziegler, 1988).

Substrate	**Example**
Endogenous substrates	
Sulfur-containing	Cysteamine, Methionine, Lipoic acid, S-farnesylcysteine, S-cysteine conjugates, selenocysteine conjugates
Nitrogen-containing	Trimethylamine, Tyramine, Phenethylamine
Exogenous substrates	
Sulfur-containing	Cimetidine, Albendazole, Sulindac sulfide, Methimazole, Ethionamide,
Nitrogen-containing	Imipramine, Clozapine, Tamoxifen, Chloro- and Bromo-pheniramine, Zimeldine, Ranitidine, Benzydamine, Olopatadine, Xanomeline, Pargyline, Itopride, Nicotine
Phosphorus-containing	Fonofos, Diethylphenylphosphine, Fenthion
Selenium-containing	2-selenylbenzanilide
Inorganics	HS^-, I^-, I_2
Boronic acid	

CHAPTER 2

Tolerance to Acetaminophen Hepatotoxicity in the Mouse Model of Autoprotection is Associated With Induction of Flavin-containing Monooxygenase-3 (FMO3) in Hepatocytes

2.1 Abstract

Acetaminophen (APAP) pretreatment with a hepatotoxic dose (400 mg/kg) in mice results in resistance to a second, higher dose (600 mg/kg) of APAP (APAP autoprotection). Recent microarray work by our group showed a drastic induction of liver flavin containing monooxygenase-3 (Fmo3) mRNA expression in our mouse model of APAP autoprotection. The role of liver Fmo3, which detoxifies xenobiotics, in APAP autoprotection is unknown. The purpose of this study was to characterize the gene regulation and protein expression of liver *Fmo3* during APAP hepatotoxicity. The functional consequences of *Fmo3* induction were also investigated. Plasma and livers were collected from male C57BL/6J mice over a period of 72 h following a single dose of APAP (400 mg/kg) to measure Fmo3 mRNA and protein expression. Although Fmo3 mRNA levels increased significantly following APAP treatment, protein expression changed marginally. In contrast, both Fmo3 mRNA and protein expression were significantly higher in APAP autoprotected livers. Unlike male C57BL/6J mice, female mice have about 80-times higher constitutive Fmo3 mRNA levels and are highly resistant to APAP hepatotoxicity. Co-administration of APAP with the FMO inhibitor

methimazole rendered female mice susceptible to APAP hepatotoxicity, with no changes in susceptibility detected in male mice. Furthermore, a human hepatocyte cell line (HC-04) clone over-expressing human FMO3 showed enhanced resistance to APAP cytotoxicity. Taken together, these findings establish for the first time induction of Fmo3 protein expression and function by xenobiotic treatment. Our results also indicate that Fmo3 expression and function plays a role in protecting the liver from APAP-induced toxicity. Although the mechanism(s) of this protection remains to be elucidated, this work describes a novel protective function for this enzyme.

2.2 Introduction

Acetaminophen (APAP) overdose is a leading cause of acute liver failure in the U.S. and Great Britain, accounting for more than 50 % of all acute liver failure cases from all etiologies (Larson et al., 2005; W. M. Lee, 2010). APAP is safe at therapeutic doses, where the majority of APAP administered is glucuronidated or sulfated and the metabolites are safely excreted into the urine and bile. Under these conditions, a small amount of APAP also undergoes bioactivation by cytochrome P450 metabolism to generate N-acetyl-p-benzoquinone imine (NAPQI), a reactive metabolite that can be detoxified by hepatic glutathione (GSH). However, when NAPQI is produced in large amounts, as in the case of APAP overdose, GSH stores are depleted and NAPQI reacts with intracellular thiols, binds covalently to cellular macromolecules, and produces oxidative stress, which ultimately results in necrosis of centrilobular hepatocytes (Cohen et al., 1997; Hinson et al., 2010). The growing concern over APAP-induced hepatotoxicity has prompted extensive research aimed at devising measures to reduce the risk of APAP heptotoxicity.

An experimental approach to modulate APAP hepatotoxicity in rodents is through auto/heteroprotection. Autoprotection is resistance to toxicant re-exposure following acute, mild injury with the same toxicant, whereas in heteroprotection, the initial toxicant used is different from the second. Mehendale and his colleagues first demonstrated autoprotection in rats in early 1990's with carbon tetrachloride (CCl_4) (Thakore & Mehendale, 1991).

Previous studies conducted in our laboratory have demonstrated both auto/heteroprotection in mice and that pre-treatment with various chemicals can reduce the severity of APAP toxicity in mice (Aleksunes et al., 2008; Manautou et al., 1994). For instance, Manautou et al. showed that peroxisome proliferators such as clofibrate at subtoxic doses protect rodents from APAP toxicity (APAP heteroprotection) (Manautou et al., 1994). Alternatively, APAP at a mild toxic dose protects mice against hepatotoxicity from higher doses of APAP (APAP autoprotection) (Aleksunes et al., 2008). This model of APAP autoprotection was used to investigate the role of hepatobiliary drug transporters during the development of resistance to APAP hepatotoxicity. In this study, an increased expression of the sinusoidal efflux transporter Mrp4 (Multidrug resistance-associated protein 4) is evidenced in the hepatocytes localized to centrilobular areas where compensatory hepatocellular proliferation following pre-treatment with mildly toxic doses of APAP is confined. The protection is shown to occur independently of changes in bioactivation or detoxification of APAP.

The utility of gene array analysis to address mechanistic toxicology questions has been demonstrated in our lab (Moffit et al., 2007). Even though our previous study demonstrated the role of the drug transporter Mrp4 in APAP autoprotection (Aleksunes et al., 2008), a gene array analysis was performed to identify any other differentially expressed genes resulting from APAP pre-treatment that might also contribute to the development of resistance to APAP hepatotoxicity upon re-exposure to this toxicant. Gene

array analysis revealed statistically significant gene expression changes unique to the APAP autoprotection mouse model (mice pretreated and re-exposed to APAP) and further analysis of these genes using causal reasoning engine (CRE) provided insights into the signaling pathways involved in autoprotection (O'Connor et al., 2014). Of several noteworthy genes that were identified to be differentially expressed in APAP autoprotected mice, *Fmo3* is one of them. *Fmo3* is unique in a way that it is considered non-inducible (Cashman & Zhang, 2002), but Fmo3 mRNA expression increased 20- and 7-fold at 4 and 24 h in the autoprotected group, respectively (O'Connor et al., 2014). Although a role of *Fmo3* in APAP hepatotoxicity is not known, it was the most biologically plausible for playing a role in autoprotection.

Fmo3 is a monooxygenase involved in drug-metabolism somewhat similar to cytochrome P450 (CYP) in that it produces many of the same metabolites, although its substrate specificity is much more limited. Fmo3 is not known to metabolize APAP and most metabolic products of Fmo3 are considered to be non-toxic (Krueger & Williams, 2005). Hepatic expression of the *Fmo3* gene is highly variable showing cell-, tissue-, gender- and developmental stage-specific expression patterns (Hines, 2006; Janmohamed et al., 2004; Koukouritaki et al., 2002). Mammalian *Fmo3* is also considered to be non-inducible (Cashman & Zhang, 2002). However, recent studies by Celius et al. showed that activation of the Aryl hydrocarbon (Ah) receptor induces Fmo3 mRNA in mice, with marginal changes in protein levels (Celius

et al., 2008; Celius et al., 2010). To our knowledge, the current study is only the second to document xenobiotic-dependent *Fmo3* induction, the importance of which is unknown. Further, the role of *Fmo3* in APAP-induced hepatotoxicity and/or autoprotection also is not known. However, it is intriguing that female mice, which contain approximately 80-times more hepatic Fmo3 mRNA than males (Janmohamed et al., 2004), are much more resistant to APAP hepatotoxicity compared to their male counterparts (Dai et al., 2006).

The initial studies reported herein describe *Fmo3* gene expression during APAP-induced hepatotoxicity. To better understand an *Fmo3* role in protection against APAP hepatotoxicity, we further attempted to establish a causal relationship between the two, i.e., *Fmo3* gene expression and APAP hepatotoxicity. Thus, the functional significance of *Fmo3* over-expression during APAP hepatotoxicity was evaluated. To date, there are no commercially available *Fmo3*-specific knockout mice because the expression of this enzyme in male mouse liver is switched off during development and male mice are essentially void of Fmo3 protein. In the absence of functional Fmo3 protein in normal male mice, there has been no need for developing a knockout model (Hernandez et al., 2009; Shephard & Phillips, 2010). As an alternative model to low Fmo3 function, inhibition of Fmo3 activity in female mice was achieved using the FMO inhibitor, methimazole. Methimazole (MMI), an antithyroid drug, is an FMO substrate and also a competitive inhibitor that has been used to block FMO-mediated conversion of various

compounds in animal models (Nace et al., 1997). Fmo3 and Fmo5 are among the most abundant FMO enzymes in female mouse liver and MMI is not a substrate for Fmo5 (Cherrington et al., 1998; Hines, 2006; Overby et al., 1995; Zhang et al., 2007). Thus, with MMI, among all FMO enzymes, Fmo3 was predominantly inhibited. Taking advantage of this observation, we could test the hypothesis that MMI inhibition of Fmo3 renders female mice susceptible to APAP-induced hepatotoxicity. In addition to the *in vivo* Fmo3 inhibitor study, we also developed an *in vitro* transgene over-expression system. We have established for the first time a stable cell line (Human hepatocyte HC-04) that over-expresses human FMO3 protein. Using this system, we could test the hypothesis that enhanced expression of FMO3 confers resistance against APAP-induced cytotoxicity.

FMO is involved in the oxygenation of sulphur-containing endogenous substrates, e.g., catalyzing the conversion of cysteamine (reduced form) to cystamine (disulfide form) (Poulsen, 1981). Although, the physiological role of cysteamine S-oxygenation by Fmo3 is not clear, in the 1970s Zieglar and Poulsen proposed that oxygenation of cysteamine may be a significant source of disulphide, maintaining the cellular thiol:disulphide potential in a cell (Ziegler et al., 1979). Upregulation of Fmo3 during APAP-induced hepatotoxicity and oxygenation of cysteamine by Fmo3 may serve to help control the overall thiol:disulphide redox state of the cell, which in turn may modulate cellular metabolism and/or activate signal transduction pathways leading to altered susceptibility to APAP (or protection). To reiterate, the

objective of the current investigation was to characterize the gene regulation and protein expression of liver Fmo3 during APAP-induced hepatotoxicity. The functional consequences of Fmo3 induction were also investigated. To our knowledge, this is the first report describing a novel protective function for this drug-metabolizing enzyme.

2.3 Materials and Methods

Chemicals

Acetaminophen, propylene glycol, methimazole and reduced GSH were purchased from Sigma-Aldrich (St Louis, MO). All other reagents were of reagent grade or better.

Animals

Male and female C57BL/6J mice, 9-10 week old, were obtained from Jackson Laboratories (Bar Harbot, ME). Upon arrival, mice were acclimated for one week prior to experimentation. Mice were housed in a 12 h dark/light cycle in a temperature and humidity controlled environment. Mice were fed laboratory rodent diet (Harlan Teklad 2018, Madison, WI) *ad libitum*.

Dosing regimen 1. Following an overnight fast, male mice (n=6) were treated with APAP (400 mg/kg, ip) in 50 % propylene glycol (PG) or vehicle. Animals were sacrificed 24, 48 and 72 h after APAP treatment. Plasma and liver were collected for measuring alanine amino transferase (ALT) activity, Fmo3 mRNA and protein levels and enzyme activity.

Dosing regimen 2. Following an overnight fasting male mice (n=6) were treated with APAP (400 mg/kg, ip) in 50 % PG or vehicle. Animals were treated with APAP (600 mg/kg, ip) in 50 % PG or vehicle, 48 h after the first treatment. Animals were sacrificed and plasma and liver were collected after 24 h for analysis.

Dosing regimen 3. Following an overnight fast, female mice (n=6) were administered a single dose of methimazole (MMI) (50 mg/kg, ip) in saline. Animals were sacrificed and plasma and livers were collected at 0.5, 4, 12 and 24 h for analysis of hepatotoxicity and GSH content. A single group of mice received a first dose of MMI (50 mg/kg, ip) and 12 h after the first dose, mice were treated with a second dose of MMI (50 mg/kg, ip). Plasma and liver were collected 12 h later for analysis.

Dosing regimen 4. Following an overnight fasting female or male mice (n=6) were administered vehicle (saline) or MMI (50 mg/kg, ip). Animals were treated with APAP (400 mg/kg, ip), 30 min later. The group receiving two doses of MMI along with APAP received the first dose of MMI 30 min prior to APAP treatment and the second dose of MMI at 12 h after the first dose. Mice in the group receiving only the second MMI dose were treated with MMI 11.5 h after APAP treatment. At 24 h after APAP treatment, animals were sacrificed and plasma and liver were collected for measuring ALT activity and GSH levels in this group of mice.

All animal studies were performed in accordance with National Institute of Health standards and the *Guide for the Care and Use of Laboratory*

Animals. This work was approved by the University of Connecticut's Institutional Animal Care and Use Committee.

Alanine Aminotransferase (ALT) Assay

Plasma ALT activity was determined as a biomarker of hepatocellular injury. Infinity ALT Liquid Stable Reagent (Thermo Fisher Scientific Inc., Waltham, MA) was used to determine ALT activity. Samples were analyzed using a Bio-Tek Power Wave X Spectrophotometer.

RNA Isolation and Quantitative Real-Time Polymerase Chain Reaction (qRT-PCR)

TRIzol reagent (Life Technologies, Carlsbad, CA) was used to extract total mouse liver RNA. cDNA was then made using an M-MLV RT kit (Invitrogen, Carlsbad, CA). Fmo3 mRNA expression was quantified by the ΔΔCT method and normalized to two housekeeping genes, β-actin and ribosomal protein S18. Data presented in this manuscript were normalized to β-actin. Primer pairs were synthesized by Integrated DNA Technologies (Coralville, IA) and are as follow: Fmo3 forward: 5′-GGA AGA GTT GGT GAA GAC CG-3′, reverse: 5′-CCC ACA TGC TTT GAG AGG AG-3′. Amplification was performed using an Applied Biosystems 7500 Fast Real-Time PCR System. Amplification was carried out in a 20 μL reaction volume containing 8 μL diluted cDNA, Fast SYBR Green PCR Master Mix (Applied Biosystems, Foster City, CA) and 1 μM of each primer.

Preparation of Crude Membrane and Microsomal Fractions

Microsomes were isolated from livers as described previously (Cashman & Hanzlik, 1981). Briefly, livers were homogenized in cold homogenization buffer (0.1 M potassium phosphate, 0.1 mM dithiothreitol (DTT), 2 % sucrose, pH 9.0) and homogenates were centrifuged at 10,000 x g for 20 min at 4°C. The supernatant was then centrifuged at 100,000 x g for 60 minutes. The resulting pellet was washed and resuspended in 0.1 M potassium phosphate buffer (pH 9.0) containing 1 mM EDTA and stored at -80°C. Protease inhibitor was added to all buffers before use. Protein concentration was determined by the method of Lowry using Bio-Rad protein assay reagents (Bio-Rad Laboratories, Hercules, CA).

Western Blot Analysis

For western blot analysis of Fmo3, microsomal proteins (10 μg) were electrophoretically resolved using 10 % polyacrylamide gels and transferred onto PVDF-Plus membrane (Micron Separations, Westboro, MA). A custom-made rabbit anti-mouse Fmo3 primary antibody (GenScript USA Inc., NJ) was used to detect Fmo3 with β-Actin as a loading control. Extensive characterization of the reactivity and/or specificity of this antibody was carried out. The antibody developed was specific for mouse Fmo3 protein. Blots were then incubated with HRP conjugated secondary antibodies against rabbit IgG. Protein-antibody complexes were detected using a

chemiluminescent kit (Thermo Scientific, IL) followed by exposure to X-ray film.

Enzyme Assay

Methimazole (MMI) metabolism was determined spectrophotometrically by measuring the rate of MMI S-oxygenation via the reaction of the oxidized product with nitro-5-thiobenzoate (TNB) to generate 5,5'-dithiobis(2-nitrobenzoate) (DTNB). The incubation mixture consisted of 50 mM sodium phosphate buffer (pH 9.0), 0.5 mM NADP+, 0.5 mM glucose-6-phosphate, 1.5 IU/mL glucose-6-phosphate dehydrogenase, 0.06 mM DTNB, 0.04 mM DTT and 100 to 150 μg/mL liver microsomes isolated from mice. Reactions were initiated by the addition of different amounts of MMI (substrate) and range of MMI concentrations used were between 1.25 and 800 μM. Incubations were done in duplicates. The disappearance of the yellow color was measured spectrophotometrically at 412 nM and specific activity (μM/min/mg) was determined using the molar extinction coefficient of NADPH (28.2 $mM^{-1}cm^{-1}$).

Immunohistochemistry

Immunohistochemical detection of Fmo3 protein was performed on 5 μm liver sections from tissues fixed in 10 % neutral-buffered zinc formalin followed by routine processing, paraffin embedding, sectioning and rehydration. Antigen retrieval was performed via microwave (950 watt) method in 10 mM sodium citrate buffer for 2 minutes at 100 % power and at

30 % power for another 8 minutes. Endogenous peroxidase activity was blocked with a 10 min incubation in 3 % H_2O_2, and avidin/biotin blocking was performed using a commercially available kit from Vector Laboratories (Burlingame, CA). Sections were incubated overnight with the previously mentioned anti-mouse Fmo3 primary antibody at a dilution of 1:8000 followed by Vector Laboratory's biotinylated goat anti-rabbit secondary antibody for 30 min. Protein-antibody complexes were detected with the Vector Elite ABC reagent and developed using a Vector ®Nova RED substrate kit for peroxidase. Slides were counterstained with hematoxylin, and mounted in "Protocol" mounting media (Fisher Scientific, IL).

GSH Assay

Total hepatic GSH concentrations were determined by the recycling method as previously described (Rahman et al., 2006). Briefly, 15-25 mg of liver tissue was added to 500 μL of 5 mM EDTA disodium salt in 0.1 M potassium phosphate buffer containing protease inhibitors. Tissues were kept on ice and homogenized by hand in a dounce homogenizer for 5-6 strokes. Equal volumes of 0.67 mg/mL 5,5´ -dithio-bis(2-nitrobenzoic acid) (DTNB) and 3.33 units/mL glutathione reductase (Sigma Aldrich, St. Louis, MO) in 0.1 M potassium phosphate buffer containing 5 mM EDTA disodium salt were mixed and 120 μL was added to 20 μL of each liver homogenate in a 96 well plate. Sixty μL of 0.67 mg/mL β-NADPH (Sigma) in 0.1 M potassium phosphate buffer containing 5 mM EDTA disodium salt was then added to each well. Absorbance was read immediately at 412 nm, taking

measurements every 30 seconds for 2 minutes. The assay was performed in duplicate for each sample and compared to a standard curve made from two fold serial dilutions (211.2 nmol/mL to 1.65 nmol/mL) of a GSH standard (Sigma).

Histopathology

Liver samples were fixed in 10 % neutral-buffered zinc formalin prior to processing and paraffin embedding. Liver sections (5 μm) were stained with hematoxylin and eosin. Sections were examined by light microscopy for the presence and severity of necrosis and degeneration using an established grading system (Manautou et al., 1994).

Lentiviral Vector Construction

The *FMO3*-T2A-luc lentiviral transfer vector was constructed by modifying the FUdeltaGW-rtTA (obtained from K. Hochedlinger via Addgene, Cambridge, MA, plasmid 19780) to replace the rtTA insert with a polylinker designed to accommodate the human *FMO3* ORF (Clone ID: 5175615 from Open Biosystems, Waltham, MA). To allow for bicistronic expression of FMO3 and luciferase, sequence encoding the T2A peptide (Szymczak et al., 2004) was inserted into the polylinker. The luciferase ORF from pGL4.10 vector (Promega, Madison, WI) was cloned in frame with FMO3 and the T2A sequence. Luciferase activity was used to normalize levels of FMO3 over-expression.

Cell Culture and Transduction

The replication-defective virus was generated in HEK 293T cells and concentrated as previously described (Maherali et al., 2008). HC-04 cells were seeded 24 h prior to transduction in complete DMEM medium and then infected with a series of volumes of untitered concentrate (100 μL, 50 μL, and 25 μL per well of a 6 well culture dish) overnight. Prior to, during, and after the viral transduction, the cells were maintained in complete DMEM containing 0.05 mM riboflavin. Media was changed daily to prevent riboflavin degradation.

Cell Culture and Treatment

HC-04 cells over-expressing human FMO3 (hFMO3-HC-04) and empty vector (EV-HC-04) were maintained in DMEM supplemented with 10 mM glucose, 10 % FBS, 0.05 mM riboflavin and 1 % antibiotic-antimycotic (100 units/mL penicillin G sodium, 100 μg/mL streptomycin sulfate, and 0.25 μg/mL amphotericin B) in a 5 % CO_2 and humidified environment (95 % relative humidity) at 37°C. For APAP treatments, cells were seeded at 200,000 cells per well in a 24-well plate. The following day, culture media was replaced with media containing APAP (1 mM to 15 mM). Twenty-four hours later, cytotoxicity was measured by the LDH assay. For MMI treatments, cells were seeded at 200,000 cells per well in a 24-well plate. The next day, cells were incubated in media containing 1 mM MMI for 30 min at 37°C. Thirty minutes following incubation with MMI, culture media containing 15 mM APAP was

added to wells. Cytotoxicity was measured using the LDH assay kit 24 h later.

LDH Leakage

As a measure of cytotoxicity following APAP treatment, percent lactate dehydrogenase (LDH) leakage in all *in vitro* experiments was determined via the Tox-7 kit. The assay was performed according to manufacturer's instructions (Sigma-Aldrich, St. Louis, MO).

Statistical Analysis

Results are expressed as means ± standard error (SE). Data were analyzed using the Student's *t-test* or ANOVA followed by a post-hoc test. While Student's *t-test* was used to compare means of two different treatment groups, ANOVA was used to compare the means of more than two means of different treatment groups that are normally distributed with a common variance. Differences were considered significant at $p<0.05$.

2.4 Results

Time Course of Plasma ALT Activity and Fmo3 mRNA Levels After APAP Treatment

Administration of 400 mg/kg APAP to male C57Bl/6J mice resulted in elevation of plasma ALT levels (Figure 2.1A). Plasma ALT activity increased to 191±18 and 219±47 IU/L at 24 and 48 h, respectively, following APAP treatment (mean plasma ALT activity in control mice was 25±5 IU/L). By 72 h,

plasma ALT activity is not statistically different from propylene glycol vehicle controls indicating recovery from APAP-induced liver injury. Fmo3 mRNA levels were quantified by qRT-PCR. The results in Figure 2.1B show that Fmo3 mRNA levels increased by 5±2.6-and 23±5.6-fold, at 24 and 48 h respectively, compared to the 0 h control group.

Time Course of Fmo3 Protein Expression After APAP Treatment

To examine the temporal changes in *Fmo3* gene expression and function following APAP treatment, Fmo3 protein levels were quantified by western blotting and by measuring catalytic activity using MMI as substrate. Representative blots and associated densitometric analysis are shown in Figure 2.2A and 2.2B, respectively. Although the expression of Fmo3 protein tended to increase by 1.1±0.3- to 1.6±0.2-fold between 24 and 72 h after APAP, these increases are statistically significant only at 72 h. An alternative method to quantitate Fmo3 protein induction is by measuring FMO catalytic activity using MMI (Zhang et al., 2007). With APAP treatment, FMO specific activity increased over time and this increase is statistically significant at 72 h only (24±1.5 μM/min/mg)(Fig. 2.2C). Figure 2.2D shows immunohistochemical analysis of Fmo3 protein localization. Cellular localization of Fmo3 protein and degree of protein expression did not change at 24 or 48 h, but marginally increased at 72 h after treatment with a single dose APAP (400 mg/kg). Unlike Fmo3 mRNA levels that peaked at 48 h, maximum Fmo3 protein expression is observed at 72 h following APAP treatment. These data demonstrate that a single dose APAP (400 mg/kg)

treatment results in a marginal, yet significant increase in Fmo3 protein levels and activity at 72 h, the longest time-point tested.

Plasma ALT Activity and Fmo3 mRNA Expression in the Mouse Model of APAP Autoprotection

Previous studies conducted in our laboratory demonstrated the phenomenon of APAP autoprotection in mice, where mice receiving an initial mild toxic dose of APAP are protected against hepatotoxicity from higher doses (Aleksunes et al., 2008). To investigate *Fmo3* gene expression in the mouse model of APAP autoprotection, male C57BL/6J mice were pretreated with either propylene glycol vehicle or 400 mg/kg APAP. Forty-eight hours following pretreatment, mice were challenged with vehicle or a higher dose of APAP (600 mg/kg). Plasma ALT activity and Fmo3 mRNA levels were measured 24 h after the challenge dose (Fig. 2.3A and 2.3B respectively). Plasma ALT levels in mice receiving vehicle pretreatment and APAP challenge (600 mg/kg; VA) increased significantly to 1600±413 IU/L compared to vehicle controls (VV). Likewise, ALT levels in mice pretreated and challenged with APAP (AA; autoprotected group) increased significantly to 230±69 IU/L compared to VV controls. However, the values are significantly lower than in the VA group. Consistent with the single dose APAP (400 mg/kg) study, APAP pretreated, vehicle challenged mice (AV) have marginal increases in ALT values in comparison to VV controls. The results in Figure 2.3B show Fmo3 mRNA levels in the mouse model of APAP autoprotection. Fmo3 mRNA transcript levels in the AV and AA groups

increased significantly by 39±5- and 70±11-fold, respectively, with APAP autoprotected mice showing the greatest (70-fold) induction.

Fmo3 Protein Expression in the Mouse Model of APAP Autoprotection

Fmo3 protein expression is not normally detectable in adult male mice livers because the expression of this enzyme is silenced during development (Cherrington et al., 1998; Falls et al., 1997; Shephard & Phillips, 2010). To determine if Fmo3 protein expression correlates with the mRNA expression seen in APAP autoprotected male mouse livers, western blot analysis was performed as described in *Materials and Methods*. Representative blots are shown in Figure 2.4A and densitometric analysis of blots are shown in Figure 2.4B. As expected, no detectable hepatic Fmo3 protein is present in VV control livers. Following treatment with APAP (dosing regimen 2) Fmo3 protein levels increased in both AV (p value 0.0743) and AA group (p value 0.041). However, the elevation is statistically significant only in APAP autoprotected group (15±2-fold change). In agreement with protein expression data, the MMI assay used to measure enzyme specific activity shows an increase in activity to 16±2 and 42 ±5μM/min/mg in AV and AA groups of mice, respectively, compared to vehicle controls (3±1μM/min/mg)(Fig. 2.4C). Figure 2.5 shows immunohistochemical analysis of Fmo3 protein localization. Protein staining is localized to centrilobular regions in both pretreated and autoprotected livers instead of its conventional periportal localization seen in non-treated female livers. This distinct zonal localization by APAP coincides with the area where damage and/or

hepatocellular compensatory repair/proliferation occurs (Figure E/F and G/H, respectively).

Effect of Methimazole Treatment on Liver in Mice

Methimazole is a drug used in the treatment of hyperthyroidism and is a high affinity substrate and effective competitive inhibitor of the Fmo-mediated oxidation of various compounds (Nace et al., 1997). Later studies described in this manuscript use MMI (50 mg/kg) to inhibit FMO activity in female as well as male mice. MMI at higher doses can by itself deplete hepatic GSH levels or cause hepatotoxicity in GSH-depleted mice (Mizutani et al., 1999; Mizutani et al., 2000). To determine whether administration of MMI by itself at doses used in our study results in hepatotoxicity, female mice were administered either one or two doses of 50 mg/kg MMI. Animals were sacrificed and plasma and livers were collected over a timecourse of 12 h for liver toxicity analysis (dosing regimen 3). Plasma ALT activity increased to 39±4 IU/L at 12 h following a single dose MMI treatment compared to vehicle controls (15±3 IU/L)(Fig. 2.6A). Even though the ALT activity increased significantly at 12 h, these levels are below the normal physiological range for hepatotoxicity (40-43 IU/L, as per the “Physiological Data Summary” provided by The Jackson Laboratory for female C57BL/6J mice). Hepatic GSH levels are shown in Figure 2.6B. GSH levels in livers from MMI treated mice are not different from that in their vehicle treated controls. In support of ALT activity data, histopathological analysis of H&E stained liver sections from MMI treated mice do not show any signs of liver injury (Fig. 2.6C). Collectively

these data suggest that MMI at two doses of 50 mg/kg does not result in hepatotoxicity nor does it deplete hepatic GSH levels, one of the key detoxification mechanisms involved during APAP exposure.

Immunohistochemical Analysis of Liver Fmo3 Protein Expression and Localization in Naïve C57BL/6J Male and Female Livers

Female mice express about eighty times higher Fmo3 mRNA levels compared to males (Janmohamed et al., 2004). To examine whether the differences in mRNA levels translate to protein levels, an immunohistochemical analysis for Fmo3 protein expression was performed in naïve livers from male and female mice using our custom-made Fmo3 primary antibody. Consistent with the literature, Fmo3 protein expression and its cellular localization is not detectable in male liver under basal conditions. Strikingly, female livers express higher Fmo3 protein levels compared to male mice. This Fmo3 expression is restricted to hepatocytes surrounding portal veins (Figure 2.7).

Effect of Methimazole Treatment on APAP-induced Liver Injury in Female and Male C57BL/6J Mice

As shown in Figure 2.7, female mice express higher Fmo3 protein levels compared to their male counterparts. It has also been demonstrated that female mice are much more resistant to APAP hepatotoxicity compared to male mice (Dai et al., 2006). If Fmo3 plays a role in conferring tolerance to APAP-induced hepatotoxicity in female mice, methimazole (FMO inhibitor)

treatment should render female mice susceptible to APAP hepatotoxicity. To investigate the effect of MMI treatment on APAP-induced hepatotoxicity in female mice, groups of mice received APAP along with either one or two doses of MMI (dosing regimen 4). Plasma ALT activity in female mice did not change compared to vehicle controls following APAP (400 mg/kg) treatment (Fig. 2.8A)(mean plasma ALT activity in control mice: 27±2 IU/L). APAP treatment along with the first and second dose of MMI (1&2MMI/APAP), significantly increased plasma ALT levels to 3343±802 IU/L. APAP treatment with only the first dose (1MMI/APAP) of MMI also increased plasma ALT values to 473±93 IU/L. Hepatic GSH levels also are shown in Figure 2.8B. Liver GSH content measured at 24 h in mice receiving APAP alone show a rebound increase to 72±3 nmol/mg protein compared to vehicle controls (48±4 nmol/mg protein). On the other hand, all three groups of mice receiving APAP and MMI co-treatment show significantly lower GSH levels (1&2MMI/APAP: 19±7, 1MMI/APAP: 30±3 and APAP/2MMI: 37±2 nmol/mg protein) compared to the group receiving APAP alone. This change correlates well with higher plasma ALT activity in these three groups. The severity of hepatocellular necrosis by APAP along with MMI was analyzed and graded using a scale ranging from 0 to 5. Liver samples with grades greater than 2 are considered to have significant injury (Manautou et al., 1994). Results of histopathological analysis are presented in Figure 2.8C and Table 2.1. Examination of liver sections from the control group revealed normal histology. Consistent with the plasma ALT activity, APAP (400 mg/kg)

treatment resulted in a minimal amount of hepatocellular injury in female mice. Even though the severity of APAP-related injury increased with MMI, there is greater injury with two doses of MMI.

Fmo5 and Fmo3 are abundant FMO enzymes in female adult mouse liver (Cherrington et al., 1998; Hines, 2006; Janmohamed et al., 2004). While Fmo3 is abundant in female mice, male mice are void of Fmo3 (Cherrington et al., 1998; Hines, 2006; Janmohamed et al., 2004). With the exception of FMO5, MMI is a substrate for all FMO enzymes (Overby et al., 1995; Zhang et al., 2007). Thus, with MMI we presume female hepatic Fmo3 is predominantly inhibited. If the susceptibility of female mice to APAP-induced hepatotoxicity is due to MMI inhibition of Fmo3 (demonstrated in Fig. 2.8A and 2.8B), then we anticipate seeing no alteration in the susceptibility of male mice to APAP hepatotoxicity with MMI administration. To investigate the effect of MMI treatment on APAP-induced hepatotoxicity in male mice, groups of mice received APAP along with either one or two doses of MMI (dosing regimen 4). Administration of APAP (400 mg/kg) in saline to male mice resulted in elevation of plasma ALT levels to 1794±222 IU/L compared to vehicle controls (45±12 IU/L) (Fig. 2.8D). APAP co-administration with MMI did not significantly change plasma ALT activity compared to APAP treated male mice (1&2MMI/APAP: 1984±592, 1MMI/APAP: 2333±126 and APAP/2MMI: 1530±328 IU/L). Hepatic GSH levels are presented in Figure 2.8E. Consistent with plasma ALT levels, hepatic GSH content following APAP (400 mg/kg) treatment decreased significantly to 16±2 nmol/mg protein

compared to vehicle controls (61±2 nmol/mg protein). Further, GSH levels did not change significantly in all groups of mice that received APAP along with one or two doses of MMI compared to the APAP only group (1&2MMI/APAP: 13±2, 1MMI/APAP: 11±2 and APAP/2MMI: 17±1 nmol/mg protein). These data demonstrate that the susceptibility of female mice to APAP-induced hepatotoxicity from MMI treatment is due to inhibition of hepatic Fmo3.

Establishment of Human Hepatocyte Cell Line (HC-04) Over-expressing Human FMO3 (hFMO3-HC-04)

To further evaluate the functional significance of FMO3 over-expression during APAP hepatotoxicity, we developed a human hepatocyte cell line (HC-04) that over-expresses human FMO3. Unlike HepG2 cells, HC-04 cells express CYPs that bioactivate APAP to its toxic metabolite NAPQI and also are susceptible to APAP-induced cellular toxicity (Lim et al., 2007). Thus, this cell line is a good model for studying the protective effects of FMO3 gene expression during APAP-induced cytotoxicity. FMO3 was incorporated into a bicistronic vector driven by the ubiquitin-C promoter, which allowed co-expression of *FMO3* and luciferase (LUC) genes in transduced HC-04 cells. We identified five clones that over-expressed human FMO3, of which three were maintained as cell lines. Results from luciferase activity assays used to measure the efficiency of transduction are presented in Figure 2.9A. The clones expressed a 33±1-, 89±2- and 455±8-fold change in luciferase activity as compared to the empty vector control (EV-HC-04). For convenience, these clones are named Low- Mid-, and High-FMO3 expressing cell lines,

respectively. FMO3 protein expression was confirmed by performing western blotting using microsomal fractions isolated from EV expressing HC-04 cells and all three FMO3-over-expressing HC-04 clones. Representative blots and densitometric analysis are shown in Figure 2.9B. Following transduction, Fmo3 protein levels increased by 5±0.1-, 10±0.3- and 33±0.5-fold in Low-, Mid- and High-FMO3 expressing HC-04 cells, respectively. The specific activity of over-expressed FMO3 protein increased to 75±1.2, 80±0.7 and 80±0.6 μM/min/mg in Low-, Mid- and High-FMO3 expressing HC-04 cells respectively compared to EV-HC-04 controls (5 μM/min/mg) (Fig. 2.9C).

Effect of APAP Treatment in HC-04 Cells Over-expressing Human FMO3 (hFMO3-HC-04)

Cell culture and treatment is described in detail in the *Materials and Methods*. Results are shown in Figure 2.10. The percent LDH leakage into the media in Low-FMO3 expressing hFMO3-HC-04 cells in response to 1, 5, 10 and 15 mM APAP treatment is significantly lower (7, 10, 17and 24 %) compared to empty vector controls (8, 13, 23 and 31 %), respectively. The amount of LDH leakage does not change in Mid-FMO3 expressing cells and is significantly greater (9, 14, 28 and 42 %) in High-FMO3 expressing cells following 1, 5, 10 and 15 mM APAP treatment. Taken together, these data suggest that over-expression of FMO3 protects against APAP-induced cytotoxicity only in Low-FMO3 expressing cells. By contrast, APAP cytotoxicity is aggravated in the High-FMO3 expressing clone.

Effect of MMI Pretreatment During APAP-induced Cytotoxicity in HC-04 Cells Over-expressing Human FMO3 (hFMO3-HC-04)

The amount of LDH leakage (%) into the media does not change with MMI treatment (Fig. 2.11A). In response to 15 mM APAP treatment, the percent LDH leakage into the media in Low-FMO3 expressing cells decreased significantly to 25 % compared to EV controls (29 %)(Fig. 2.11B). Following pretreatment with 1 mM MMI, the susceptibility of Low-FMO3 expressing cells to APAP-induced cytotoxicity restored to 29 %. On the contrary, Mid- and High-FMO3 expressing cells did not exhibit any protection against APAP-induced cytotoxicity. These cell lines also show enhanced cytotoxicity during MMI pretreatment.

Figure 2.1

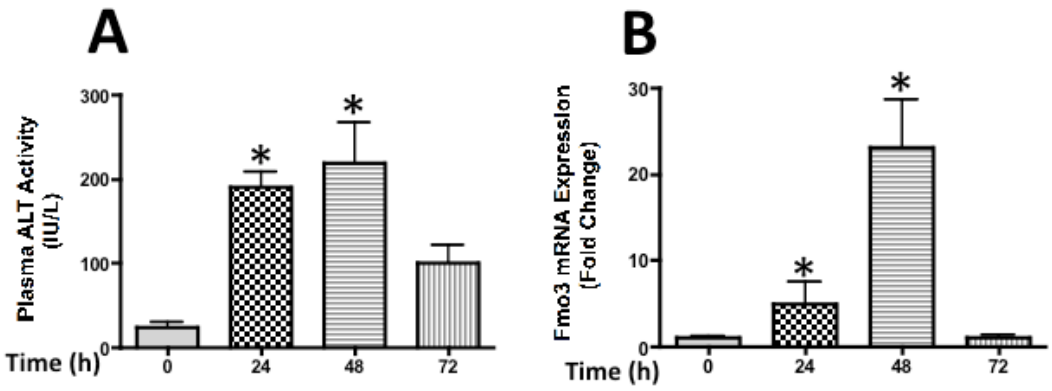
A
Plasma ALT Activity (IU/L)
300
200
100
0
*
*
Time (h)
0
24
48
72
B
Fmo3 mRNA Expression (Fold Change)
30
20
10
0
*
*
Time (h)
0
24
48
72

Figure 2.1 *Plasma ALT activity and quantitative RT-PCR analysis of liver Fmo3 transcripts following a single dose APAP treatment.* Plasma and livers were collected from mice 24, 48 and 72 h following APAP (400 mg/kg) or vehicle treatments. **(A)** The data are presented as mean plasma ALT (IU/L) ± SE. **(B)** RNA was isolated from livers and further cDNA was made using a commercial MMLV-RT kit. The cDNA samples were analyzed by quantitative RT-PCR using Fmo3 mouse-specific primers. Gene expression was normalized to housekeeping gene β-Actin. Fmo3 mRNA expression are presented as mean Fold Change ± SE. One-way ANOVA was performed followed by the Dunnett's post-test. Asterisks (*) represent a statistical difference ($p < 0.05$) between 0 h vehicle and APAP-treated groups.

Figure 2.2

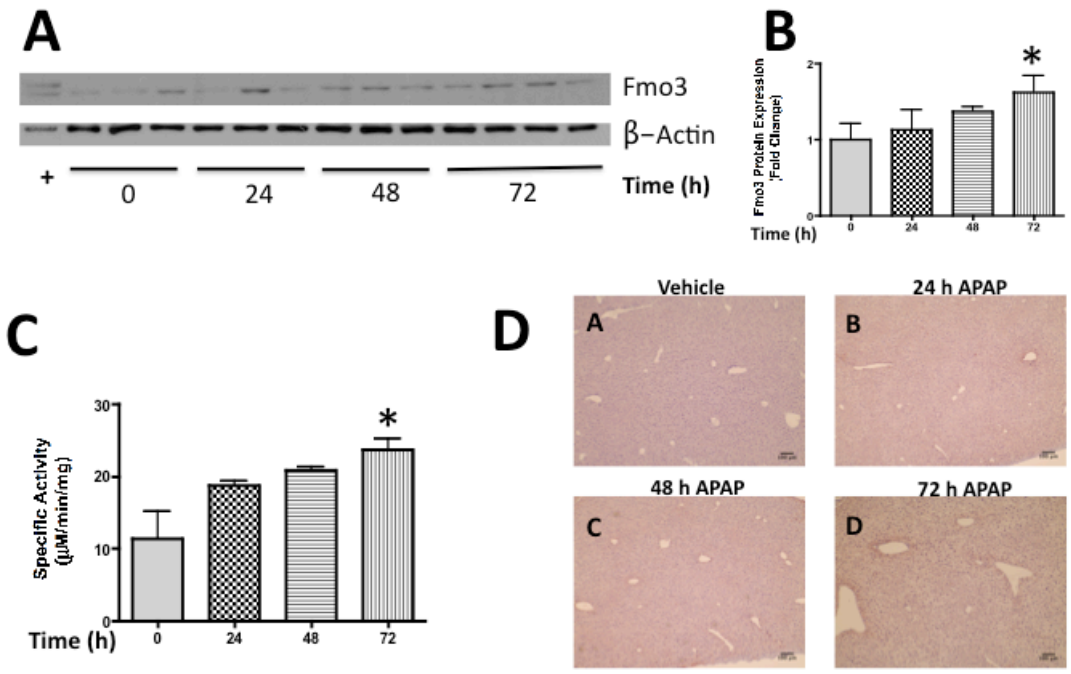
A
Fmo3
β−Actin
+
0
24
48
72
Time (h)
B
Fmo3 Protein Expression (Fold Change)
Time (h)
0
24
48
72
*
C
Specific Activity (μM/min/mg)
Time (h)
0
24
48
72
*
D
Vehicle
A
24 h APAP
B
48 h APAP
C
72 h APAP
D

Figure 2.2 *Analysis of liver Fmo3 protein expression following a single dose APAP treatment by western blotting, enzyme activity assay as well as by immunohistochemistry.* After overnight fasting, mice received a single dose of 400 mg/kg APAP or vehicle. Livers were collected at 24, 48 and 72 h following APAP or vehicle treatments. Western blots for Fmo3 were performed using liver microsomes from control and APAP-treated mice. A custom-made rabbit anti-mouse Fmo3 primary antibody, described in *Materials and Methods* section was used to detect Fmo3. Equal protein loading (10 µg protein/lane) was confirmed by detection of β-actin. Microsomal protein isolated from naïve female mouse liver was used as a positive control indicated by "**+"** sign. The data are presented as blots **(A)** and as mean Fmo3 protein expression (Fold Change) ± SE **(B)**. FMO activity was measured in liver microsomes from control and APAP-treated mice using methimazole as substrate as described under *Materials and Methods.* Data are presented as mean Specific Activity (µM/min/mg) ± SE **(C)**. Asterisks (*) represent a statistical difference ($p < 0.05$) between 0 h vehicle and APAP-treated groups. Immunohistochemical staining to detect Fmo3 was conducted on zinc formalin fixed, paraffin-embedded liver sections from control and APAP-treated mice. Immunochemical staining was performed with the same antibody used for Western blotting. Representative images are shown **(D)**. Scale bar: 100 µm. **(A)** Vehicle-treated 0 h; **(B)** APAP-treated 24 h; **(C)** APAP-treated 48 h; **(D)** APAP-treated 72 h.

Figure 2.3

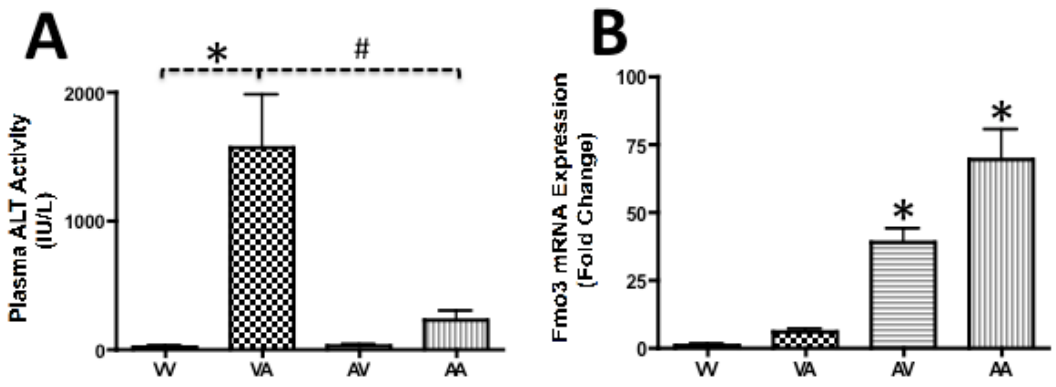
A
*
#
Plasma ALT Activity (IU/L)
2000
1000
0
W
VA
AV
AA
B
Fmo3 mRNA Expression (Fold Change)
100
75
50
25
0
*
*
W
VA
AV
AA

Figure 2.3 *Plasma ALT activity in the mouse model of APAP autoprotection*. Groups of mice were treated with vehicle or APAP 400 mg/kg. 48 h after pretreatment, mice were challenged with vehicle or APAP 600 mg/kg. Plasma and livers were collected 48 h following APAP challenge. (A) The data are presented as mean plasma ALT (IU/L) ± SE. One-way ANOVA was performed followed by the Dunnett's post-test. While asterisks (*) represent a statistical difference ($p < 0.05$) between VV group and VA groups, pound (#) represent a statistical difference ($p < 0.05$) between VA and AA groups. (B) RNA was extracted from livers and cDNA was prepared using a commercial MMLV-RT kit as described in *Materials and Methods*. The cDNA samples were analyzed for Fmo3 mRNA levels by quantitative RT-PCR using Fmo3 mouse-specific primers. Gene expression was normalized to housekeeping gene β-Actin. Fmo3 mRNA expression are presented as mean Fold Change ± SE. One-way ANOVA was performed followed by the Dunnett's post-test. Asterisks (*) represent a statistical difference ($p < 0.05$) from VV groups and pound (#) represent a statistical difference ($p<0.05$) between VA and AA groups.

Figure 2.4

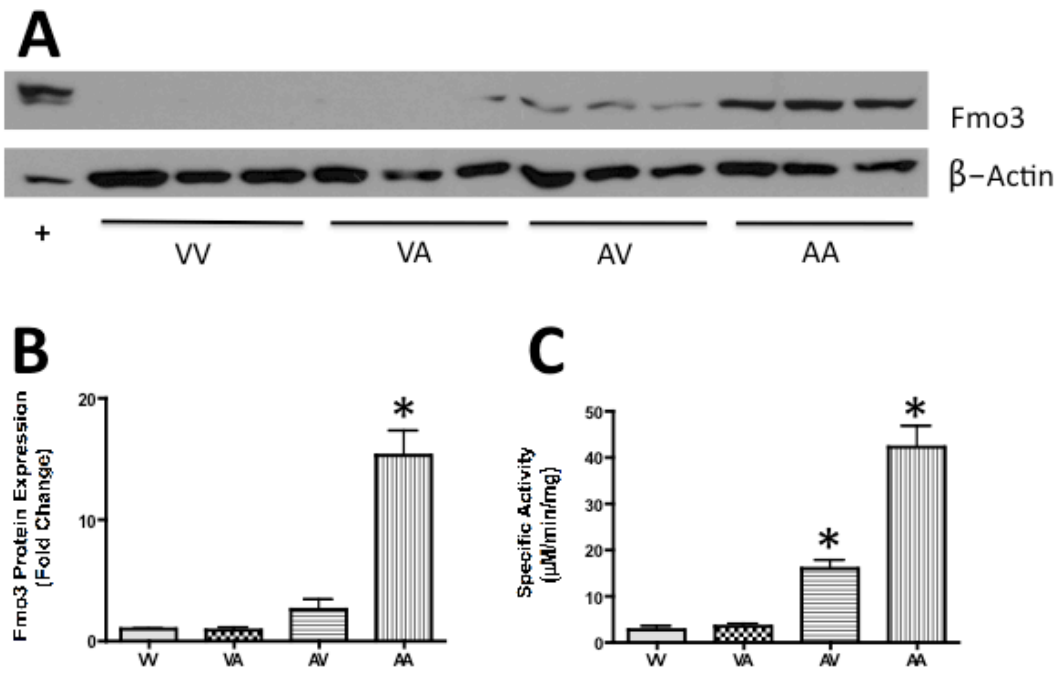
A
Fmo3
β−Actin
+
VV
VA
AV
AA
B
Fmo3 Protein Expression
(Fold Change)
20
10
0
*
VV
VA
AV
AA
C
Specific Activity
(μM/min/mg)
50
40
30
20
10
0
*
*
VV
VA
AV
AA

Figure 2.4 *Analysis of liver Fmo3 protein expression in the mouse model of APAP autoprotection by western blotting and enzyme activity assay.* Dosing regimen is described in detail in *Materials and Methods* section. Briefly, groups of mice were administered with vehicle or APAP (400 mg/kg) and 48 h later challenged with vehicle or APAP (600 mg/kg). Livers were collected 24 h following the last treatment. Western blots for Fmo3 was performed using liver microsomes from all groups of mice. A custom-made rabbit anti-mouse Fmo3 primary antibody, described before was used to detect Fmo3. Equal protein loading (10 µg protein/lane) was confirmed by detection of β-actin. Microsomal protein isolated from naïve female mouse liver was used as a positive control indicated by "**+"** sign. The data are presented as blots **(A)** and as mean Fmo3 protein expression (Fold Change) ± SE **(B)**. Liver microsomes isolated from all groups of mice were used to measure FMO activity using methimazole as substrate. Data are presented as mean Specific Activity (µM/min/mg) ± SE **(C)**. Asterisks (*) represent a statistical difference ($p < 0.05$) from VV groups.

Figure 2.5

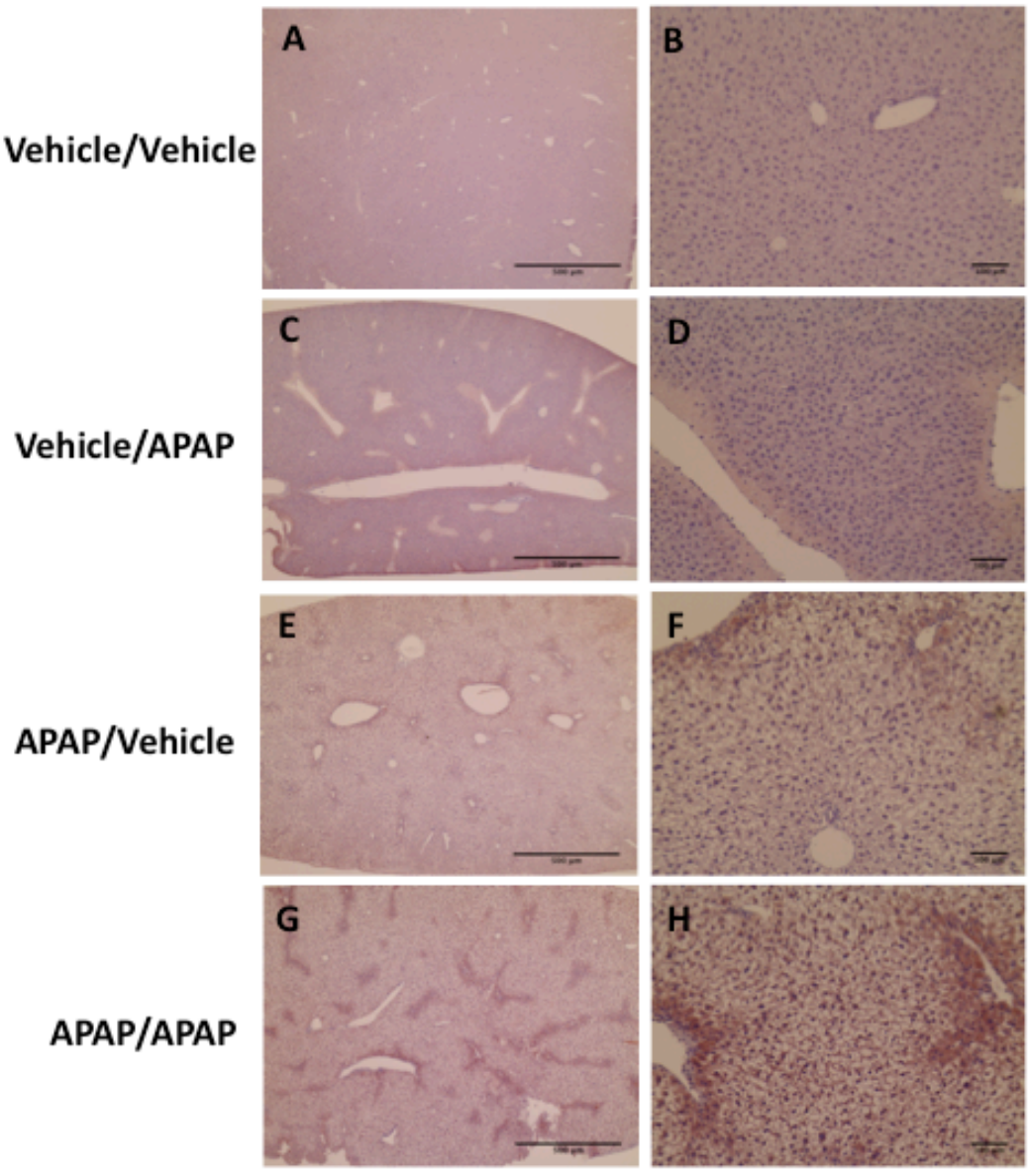
Vehicle/Vehicle
Vehicle/APAP
APAP/Vehicle
APAP/APAP
A
B
C
D
E
F
G
H

Figure 2.5 *Immunohistochemical analysis of liver Fmo3 protein expression and localization in the mouse model of APAP autoprotection.* Details of APAP autoprotection treatment regimen are described in *Materials and Methods*. Groups of mice were pretreated with vehicle or APAP (400 mg/kg) and challenged with vehicle or APAP (600 mg/kg) 48 h later. Twenty-four hours after the challenge dose livers were collected and fixed in zinc formalin and paraffin embedded. Immunochemical staining to detect Fmo3 was performed with the same antibody used for Western blotting. Representative images from all groups of mice are shown at two magnifications. Scale bar: 100 and 500 µm. (A/B) VV – Vehicle pretreated and vehicle challenge group; (C/D) VA – Vehicle pretreated and APAP (600 mg/kg) challenge group; (E/F) AV – APAP (400 mg/kg) pretreated and Vehicle challenge group; (G/H) AA – APAP (400 mg/kg) pretreated and APAP (600 mg/kg) challenge group liver sections.

Figure 2.6

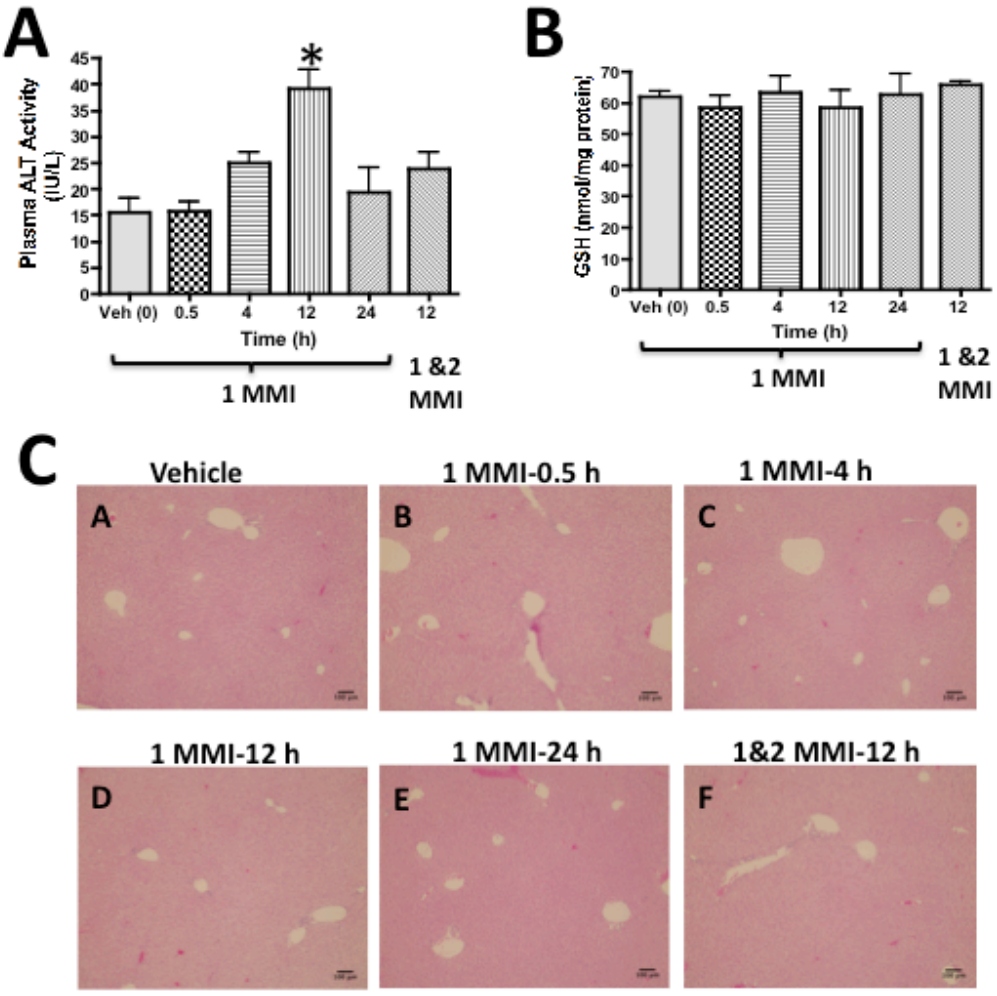
A
Plasma ALT Activity (IU/L)
45
40
35
30
25
20
15
10
5
0
*
Veh (0)
0.5
4
12
24
12
Time (h)
1 MMI
1 &2 MMI
B
GSH (nmol/mg protein)
70
60
50
40
30
20
10
0
Veh (0)
0.5
4
12
24
12
Time (h)
1 MMI
1 &2 MMI
C
Vehicle
A
1 MMI-0.5 h
B
1 MMI-4 h
C
1 MMI-12 h
D
1 MMI-24 h
E
1&2 MMI-12 h
F

Figure 2.6 *Plasma ALT activity, hepatic GSH levels and histopathology of liver sections after 50 mg/kg methimazole (MMI) treatment in female mice.* Dosing regimen is described in detail in *Materials and Methods* section. Briefly, groups of mice were administered a single dose of MMI (50 mg/kg) and plasma and livers were collected 0.5, 4, 12 and 24 h later. A single group of mice received both the first and the second dose of MMI and 12 h after the second dose, plasma and livers were collected for analysis. **(A)** The data are presented as mean plasma ALT (IU/L) ± SE. **(B)** GSH levels are expressed as GSH nmol/mg protein ± SE. One-way ANOVA was performed followed by the Dunnett's post-test. Asterisks (*) represent a statistical difference ($p < 0.05$) between vehicle and MMI-treated groups. **(C)** Histopathology of formalin-fixed, paraffin-embedded liver sections from MMI treated mice. Representative images are shown. Scale bar: 100 µm. (A) Control; (B) First dose MMI-treated 0.5 h; (C) First dose MMI-treated 4 h; (D) First dose MMI-treated 12 h; (E) First dose MMI-treated 24 h; (F) First and second dose MMI-treated 12 h.

Figure 2.7

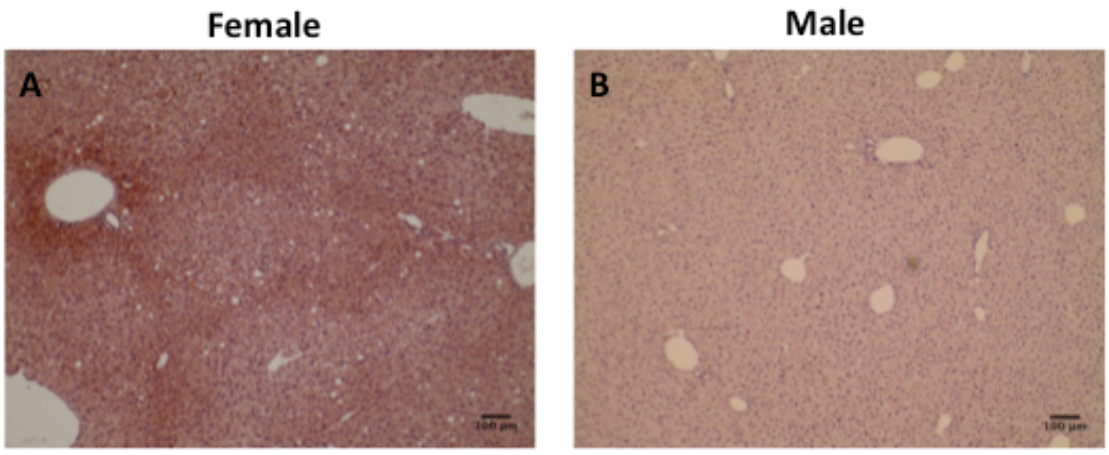

Figure 2.7 *Immunohistochemical analysis of Fmo3 in naïve female and male liver.* Livers from untreated female and male mice were collected and fixed in zinc formalin and paraffin embedded. Immunochemical staining of Fmo3 was performed on paraffin sections using the custom-antibody used before. Representative images are shown. Scale bar: 100 µm. (A) Female (B) Male liver specimens.

Figure 2.8

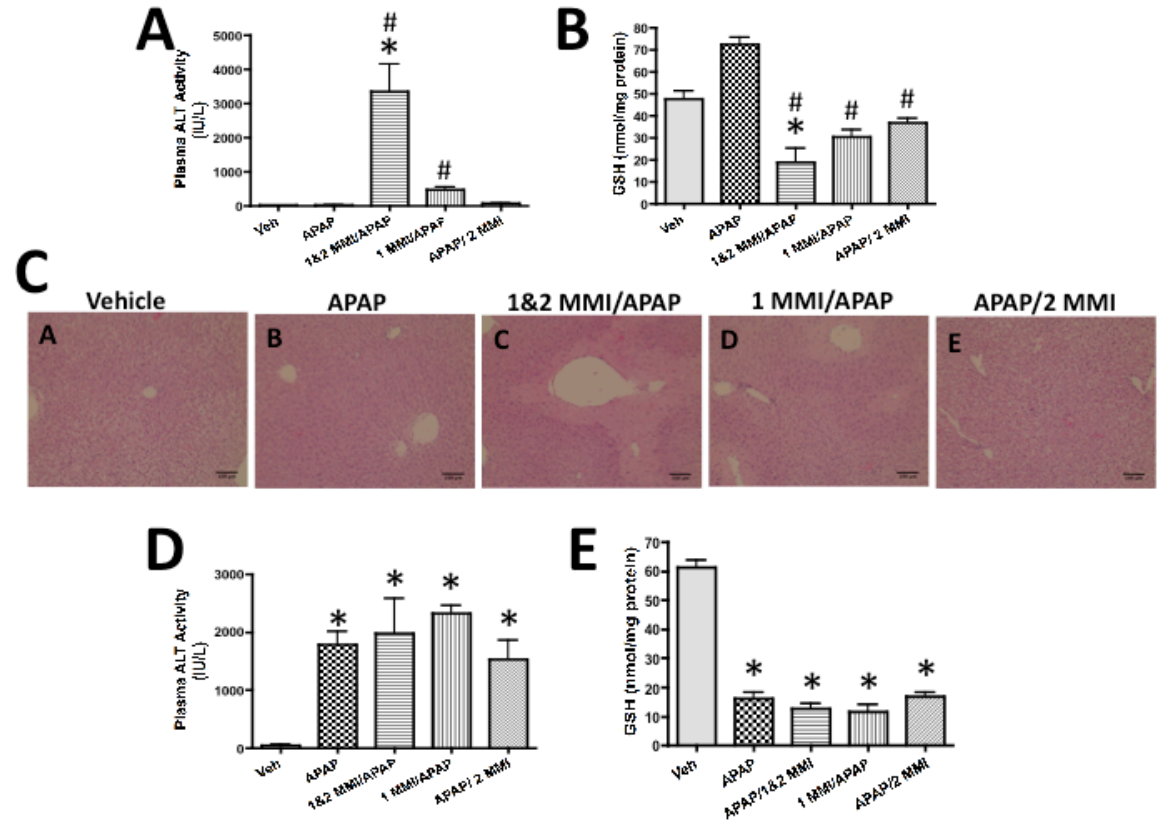
A
Plasma ALT Activity (IU/L)
5000
4000
3000
2000
1000
0
Veh
APAP
1&2 MMI/APAP
1 MMI/APAP
APAP/2 MMI
B
GSH (nmol/mg protein)
80
70
60
50
40
30
20
10
0
C
Vehicle
APAP
1&2 MMI/APAP
1 MMI/APAP
APAP/2 MMI
D
Plasma ALT Activity (IU/L)
3000
2000
1000
0
E
GSH (nmol/mg protein)
70
60
50
40
30
20
10
0
APAP/1&2 MMI

Figure 2.8 *Plasma ALT activity, hepatic GSH levels and histopathology of liver sections after MMI intervention in APAP treated mice.* Female or male mice were treated with vehicle or APAP (400 mg/kg) or APAP along with MMI (50 mg/kg). The first dose of MMI was administered 30 min prior to APAP treatment and the second dose 12 h after the first dose. 24 h after APAP treatment, plasma and livers were collected for analysis. **(A)** The data from female mice are presented as mean plasma ALT (IU/L) ± SE. **(B)** GSH levels in female mice livers are expressed as GSH nmol/mg protein ± SE. One-way ANOVA was performed followed by the Dunnett's post-test post-test. Asterisks (*) represent a statistical difference ($p < 0.05$) compared to vehicle treated group and pound (#) represent a statistical difference ($p<0.05$) from APAP treated group. **(C)** Histopathology of formalin-fixed, paraffin-embedded liver sections after MMI intervention in APAP treated female mice. Representative images are shown. Scale bar: 100 µm. (A) Vehicle – Vehicle treated group; (B) APAP – APAP (400 mg/kg) treated group; (C) 1&2 MMI/APAP – APAP (400 mg/kg) with both the first and second dose MMI (50 mg/kg) treated group; (D) 1 MMI/APAP – APAP (400 mg/kg) with the first dose MMI (50 mg/kg) treated group; (E) APAP/2MMI – APAP (400 mg/kg) with the second dose MMI (50 mg/kg) treated group. **(D)** The data from male mice are presented as mean plasma ALT (IU/L) ± SE. **(E)** GSH levels in male mice livers are expressed as GSH nmol/mg protein ± SE. One-way ANOVA was performed followed by the Dunnett's post-test. Asterisks (*) represent a statistical difference ($p < 0.05$) compared to vehicle treated group.

Figure 2.9

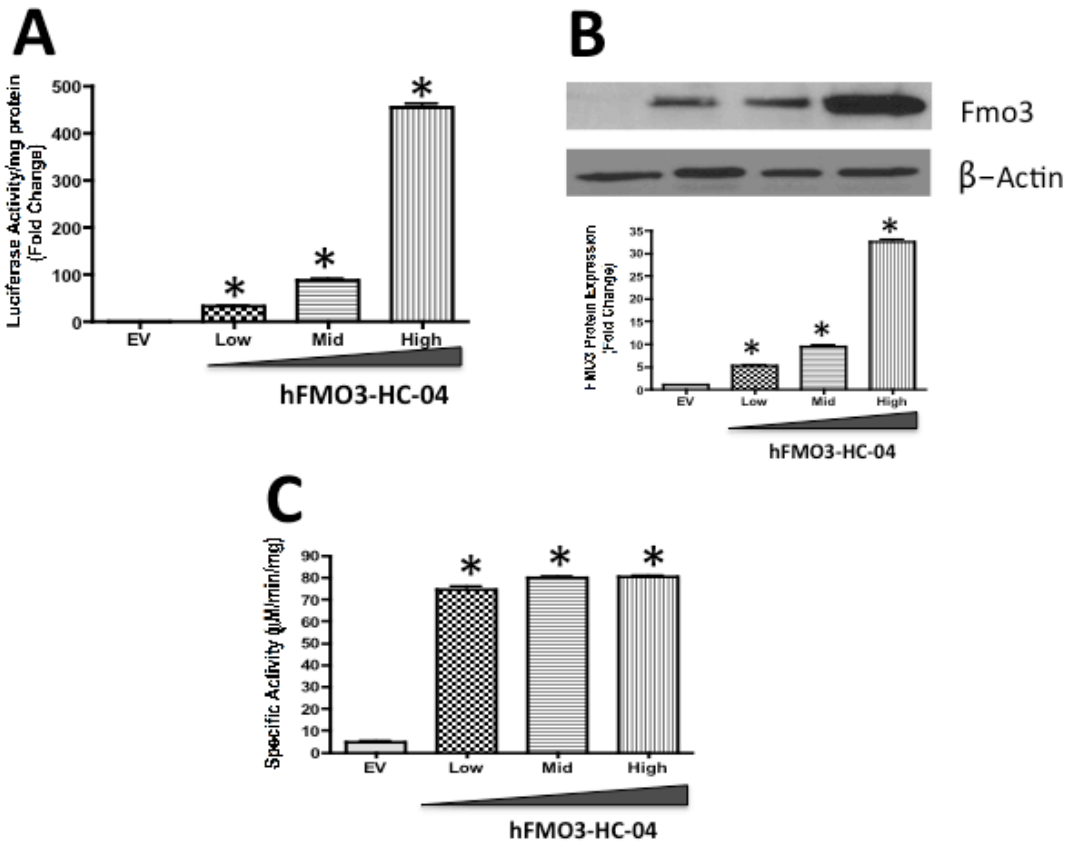
A
Luciferase Activity/mg protein (Fold Change)
500
400
300
200
100
0
EV
Low
Mid
High
hFMO3-HC-04
B
Fmo3
β−Actin
EV
Low
Mid
High
hFMO3-HC-04
C
90
80
70
60
50
40
30
20
10
0
EV
Low
Mid
High
hFMO3-HC-04

Figure 2.9 *Establishment of HC-04 cells over-expressing human FMO3 (hFMO3-HC-04).* Lentiviral vector construction and transduction are described in detail in *Materials and Methods* section. **(A)** Luciferase activity to measure the efficiency of transduction in hFMO3-HC-04 clones. The data are presented as mean luciferase activity/mg protein (Fold Change) ± SE. **(B)** Western blot for Fmo3 was performed using microsomal protein isolated from empty vector (EV), Low-, Mid- and High-FMO3 expressing cell lines. Rabbit anti-human FMO3 primary antibody was used to detect FMO3 protein expression. Equal protein loading (10 µg protein/lane) was confirmed by detection of β-actin. The data are presented as blots as well as mean FMO3 protein expression (Fold Change) ± SE. **(C)** Microsomes isolated from EV expressing HC-04 cells and all three FMO3-over-expressing HC-04 clones were used to measure FMO activity using methimazole as substrate. Data are presented as mean Specific Activity (µM/min/mg) ± SE Protein. One-way ANOVA was performed followed by the Dunnett's post-test. Asterisks (*) represent a statistical difference ($p < 0.05$) compared to EV controls.

Figure 2.10

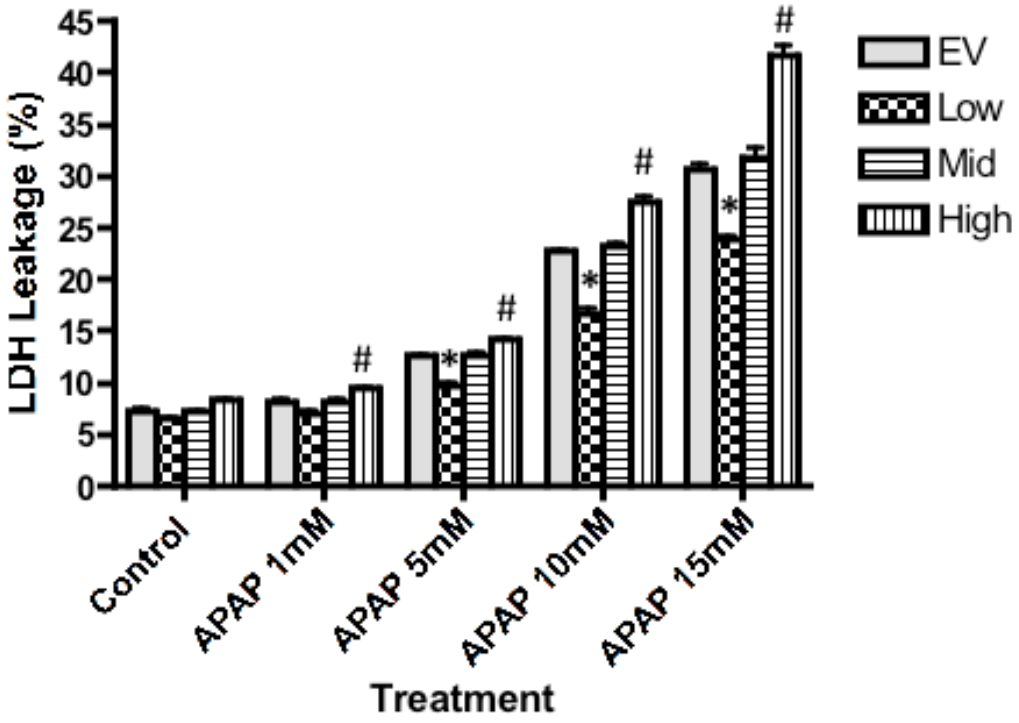
LDH Leakage (%)
45
40
35
30
25
20
15
10
5
0
Control
APAP 1mM
APAP 5mM
APAP 10mM
APAP 15mM
Treatment
EV
Low
Mid
High
#
*

Figure 2.10 *Effect of APAP treatment in HC-04 cells over-expressing human FMO3 (hFMO3-HC-04).* Empty vector, Low-, Mid- and High-FMO3 expressing cell lines were treated with a range of APAP concentrations from 1 mM to 15 mM. 24 h later, percent LDH leakage into the medium was measured using a commercial kit. The data are presented as mean LDH leakage (%) ± SE. Two-way ANOVA was performed followed by the Bonferroni's post-test. Asterisks (*) represent a significant decrease ($p < 0.05$) compared to EV controls and pound (#) represent a significant increase ($p<0.05$) compared to EV controls.

Figure 2.11

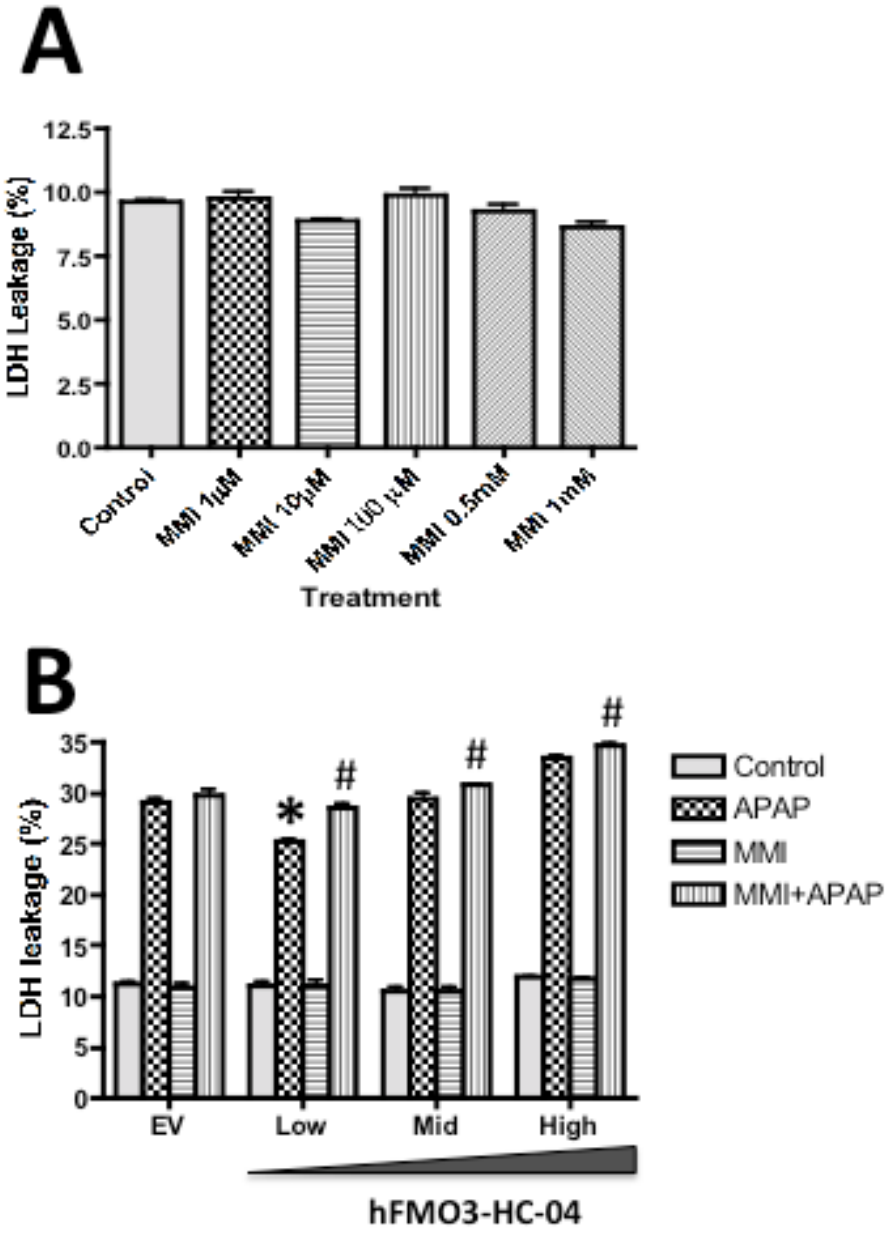
A
LDH Leakage (%)
12.5
10.0
7.5
5.0
2.5
0.0
Control
MMI 1μM
MMI 10μM
MMI 100 μM
MMI 0.5mM
MMI 1mM
Treatment
B
LDH leakage (%)
35
30
25
20
15
10
5
0
*
#
#
#
EV
Low
Mid
High
hFMO3-HC-04
Control
APAP
MMI
MMI+APAP

Figure 2.11 *Effect of MMI pretreatment during APAP-induced cytotoxicity in HC-04 cells over-expressing human FMO3 (hFMO3-HC-04).* Empty vector, Low-, Mid- and High-FMO3 expressing cell lines were incubated with MMI (1 mM) for 30 min before APAP (15 mM) treatment. 24 h after APAP treatment, percent LDH leakage into the medium was measured. The data are presented as mean LDH leakage (%) ± SE. Two-way ANOVA was performed followed by the Bonferroni's post-test. Asterisks (*) represent a significant decrease ($p<0.05$) compared to APAP treated EV control and pound (#) represent a significant increase ($p<0.05$) compared to respective APAP treated EV and hFMO3-HC-04 cell lines.

TABLE 2.1

Histopathological Analysis of Livers after MMI Intervention in APAP Treated Mice. Liver sections were examined for severity of degenerative and necrotic changes in centrilobular region as described previously (Manautou et al., 1994). Liver samples with grades greater than 2 are considered to have significant injury. Data were rank ordered prior to statistical analysis. Asterisks (*) represent a statistical difference ($p<0.05$) from vehicle control group and pound (#) represent a statistical difference ($p<0.05$) from APAP treated group.

Treatment Group	Histological Grade						Percent >2
	0	1	2	3	4	5	
Control	5	0	0	0	0	0	0
APAP	0	5	0	0	0	0	0
1&2MMI / APAP*#	0	0	0	1	1	2	100
1MMI / APAP*	0	0	4	1	0	0	20
APAP / 2MMI	0	5	0	0	0	0	0

2.5 Discussion

The mechanism of APAP-induced cellular and liver organ toxicity is multifactorial and complex (Jaeschke & Bajt, 2006; Jaeschke et al., 2012). Examining novel genes and pathways differentially regulated in experimental models of xenobiotic hepatotoxicity resistance can provide novel avenues to develop new modalities of treatment for liver diseases. Our laboratory has previously developed a mouse model of APAP autoprotection for studying the mechanisms of hepatic injury/recovery (Aleksunes et al., 2008). This study also elucidated the role of efflux transporter MRP4 and compensatory cellular proliferation in protecting against APAP-induced hepatotoxicity in this model of APAP autoprotection. However, it is possible that factors other than MRP4 also can contribute to the development of APAP toxicity tolerance. A gene array analysis recently conducted in our lab provided insights into signaling pathways potentially involved in APAP autoprotection (O'Connor et al., 2014). *Fmo3* was among the genes with the most significant change in APAP autoprotected mice. Even though a role of *Fmo3* expression in APAP hepatotoxicity is not known, it was the most biologically plausible for playing a role in autoprotection.

In this study, we investigated the hepatic expression of Fmo3 protein during APAP-induced hepatotoxicity. Historically, Fmo3 was considered to be a non-inducible drug-metabolizing enzyme (Cashman & Zhang, 2002; Cashman & Zhang, 2006; Hines, 2006; Krueger & Williams, 2005). However, recent studies show that activation of the Ah receptor induces Fmo3 mRNA

levels (Celius et al., 2008; Celius et al., 2010). In these studies, although there is a very large increase in Fmo3 mRNA levels, protein levels measured by methimazole oxidation show only modest increases in protein function. Similarly, our results show that the dramatic elevation in liver Fmo3 mRNA expression following administration of a single APAP dose is accompanied by marginal increases in Fmo3 protein expression and catalytic activity. It is worth noting that the Fmo3 mRNA expression is variable between studies, which is again similar to the observations with ligand dependent activation of AhR and Fmo3 mRNA expression (Celius et al., 2008). These differences in expression cannot be due to diurnal variation in basal expression because animals were dosed and tissue harvested at approximately the same time of the day every time we conducted independent studies. Fmo3 is subject to hormone regulation (Cherrington et al., 1998; Falls et al., 1997; Janmohamed et al., 2004), and such, 9 to 10 weeks old mice were used in the current study. Irrespective of the level and degree of increased Fmo3 mRNA expression following a single dose APAP treatment, increases in protein expression remained marginal.

In contrast to what was observed with a single APAP hepatotoxic dose, both liver Fmo3 mRNA and protein expression are significantly higher in mice treated with the APAP autoprotection regimen (pre- and post-APAP treatment). In agreement with greater Fmo3 protein expression, Fmo3 catalytic activity and centrilobular zonal expression also are significantly greater in the APAP autoprotection group. These findings suggest the

regulation of Fmo3 gene expression (transcriptional and/or translational) is different under the conditions of treatment with a single APAP dose versus an autoprotection treatment regimen. Because the level of damage from a mildly toxic dose of APAP is minimal, the need for restoration of balance in cellular processes may also be less. Thus all mRNA transcribed in response to the minimally toxic APAP exposure may not be translated into functional protein. In contrast, after an autoprotected dosing regimen, the initial exposure to a mildly toxic APAP dose would prime the tissue for faster recovery from re-exposure to a second toxic insult. Indeed, the possibility exists that at least a portion of the dramatic increases in Fmo3 protein observed with the second APAP dose results from rapid translation of Fmo3 mRNA stabilized in ribonucleoprotein complexes. Such translational control has been well documented in other systems where a rapid response to a potentially toxic exposure occurs (e.g., translation of stored ferritin mRNA in response to iron exposure). This overall concept is well accepted and referred to by some scientists as “hormesis”. The precise cellular and molecular events leading to this adaptation is not known. Moreover, immunohistochemical analysis of APAP autoprotected livers show the Fmo3 expression is localized to the hepatic centrilobular regions, where APAP induced damage and/or hepatocellular compensatory repair/proliferation occurs, instead of the conventional periportal localization seen in female livers. This expression pattern is again suggestive of a potential Fmo3 role in the development of APAP hepatotoxicity resistance via an unknown cytoprotective function.

Female mice exhibit higher *Fmo3* gene expression than male mice (Cherrington et al., 1998; Hines, 2006; Janmohamed et al., 2004), and are much more resistant to APAP hepatotoxicity compared to males (Dai et al., 2006). Our findings with the FMO inhibitor methimazole in female mice demonstrate that MMI inhibition of Fmo3 makes female mice susceptible to APAP-induced hepatotoxicity. The caveats of any inhibitor study are the specificity of inhibition as well as potential off target effects exhibiting toxicity comparable to that seen in males. Historically, MMI is known to interfere with the synthesis of thyroid hormones by inhibiting the enzyme, thyroperoxidase and is capable of inhibiting other enzymes involved in oxygenation reactions such as FMO and CYP dependent monooxygenases (Hunter & Neal, 1975). If MMI was contributing to changing female mice susceptibility to APAP hepatotoxicity by inhibiting CYP-dependent metabolism, we would have anticipated seeing less liver damage. Clearly, this is not the case because MMI treatment makes female mice sensitive to APAP hepatotoxicity. This is quite remarkable since C57BL/6J female mice are quite resilient to APAP hepatotoxicity. Undesirable side effects such as cholestasis can develop from MMI treatment due to extrathyroidal actions in humans (Schmidt et al., 1986). However, a cholestatic liver is less susceptible to APAP-induced hepatotoxicity in mice (Silva et al., 2006). Lastly, MMI at higher doses can deplete hepatic GSH levels or in GSH-depleted mice induce centrilobular necrosis (Mizutani et al., 1999; Mizutani et al., 2000). However, under the conditions used in the current study, MMI treatment alone does not result in

GSH depletion or hepatotoxicity in mice. Furthermore, MMI treatment in male mice did not alter APAP-induced hepatotoxicity negating any potential non-specific functions of MMI. Collectively, these results suggest that the susceptibility of female mice to APAP hepatotoxicity following MMI treatment is the result of inhibiting Fmo3 function.

To further study the importance of FMO3 over-expression, we established an *in vitro* over-expression system using HC-04 cells. While the percent LDH leakage into the media in Low-FMO3 expressing hFMO3-HC-04 cells in response to APAP treatment is significantly lower compared to empty vector controls, the amount of LDH leakage by APAP does not change in the Mid-FMO3 expressing clone and is significantly greater in High-FMO3 cells. Taken together, these data suggest that over-expression of FMO3 significantly alters susceptibility to APAP induced cytotoxicity. Even though the percent protection from APAP cytotoxicity in the Low-FMO3 expressing clone is only about 20 percent, one must keep in mind that FMO3 over-expressing cells are a mono cell culture. The possible contribution from other cell types, such as Kupffer cells and endothelial cells known to play an important role in signaling mechanisms should not be overlooked. The data also suggest that there is a threshold for FMO3 over-expression in protecting against APAP-induced cytotoxicity. This is evidenced by the enhanced APAP cytotoxicity in the High-expressing FMO3 cells. MMI treatment did not result in elevation of basal LDH leakage into the medium in all FMO3-over-expressing clones. This suggests that MMI by itself at doses used *in vitro* did

not result in cytotoxicity. Inhibition of FMO3 activity by MMI in all three Low-, Mid- and High-FMO3 expressing cell lines resulted in rescue of sensitivity to APAP in Low-FMO3 expressing cell line compared to EV controls. Since High-FMO3 expressing cells exhibit greater LDH leakage in comparison to EV controls following APAP treatment (threshold for FMO3 over-expression), one might anticipate seeing lower APAP cytotoxicity following MMI co-treatment. Considering this is not the case, it is possible that MMI at 1mM concentration results in inhibition of FMO3 activity in Low-FMO3 expressing cell line but is metabolized in High-FMO3 expressing cells. To emphasize, MMI is a substrate for Fmo3 as well as a competitive inhibitor with IC_{50} value of 60.2±16.2 μM (Attar et al., 2003; Rettie & Fisher, 1999).

FMO is involved in oxygenation of phosphorus, nitrogen and sulphur-containing xenobiotics. FMO's also are involved in the oxidation of endogenous substrates such as cysteamine to cystamine (Poulsen, 1981). Although, the physiological role of FMO3 cysteamine S-oxygenation is not clear, Zieglar and Poulsen proposed in the 1970's that FMO might be involved in protein disulphide bond formation through oxidation of cysteamine. It was also proposed that oxygenation of cysteamine may be a significant source of disulphide, maintaining the cellular thiol:disulphide potential in a cell (Ziegler et al., 1979). Further, Suh and Robertus showed that yeast FMO serve as a modulator of cellular thiols and maintains optimum redox potential within the endoplasmic reticulum, allowing for proper folding of disulfide bond-containing proteins (Suh & Robertus, 2002). The cytoprotective functions of

Fmo3 and its possible involvement in APAP autoprotection are summarized below. The relationship between cellular thiol:disulphide ratios and the regulation of metabolic reactions has been recognized for a long time (Barron, 1953). Oxygenation of cysteamine during APAP hepatotoxicity may serve to help control the overall thiol:disulphide redox state of the cell, which in turn may modulate cellular metabolism and/or activate signal transduction pathway leading to altered susceptibility to APAP (or protection). Oxygenation of cysteamine to cystamine by Fmo3 and transport out of the cell also may represent a detoxication mechanism or protective function, because cysteamine is toxic to cells at concentrations as low as 39 μM through the transition metal-dependent formation of hydrogen peroxide (Jeitner & Lawrence, 2001). To investigate whether oxygenation of cysteamine to cystamine by Fmo3 is important during APAP hepatotoxicity, follow-up studies will measure the total hepatic cysteamine and cystamine concentrations in the mouse model of APAP autoprotection.

In the present study, up-regulation of Fmo3 gene expression in the mouse APAP autoprotection model and its role in protecting against APAP-induced cytotoxicity or hepatotoxicity has led to the conclusion that Fmo3 is important for development of resistance to APAP-induced hepatotoxicity. The phenomenon of autoprotection is also seen in patients who are repeatedly exposed to supratherapeutic doses of APAP (Shayiq et al., 1999; Watkins et al., 2006). These clinical data suggest that human liver can adapt to APAP-induced hepatotoxicity similar to that seen in our APAP autoprotection mouse

model. C57BL/6J wild type mice are commonly used for studies of APAP hepatotoxicity and the mechanisms of toxicity in these animals are not completely understood. Although, key events such as NAPQI formation, GSH depletion, protein arylation, peroxynitrate formation and mitochondrial damage play an important role in APAP hepatotoxicity (Cohen et al., 1997; Hinson et al., 2010; Jaeschke & Bajt, 2006; Jaeschke et al., 2011; McGill et al., 2012). Even though primary human hepatocytes are the gold standard tool for studying APAP hepatotoxicity mechanisms, they have major drawbacks. The availability of these cells is limited, and the drug response can vary significantly due to differences in donors. Most importantly, the lifespan of primary human hepatocytes is short and they undergo changes in CYP expression levels over time in culture. Hepatoma cell lines like HepG2 express very low CYP levels compared to primary human hepatocytes or human liver especially those that are involved in the metabolism of APAP (Rodriguez-Antona et al., 2002). Using the more recently available human hepatoma cell line, HepaRG, which expresses a more normal spectrum of drug metabolizing enzymes, studies have demonstrated that the mechanistic features of APAP-induced hepatotoxicity are the same as reported for human hepatocytes and mouse liver *in vivo* (McGill et al., 2011). Thus, it is very likely that the phenomenon of APAP autoprotection seen in human might also involve FMO3 over-expression. Although this is a subject of current investigation in our laboratory the mere fact that the protein once thought to be non-inducible is being induced following treatment with a commonly used,

over-the-counter drug like acetaminophen is quite alarming. Importantly, one also must be concerned about the number of other drugs that are co-administered with APAP and are FMO3 substrates.

CHAPTER 3

Differential FMO3 Gene Expression in Various Liver Injury Models Involving Hepatic Oxidative Stress in Mice

3.1 Abstract

Flavin-containing monooxygenase-3 (FMO3) catalyzes metabolic reactions similar to cytochrome P450 monooxygenase however, most metabolites of FMO3 are considered non-toxic. Recent findings in our laboratory demonstrated *Fmo3* gene induction following toxic acetaminophen (APAP) treatment in mice. The goal of this study was to evaluate *Fmo3* gene expression in diverse other mouse models of hepatic oxidative stress and injury. *Fmo3* gene regulation by Nrf2 was also investigated using Nrf2 knockout (Nrf2 KO) mice. In our studies, male C57BL/6J mice were treated with toxic doses of hepatotoxicants or underwent bile duct ligation (BDL, 10d). Hepatotoxicants included APAP (400 mg/kg, 24 to 48 h), alpha-naphthyl isothiocyanate (ANIT; 50 mg/kg, 2 to 48 h), carbon tetrachloride (CCl_4; 10 or 30 μL/kg, 24 and 48 h) and allyl alcohol (AlOH; 30 or 60 mg/kg, 6 and 24 h). Because oxidative stress activates nuclear factor (erythroid-derived 2)-like 2 (Nrf2), additional studies investigated *Fmo3* gene regulation by Nrf2 using Nrf2 knockout (Nrf2 KO) mice. At appropriate time-points, blood and liver samples were collected for assessment of plasma alanine aminotransferase (ALT) activity, plasma and hepatic bile acid levels, as well as liver Fmo3 mRNA and protein expression. Fmo3 mRNA expression increased

significantly by 43-fold at 12 h after ANIT treatment, and this increase translates to a 4-fold change in protein levels. BDL also increased Fmo3 mRNA expression by1899-fold, but with no change in protein levels. Treatment of mice with CCl_4 decreased liver *Fmo3* gene expression, while no change in expression is detected with AlOH treatment. Nrf2 KO mice are more susceptible to APAP (400 mg/kg, 72 h) treatment compared to their wild-type (WT) counterparts, which is evidenced by greater plasma ALT activity. Fmo3 mRNA and protein expression increased in Nrf2 KO mice after APAP treatment. Collectively, not all hepatotoxicants that produce oxidative stress alter *Fmo3* gene expression. Along with APAP, toxic ANIT treatment in mice markedly increases *Fmo3* gene expression. While BDL increases Fmo3 mRNA expression, protein level does not change. The discrepancy with *Fmo3* induction in cholestatic models, ANIT and BDL, is not entirely clear. Results from Nrf2 KO mice with APAP suggest that the transcriptional regulation of *Fmo3* during liver injury may not involve Nrf2.

3.2 Introduction

Drug-induced liver injury (DILI) is a significant challenge for both drug development and clinical care. It accounts for more than 50 % of all acute liver failure cases in the U.S. (Larson et al., 2005; W. M. Lee, 2010). Many chemicals, such as acetaminophen (APAP), carbon tetrachloride (CCl_4) and allyl alcohol (AlOH) have been used to model hepatotoxicity relevant to human exposure. Alpha-naphthyl isothiocyanate (ANIT) and bile duct ligation (BDL) on the other hand are used to model cholestasis, a pathological condition caused by impairment of hepatic bile flow. While ANIT produces intrahepatic cholestasis, BDL produces extrahepatic cholestasis. With APAP and CCl_4, the parent compound is metabolized by cytochrome P450 (CYP) to generate reactive metabolites, N-acetyl-p-benzoquinone imine (NAPQI) and tricholoromethyl radical ($^{\cdot}CCl_3$), respectively. AlOH in turn is metabolized in the liver by alcohol dehydrogenase to its reactive metabolite, acrolein. The glutathione adduct of acrolein is converted by CYPs to glycidaldehyde. Toxicity resulting from these reactive metabolites is multifactorial and includes lipid peroxidation, generation of oxidative stress, altered cellular redox status and protein adduct formation (Burcham & Fontaine, 2001; Cohen et al., 1997; Jaeschke et al., 2012; Ohno et al., 1985; Tom et al., 1984). During cholestasis resulting from either BDL or ANIT treatment, increase in bile acid concentration stimulates production of reactive oxygen species eventually leading to hepatocellular necrosis and apoptosis (Sokol et al., 1995; Trauner et al., 1998).

The role of nuclear factor (erythroid-derived 2)-like 2 (Nrf2) role as a master defense against hepatotoxicity produced by various chemicals has been investigated in several studies. Nrf2 belongs to the cap 'n' collar family of transcription factors that promotes transcription of a battery of cytoprotective genes (Aleksunes & Manautou, 2007; Kensler et al., 2007). Under basal conditions, Nrf2 is largely bound to the cytoskeletal anchoring protein Kelch-like ECH-associated protein 1 (Keap1) also known as cytosolic Nrf2 inhibitor in the cytoplasm. In response to oxidative stress, Nrf2 is released from Keap1 and translocates to the nucleus. In the nucleus, Nrf2 binds to the GTGACA***GC core sequence of the antioxidant response element (ARE) (Rushmore et al., 1991) and promotes ARE-mediated antioxidant gene expression.

A low toxic APAP dose causes nuclear accumulation of Nrf2 in mouse liver, which is accompanied by increased expression of Nrf2 dependent cytoprotective genes such as heme oxygenase-1 (*Hmox1*), NAD(P)H:quinone oxidoreductase-1 (*Nqo1*) and glutamate cysteine ligase catalytic subunit (*Gclc*) (Aleksunes et al., 2005; Aleksunes et al., 2006; Bauer et al., 2000; Chiu et al., 2002; Goldring et al., 2004). Similar results have been reported with ANIT, BDL, CCl_4 and AlOH, other models of hepatic oxidative stress used in the present study (Aleksunes et al., 2005; Aleksunes et al., 2006; Liu et al., 2013; Randle et al., 2008; Tanaka et al., 2009). On the other hand, Nrf2 KO mice are more susceptible to APAP-induced liver injury compared to their wild-type counterparts (Chan et al., 2001; Enomoto et al., 2001). Likewise,

Nrf2 KO mice are also more susceptible to CCl_4- and AlOH-induced hepatoxicity compared to wild-type mice (Liu et al., 2013). However, Nrf2-null mice do not exhibit any difference in susceptibility to either BDL or ANIT treatment (Tanaka et al., 2009; Weerachayaphorn et al., 2012). This response is attributed to the adaptive compensatory changes involving nuclear transcription factors, including Fxr, Shp, Pxr and Hnf1α, efflux bile acid transporters, altered GSH levels and bile flow rates in Nrf2 KO mice (Tanaka et al., 2009; Weerachayaphorn et al., 2012). Collectively, the models of hepatic injury selected for the current study not only result in hepatic oxidative stress but also activate the Nrf2-Keap1 regulatory pathway.

Despite *Fmo3* being considered non-inducible, studies with aryl hydrocarbon receptor (AhR) agonists in mice show liver *Fmo3* gene induction (Celius et al., 2008; Celius et al., 2010). A recent gene array analysis performed in our laboratory also demonstrated *Fmo3* gene induction in the APAP autoprotection mouse model (mice receiving a low hepatotoxic APAP dose that become resistant to a subsequent higher APAP dose) (O'Connor et al., 2014). Unlike with AhR agonists that result in marginal increases in Fmo3 protein expression in mouse liver, we show significant increases in Fmo3 protein levels in APAP autoprotected mice (Rudraiah et al., 2014). *Fmo3* induction by other hepatotoxicants that produce oxidative stress is not currently known.

In human liver, transcription factors regulating constitutive *FMO3* expression as well as those involved in developmental expression pattern are

extensively studied (Klick & Hines, 2007; Klick et al., 2008; Shimizu et al., 2008). Because the mammalian FMOs were considered non-inducible by xenobiotics (Cashman & Zhang, 2002; Krueger & Williams, 2005), the transcriptional regulation of FMO involving stress-activated transcription factors or receptors that bind ligands and interact with DNA was not studied as other forms of regulation. Thus, little is known about the transcriptional regulation of *Fmo3* in response to toxicant exposure. Recently, Celius et al. show that the Fmo3 mRNA up-regulation by 3-methylcholanthrene (3MC) and benzo(a)pyrene (BaP) but not TCDD in Hepa-1 cells is mediated by p53 and its binding to a p53-response element in the promoter region of *Fmo3* (Celius et al., 2010).

Differentially expressed genes in the APAP autoprotection model were further analyzed using Causal Reasoning Engine (CRE), a recently developed computational platform (O'Connor et al., 2014). CRE analysis provides hypotheses on the upstream molecular events that best explain gene expression profiles based on prior biological knowledge. CRE analysis of differentially expressed genes in APAP autoprotection study supports an induction of the Nrf2 pathway (O'Connor et al., 2014). Additionally, the 5'-flanking region of the mouse *Fmo3* contains multiple copies of the ARE (Celius et al., 2008). Therefore, the purpose of the present study was to investigate liver *Fmo3* gene expression under oxidative stress conditions involving activation of the Nrf2-Keap1 regulatory pathway. Mice were dosed with hepatotoxicants APAP (400 mg/kg, 24 to 48 h), ANIT (50 mg/kg, 2 to 48

h), CCl_4 (10 or 30 μL/kg, 24 and 48 h) or AlOH (30 or 60 mg/kg, 6 and 24 h) or underwent sham surgery or bile duct ligation (10 d). Doses selected for hepatotoxicants are based upon previous studies conducted in our laboratory resulting in oxidative stress and tissue injury. The inclusion of multiple time-points following hepatotoxicants exposure enabled comprehensive characterization of temporal changes in *Fmo3* in relation to injury and recovery. Further, in order to investigate whether Nrf2 mediates *Fmo3* gene expression, Nrf2 KO mice were employed. APAP was used as a model toxicant in the Nrf2 KO mice study. From these experiments, it is concluded that not all hepatotoxicants that produce oxidative stress in mice induce liver *Fmo3* gene expression. Toxic ANIT treatment, along with the previously demonstrated APAP treatment, markedly increases *Fmo3* gene expression. While BDL increases Fmo3 mRNA expression, protein levels do not change. APAP treatment induces *Fmo3* gene expression in Nrf2 KO mice liver suggesting that the transcriptional regulation of *Fmo3* might not involve Nrf2.

3.3 Materials and Methods

Chemicals

Acetaminophen, alpha-naphthyl isothiocyanate, carbon tetrachloride, allyl alcohol, propylene glycol and corn oil were purchased from Sigma-Aldrich (St Louis, MO). All other reagents were of reagent grade or better and commercially available.

Animals

Male C57BL/6J mice (9- to 10-week old) were purchased from Jackson Laboratories (Bar Harbor, ME) for this study. Upon arrival, mice were acclimated for one week prior to experimentation. Mice were housed in a temperature-, light- and humidity-controlled environment. Mice were fed laboratory rodent diet (Harlan Teklad 2018, Madison, WI) *ad libitum*.

Experimental Design 1. Following an overnight fast, male mice (n=6) were treated with APAP (400 mg/kg in 50 % propylene glycol, ip, 24, 48 and 72 h), ANIT (50 mg/kg in corn oil, po, 2, 4, 8, 12, 24 and 48 h), CCl_4 (10 or 30 μL/kg in corn oil, ip, 24 and 48 h), AlOH (30 or 60 mg/kg in saline, ip, 6 and 24 h) or vehicle. At the end of each experiment, animals were sacrificed at the specified time-points for each hepatotoxicant and plasma and livers were collected for analysis. BDL liver samples were obtained from a previously described cohort (Donepudi et al., 2012). Briefly, sham or BDL surgery was performed under phenobarbital-induced anesthesia (65 mg/kg, ip). The surgeries were performed at the University of Rhode Island, College of Pharmacy animal facility with IACUC approval. Serum and liver were collected 10 d after surgery for analysis.

Experimental Design 2. Following overnight fasting, male Nrf2 KO mice and their wild-type counterparts (C57BL/6J) were treated with APAP (400 mg/kg, ip) in 50 % PG or vehicle. Plasma and livers were collected 72 h after APAP treatment for analysis.

All animal studies were performed in accordance with National Institute of Health standards and the Guide for the Care and Use of Laboratory Animals. This work was approved by the University of Connecticut's Institutional Animal Care and Use Committee.

Alanine Aminotransferase (ALT) Assay

Plasma or serum ALT activity was determined as a biochemical indicator of hepatocellular injury. Infinity ALT Liquid Stable Reagent (Thermo Fisher Scientific Inc., Waltham, MA) was used to determine ALT activity. Briefly, 100 μL of reagent was added to 10 μL serum or plasma samples, and absorbance was measured spectrophotometrically at 340 nm using a Bio-Tek Power Wave X Spectrophotometer. ALT activity (IU/L) was determined using the molar extinction coefficient of NADH (6.3 $mM^{-1}cm^{-1}$).

Total Bile acid Assay

Total bile acids were extracted from whole liver homogenates using a t-butanol extraction method. Briefly, livers were homogenized in extraction solution (1:1, water: t-butanol) and bile acids extracted overnight at room temperature in the dark. Blood levels of total bile acid and hepatic bile acid levels were measured using a spectrophotometric bile acid assay kit (Bioquant, San Diego, CA) according to manufacturer's protocol.

RNA Isolation and Quantitative Real-Time Polymerase Chain Reaction (qRT-PCR)

Total RNA was extracted from mouse liver samples using TRIzol reagent (Life Technologies, Carlsbad, CA) according to the manufacturer's instructions. Total RNA was then reverse-transcribed into cDNA using an M-MLV RT kit (Invitrogen, Carlsbad, CA). Fmo3 mRNA expression was quantified by the ΔΔCT method and normalized to two housekeeping genes, β-actin and ribosomal protein S18. Data presented were normalized to β-actin. Primer pairs were synthesized by Integrated DNA Technologies (Coralville, IA) and are as follow: Fmo3 forward: 5′-GGA AGA GTT GGT GAA GAC CG-3′, reverse: 5′-CCC ACA TGC TTT GAG AGG AG-3′. Amplification was performed using an Applied Biosystems 7500 Fast Real-Time PCR System. Amplification was carried out in a 20 µL reaction volume containing 8 µL diluted cDNA, Fast SYBR Green PCR Master Mix (Applied Biosystems, Foster City, CA) and 1 µM of each primer.

Preparation of Microsomal Fraction and Western Blot Analysis

Microsomes were isolated from livers as described previously (Cashman & Hanzlik, 1981; Rudraiah et al., 2014) and stored at -80°C until use. Protein concentration was determined by the method of Lowry using Bio-Rad protein assay reagents (Bio-Rad Laboratories, Hercules, CA). For western blot analysis, microsomal proteins (10 µg) were electrophoretically resolved using 10 % polyacrylamide gels and transferred onto PVDF-Plus

membrane (Micron Separations, Westboro, MA). Membranes were blocked with 5 % non-fat powdered milk in tris buffered saline containing 0.05% tween-20 (TBS-T) for 8 h. A rabbit anti-mouse Fmo3 primary antibody (GenScript USA Inc., NJ) (1:5000) was used to detect Fmo3 with β-actin as a loading control. Blots were then incubated with HRP conjugated secondary antibodies against rabbit IgG (1:2000) (Sigma-Aldrich, St Louis, MO). Protein-antibody complexes were detected using a chemiluminescent kit (Thermo Scientific, IL) with visualization using GeneMate blue autoradiography film (Bioexpress, Kaysville, UT).

Enzyme Assay

Methimazole (MMI) metabolism was determined spectrophotometrically by measuring the rate of MMI *S*-oxygenation via the reaction of the oxidized product with nitro-5-thiobenzoate (TNB) to generate 5,5'-dithiobis(2-nitrobenzoate) (DTNB). The incubation mixture consisted of 50 mM sodium phosphate buffer (pH 9.0), 0.5 mM $NADP^+$, 0.5 mM glucose-6-phosphate, 1.5 IU/mL glucose-6-phosphate dehydrogenase, 0.06 mM DTNB, 0.04 mM dithiothreitol and 100 to 150 µg/mL liver microsomes isolated from mice. Reactions were initiated by the addition of different amounts of MMI (substrate), with a concentration range from 1.25 to 800 µM. Incubations were done in duplicates. The disappearance of the yellow color was measured spectrophotometrically at 412 nm and specific activity (µM/min/mg) was determined using the molar extinction coefficient of NADPH (28.2 $mM^{-1}cm^{-1}$).

Statistical Analysis

The statistical significance between groups was determined using the Student's t-test, one-way ANOVA with Dunnett's post-hoc test or two-way ANOVA followed by the Bonferroni's post-hoc test. While Student's t-test was used to compare means of two different treatment groups, ANOVA was used to compare the means of more than two treatment groups that are normally distributed with a common variance. All statistical analysis was performed using GraphPad Prism version 4.00 for Macintosh (GraphPad Software, Inc., San Diego, CA). Data are presented as mean ± standard error (SE), with $p<0.05$ considered statistically significant.

3.4 Results

Plasma ALT Activity in the Mouse Liver Injury Models

The hepatotoxicity of APAP (400 mg/kg) at 24, 48 and 72 h as assessed by plasma ALT activity has been reported previously (Rudraiah et al., 2014). Briefly, APAP increased plasma ALT activity to 191±18 and 219±47 IU/L at 24 and 48 h, respectively (mean plasma ALT activity in control mice was 25±5 IU/L). Plasma ALT activity is not statistically different from vehicle controls by 72 h, indicating recovery from APAP-induced liver injury. Plasma ALT activity in all mouse models of liver injury is shown in Figure 3.1. ANIT increased ALT activity at 12 h (182±9 IU/L), which continued to increase at 24 and 48 h (715±126 IU/L and 781±45 IU/L, respectively) compared to vehicle control group (9±1 IU/L). BDL for 10 d results in an elevation of ALT

activity to 185±10 IU/L. A high CCl_4 dose (30 µL/kg) increased plasma ALT at 24 and 48 h to 6367±1135 and 397±111 IU/L, respectively. A low CCl_4 dose (10 µL/kg) also increased plasma ALT activity at 24 and 48 h to 757±106 and 416±68 IU/L, respectively. The greatest increase in plasma ALT with both doses of CCl_4 is observed at 24 h. While AlOH treatment (low dose, 30 mg/kg) did not result in significant increases in ALT levels at 6 h and 24 h (36±4 and 73±24 IU/L, respectively), a high AlOH dose (60 mg/kg) results in significantly higher ALT levels at both 6 h and 24 h (153±50 and 4440±2428 IU/L, respectively). The associated histopathological damage with all hepatotoxicants has been reported previously (Aleksunes et al., 2005; Aleksunes et al., 2006; Campion et al., 2009; Donepudi et al., 2012; Rudraiah et al., 2014). With acute toxicity models, plasma ALT activity lesser than 1000 IU/L is usually associated with a minimal to mild hepatocellular damage (histological grade of 2 or less than 2), and an ALT activity higher than 1000 IU/L is associated with moderate, marked or severe hepatocellular damage (histological grade of 3, 4, or 5) (Aleksunes et al., 2008; Manautou et al., 1994). Alternatively, a 10 d BDL with an associated ALT activity of less than 200 IU/L, exhibit a chronic hepatocellular damage involving fibrosis (Donepudi et al., 2012).

Hepatic Fmo3 mRNA Expression in the Mouse Liver Injury Models

Fmo3 mRNA levels were quantified by qRT-PCR and the results are presented in Figure 3.2. Fmo3 mRNA expression following 400 mg/kg APAP treatment has been previously reported (Rudraiah et al., 2014). Briefly, Fmo3

mRNA levels increased by 5±2.6-and 23±5.6-fold, at 24 and 48 h after APAP, respectively, compared to the 0 h control group. ANIT increased Fmo3 mRNA levels as early as 2 h after treatment. This increase peaked and is statistically significant only at 12 h (43±10-fold increase), compared to 0 h vehicle control group. BDL also increased Fmo3 mRNA expression by 1899±625-fold, compared to sham operated mice. Both the low and high dose of CCl_4 decreased Fmo3 mRNA levels at both time points examined, and this decrease is statistically significant only at 48 h (10 μL/kg: 0.2±0.06-fold and 30 μL/kg: 0.2±0.08-fold). No change in liver Fmo3 mRNA levels is observed with AlOH treatment.

Hepatic Bile Acid Concentrations in the Mouse Liver Injury Models

To determine the extent of cholestasis induced by different hepatotoxicants used in the current study, total hepatic bile acid levels were measured (Figure 3.3). As expected ANIT increased hepatic bile acid levels to 1.7±0.2 and 1.6±0.4 μmol/g at 24 and 48 h, respectively, compared to 0 h vehicle control group (0.2±0.02 μmol/g). BDL also increased hepatic bile acid concentrations to 19.49±0.85 μmol/g compared to sham operated group (10.61±1.65 μmol/g). No significant changes were observed in mice treated with APAP, CCl_4 and AlOH.

Total bile Acid Concentrations in the Blood in the Mouse Liver Injury Models

Bile acid concentration in plasma is also a biomarker of cholestasis. In order to determine the extent of cholestasis, plasma bile acid levels were also

quantified in all mouse models of liver injury (Figure 3.4). Plasma bile acid concentration increased in ANIT treated mice at 24 and 48 h to 210±20 and 330±128 μmol/L, respectively, compared with vehicle treated mice (2±0.2 μmol/L). Bile duct ligation significantly increased serum bile acid levels to 1359±142 μmol/L compared to sham operated mice (86±11 μmol/L). Significant increases in plasma bile acid concentrations are seen in high dose CCl_4 treated mice at both 24 and 48 h (112±15 μmol/L and 29±2 μmol/L, respectively). Exposure to APAP and AlOH did not result in any significant change in plasma bile acid levels.

Fmo3 Protein Expression in the Mouse Liver Injury Models

Temporal expression of the Fmo3 protein following exposure to hepatotoxicants and BDL were quantified by western blotting. Representative blots and associated densitometric analyses are shown in Figure 3.5. Fmo3 protein increase following APAP treatment has been previously reported (Rudraiah et al., 2014). Although the expression of Fmo3 protein tended to increase by 1.1±0.3- to 1.6±0.2-fold between 24 and 72 h after APAP, the increase is statistically significant only at 72h. Consistent with Fmo3 mRNA changes evidenced with ANIT treatment, Fmo3 protein levels also tend to increase as early as 2 h. However, this increase is significant only at 12 h (3.5±0.9-fold) compared to 0 h vehicle treated group. Fmo3 protein levels decreased to 0.7±0.08- and 0.3±0.1-fold at 24 and 48 h, respectively, after exposure to ANIT. Conversely, in spite of the dramatic increase in Fmo3 mRNA levels after BDL, Fmo3 protein levels did not change. No significant

changes in Fmo3 protein expression are observed with CCl_4 or AlOH treatment.

Plasma ALT Activity and Fmo3 mRNA Levels After APAP Treatment in Wild-Type and Nrf2 Knockout Mice

All models of hepatic injury used in the current study activate the Nrf2-Keap1 regulatory pathway. Furthermore, CRE analysis of differentially expressed genes in our APAP autoprotection study supported an induction of the Nrf2 pathway (O'Connor et al., 2014). To investigate whether Nrf2 mediates *Fmo3* gene expression, APAP was used as a model toxicant for Nrf2 activation in Nrf2 KO and WT mice. Mice were administered a 400 mg/kg APAP dose for 72 h. Dose and time-point selected were based on our single dose APAP study performed previously (Rudraiah et al., 2014), where a 400 mg/kg APAP treatment increased Fmo3 protein levels at 72 h. Administration of 400 mg/kg APAP to male C57BL/6J WT mice did not result in significantly different plasma ALT values at 72 h from vehicle controls. This is consistent with the previously reported results, indicating recovery from APAP-induced liver injury and increased Fmo3 protein expression in WT mice (Rudraiah et al., 2014). In contrast, plasma ALT activity is elevated at 72 h in Nrf2 KO mice receiving the same dose of APAP (176±12 IU/L) compared to vehicle control group (23±5 IU/L) (Figure 3.6A). This is again consistent with the literature and confirms that Nrf2 plays an important role not only in the magnitude of toxicity, but also in the degree and rate of recovery from APAP-induced liver injury. Fmo3 mRNA levels were quantified by qRT-PCR. The results in Figure

3.6B show that there is no change in Fmo3 mRNA levels at 72 h in wild-type mice administered 400 mg/kg APAP. This is again consistent with previous reports, where maximal Fmo3 mRNA expression is seen at 48 h after APAP administration and returns to normal by 72 h (Rudraiah et al., 2014). Notably, Fmo3 mRNA expression is significantly higher in Nrf2 KO mice 72 h after APAP treatment by 140±43-fold change compared to vehicle control group.

Fmo3 Protein Expression After APAP Treatment in Wild-Type and Nrf2 Knockout Mice

To examine the temporal changes in *Fmo3* gene expression following APAP treatment in WT and Nrf2 KO mice, Fmo3 protein levels were quantified by western blotting and by measuring catalytic activity using MMI as substrate. Representative blots and associated densitometric analysis are shown in Figure 3.7A. Consistent with increased Fmo3 mRNA expression in Nrf2 KO mice administered APAP (400 mg/kg) at 72 h, Fmo3 protein levels are also significantly higher (5.1±1.3-fold) compared to vehicle control group. Measuring FMO catalytic activity using MMI can also quantitate Fmo3 protein induction (Zhang et al., 2007). FMO specific activity increased significantly in Nrf2 KO livers (48±6 μM/min/mg) at 72 h after APAP compared to vehicle controls of either genotype (Figure 3.7B).

Figure 3.1

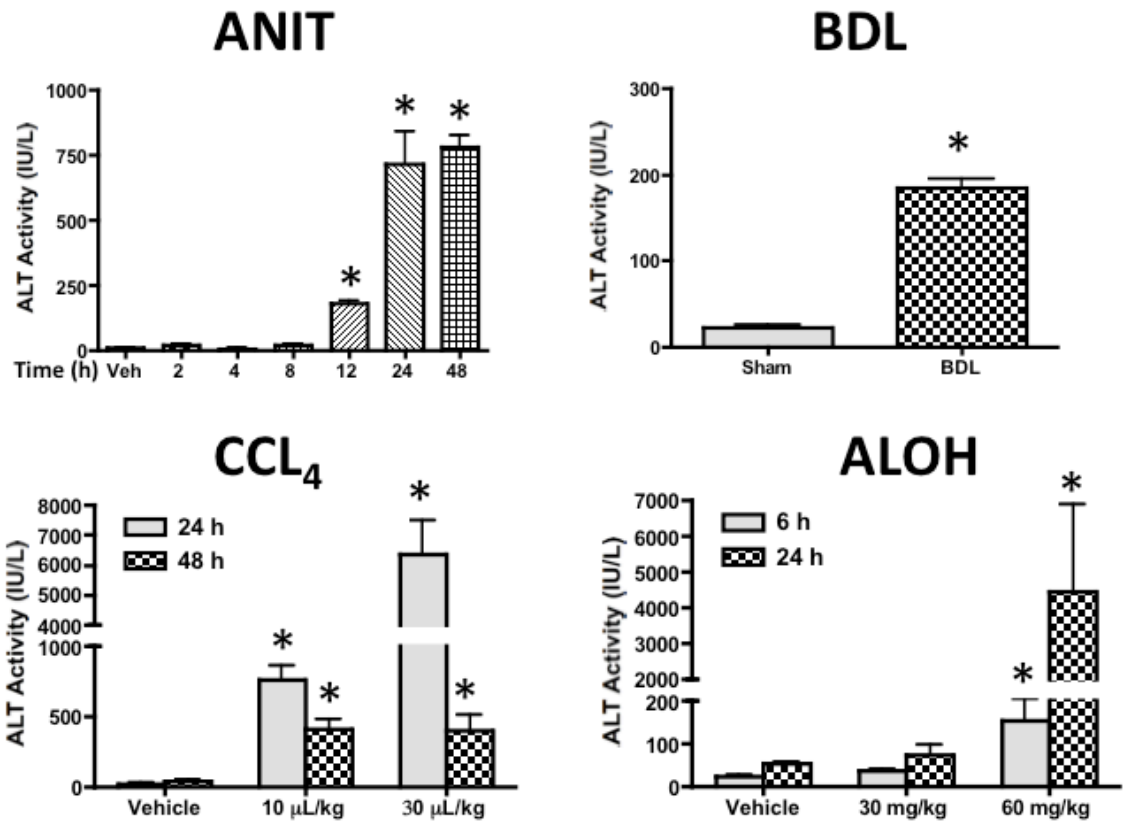
ANIT
ALT Activity (IU/L)
1000
750
500
250
0
Time (h) Veh 2 4 8 12 24 48
BDL
ALT Activity (IU/L)
300
200
100
0
Sham
BDL
CCL4
24 h
48 h
ALT Activity (IU/L)
8000
7000
6000
5000
4000
1000
500
0
Vehicle
10 µL/kg
30 µL/kg
ALOH
6 h
24 h
ALT Activity (IU/L)
7000
6000
5000
4000
3000
2000
200
100
0
Vehicle
30 mg/kg
60 mg/kg

Figure 3.1 *Plasma ALT activity in mice treated with hepatotoxicants or BDL.* Male C57BL/6J mice were treated with ANIT (50 mg/kg, po, 2,4,8,12,24 & 48 h), CCl_4 (10 & 30 µL/kg, ip, 24 & 48 h), AlOH (30 & 60 mg/kg, ip, 6 & 24 h) or BDL (10 d). Plasma was collected from mice at various time points following hepatotoxicant treatment or the appropriate vehicle. The data are presented as mean plasma ALT (IU/L) ± SE. One-way ANOVA, t-test or two-way ANOVA was performed, appropriately, followed by the Dunnett's posttest for One-way ANOVA and the Bonferroni posttest for two-way ANOVA. Asterisks (*) represent a statistical difference ($p < 0.05$) between vehicle-treated and hepatotoxicant-treated group.

Figure 3.2

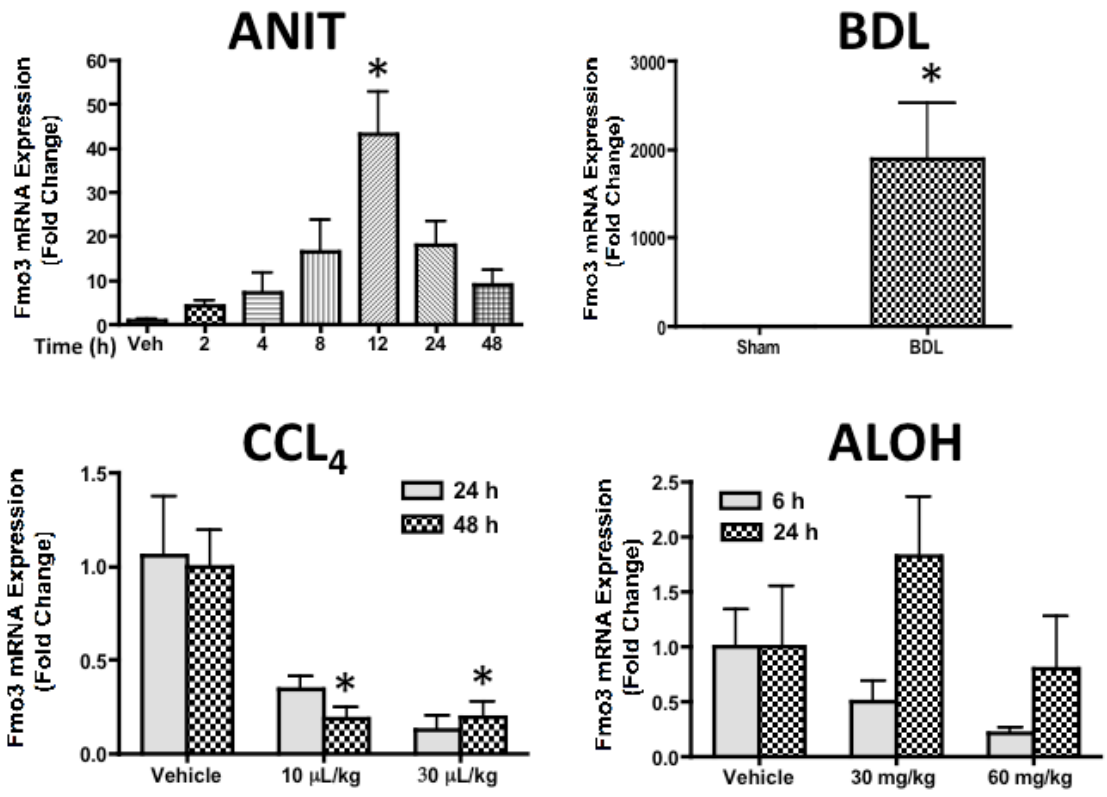
ANIT
Fmo3 mRNA Expression (Fold Change)
Time (h)
Veh
2
4
8
12
24
48
BDL
Sham
BDL
CCL4
24 h
48 h
Vehicle
10 µL/kg
30 µL/kg
ALOH
6 h
24 h
Vehicle
30 mg/kg
60 mg/kg

Figure 3.2 *Quantitative RT-PCR analysis of liver Fmo3 transcripts after hepatotoxicant treatment or BDL.* Livers were collected from mice sacrificed at respective time-points (2,4,8,12,24 & 48 h for ANIT; 24 & 48 h for CCl_4; 6 & 24 h for AlOH; and 10 d for BDL). RNA was isolated and cDNA was made using a commercial MMLV-RT kit. The cDNA samples were analyzed by quantitative RT-PCR using Fmo3 mouse-specific primers. Gene expression was normalized to the housekeeping gene β-actin. Fmo3 mRNA expression is presented as mean Fold Change ± SE. One-way ANOVA, t-test or two-way ANOVA was performed, appropriately, followed by the Dunnett's posttest for One-way ANOVA and the Bonferroni posttest for two-way ANOVA. Asterisks (*) represent a statistical difference ($p < 0.05$) between vehicle-treated and hepatotoxicant-treated or BDL group.

Figure 3.3

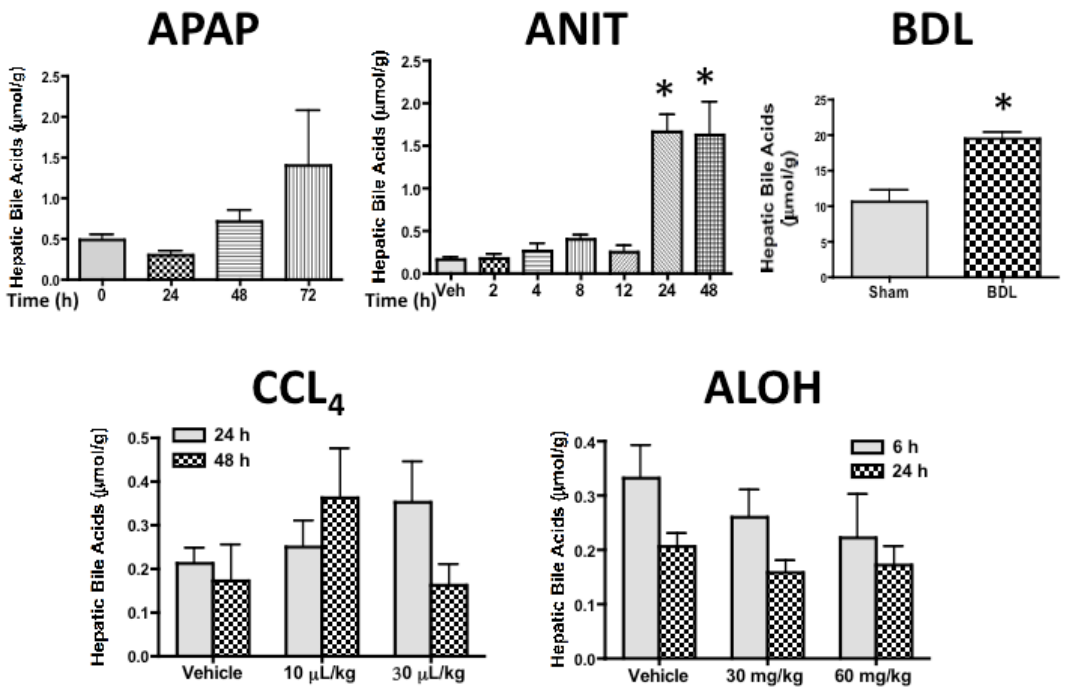
APAP
Hepatic Bile Acids (µmol/g)
Time (h)
0
24
48
72
ANIT
Hepatic Bile Acids (µmol/g)
Time (h)
Veh
2
4
8
12
24
48
*
*
BDL
Hepatic Bile Acids (µmol/g)
Sham
BDL
*
CCL4
Hepatic Bile Acids (µmol/g)
24 h
48 h
Vehicle
10 µL/kg
30 µL/kg
ALOH
Hepatic Bile Acids (µmol/g)
6 h
24 h
Vehicle
30 mg/kg
60 mg/kg

Figure 3.3 *Hepatic bile acid levels after hepatotoxicant administration or BDL.* Livers were collected at the end of each study (24, 48 & 72 h for APAP; 2,4,8,12,24 & 48 h for ANIT; 10 d for BDL; 24 & 48 h for CCl_4; and 6 & 24 h for AlOH). Liver total bile acids were measured spectrophotometrically using a commercial bile acid assay kit. Hepatic total bile acids are expressed as mean hepatic bile acids (µmol/g) ± SE. One-way ANOVA, t-test or two-way ANOVA was performed, appropriately, followed by the Dunnett's posttest for one-way ANOVA and the Bonferroni posttest for two-way ANOVA. Asterisks (*) represent a statistical difference ($p < 0.05$) between vehicle-treated and hepatotoxicant-treated or BDL group.

Figure 3.4

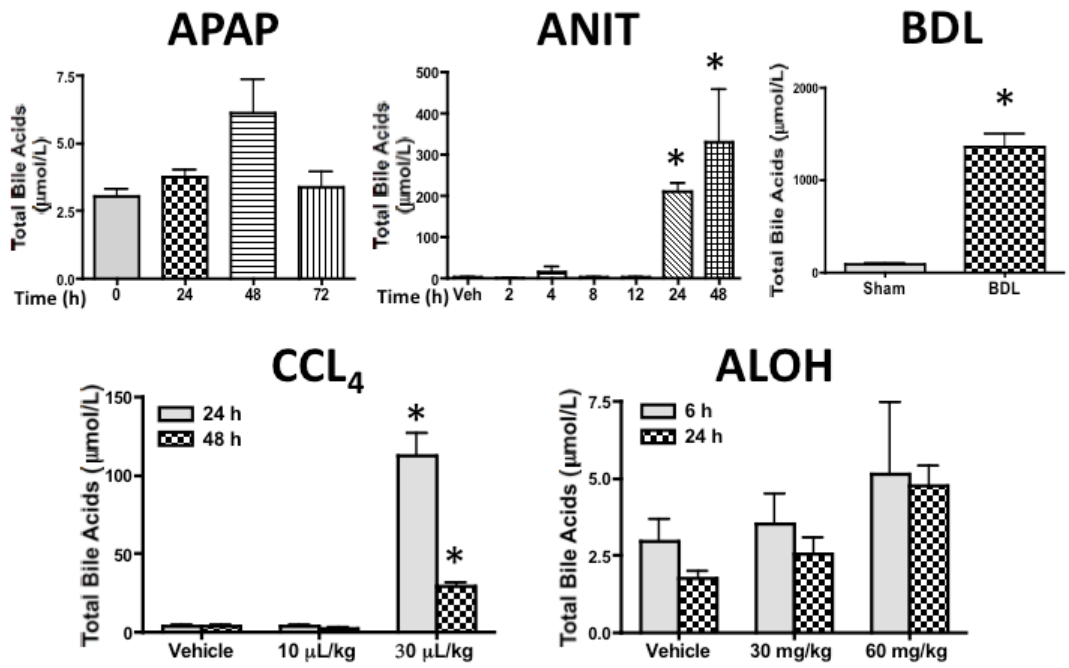
APAP
Total Bile Acids (µmol/L)
7.5
5.0
2.5
0.0
Time (h)
0
24
48
72
ANIT
Total Bile Acids (µmol/L)
500
400
300
200
100
0
Time (h)
Veh
2
4
8
12
24
48
*
BDL
Total Bile Acids (µmol/L)
2000
1000
0
Sham
BDL
*
CCL4
Total Bile Acids (µmol/L)
150
100
50
0
24 h
48 h
Vehicle
10 µL/kg
30 µL/kg
*
ALOH
Total Bile Acids (µmol/L)
7.5
5.0
2.5
0.0
6 h
24 h
Vehicle
30 mg/kg
60 mg/kg

Figure 3.4 *Blood levels of Total Bile acid in the mouse models of liver injury.* Mice were administered APAP (400 mg/kg, ip, 24, 48 & 72 h), ANIT (50 mg/kg, po, 2,4,8,12,24 & 48 h), CCl_4 (10 & 30 µL/kg, ip, 24 & 48 h), AlOH (30 & 60 mg/kg, ip, 6 & 24 h) or BDL (10 d). Blood was collected and the plasma or serum (for BDL) was isolated by centrifugation. Total bile acid levels were measured spectrophotometrically using a commercial bile acid assay kit. Total bile acids are expressed as mean total bile acids (µmol/L) ± SE. Student's t-test, one-way ANOVA, or two-way ANOVA was performed, appropriately, followed by the Dunnett's posttest for one-way ANOVA and the Bonferroni posttest for two-way ANOVA. Asterisks (*) represent a statistical difference ($p < 0.05$) between vehicle-treated and hepatotoxicant-treated or BDL group.

Figure 3.5

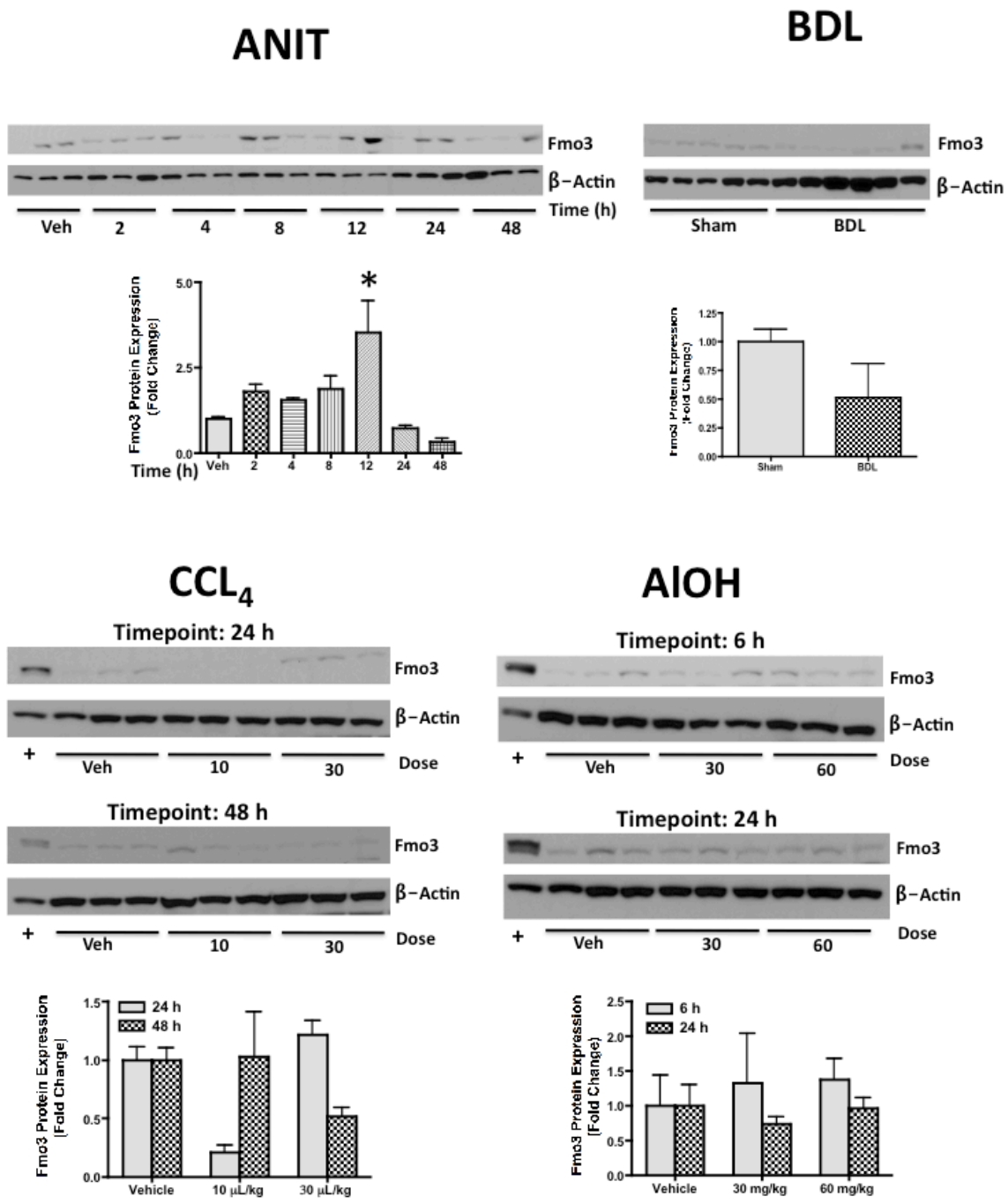
ANIT
BDL
Fmo3
β−Actin
Time (h)
Veh
2
4
8
12
24
48
Sham
BDL
Fmo3 Protein Expression (Fold Change)
CCL4
AlOH
Timepoint: 24 h
Timepoint: 48 h
Timepoint: 6 h
Timepoint: 24 h
Dose
10
30
60
24 h
48 h
6 h
Vehicle
10 µL/kg
30 µL/kg
30 mg/kg
60 mg/kg

Figure 3.5 *Analysis of liver Fmo3 protein expression in the mouse models of liver injury by western blotting.* Western immunoblots for Fmo3 were performed using liver microsomes from control and hepatotoxicant-treated or BDL mice. A custom-made rabbit anti-mouse Fmo3 primary antibody, described in *Materials and Methods* was used to detect Fmo3. Fmo3 protein levels were normalized to β-actin loading control. Microsomal proteins isolated from naïve female mouse liver was used as a positive control (indicated by "**+**" sign). The data are presented as blots and as mean Fmo3 protein expression (Fold Change) ± SE. One-way ANOVA, t-test or two-way ANOVA was performed, appropriately, followed by the Dunnett's posttest for One-way ANOVA and the Bonferroni posttest for two-way ANOVA. Asterisks (*) represent a statistical difference ($p < 0.05$) between vehicle-treated and hepatotoxicant-treated or BDL group.

Figure 3.6

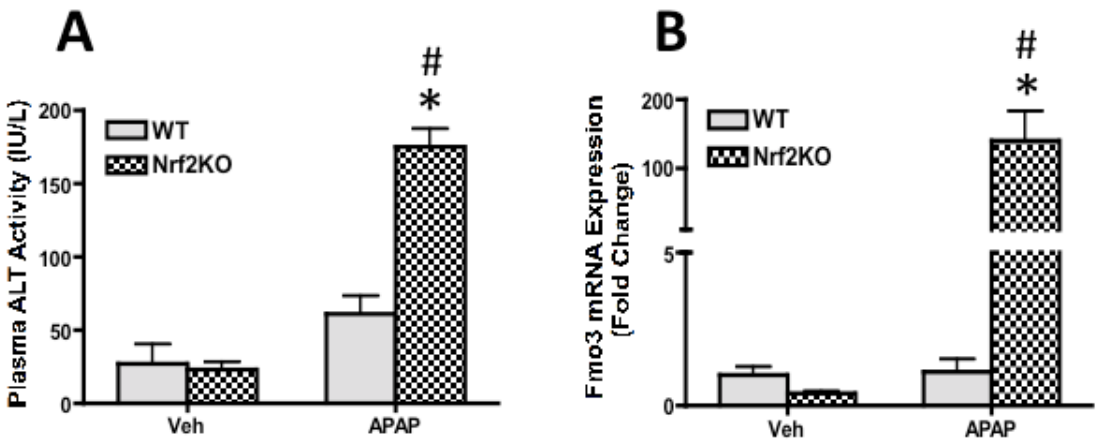
A
Plasma ALT Activity (IU/L)
200
150
100
50
0
WT
Nrf2KO
#
*
Veh
APAP
B
Fmo3 mRNA Expression
(Fold Change)
200
100
5
0
WT
Nrf2KO
#
*
Veh
APAP

Figure 3.6 *Plasma ALT activity and quantitative RT-PCR analysis of liver Fmo3 transcripts following a single dose APAP treatment in wild-type and Nrf2-knockout mice.* Plasma and livers were collected from mice 72 h following APAP (400 mg/kg) or vehicle treatment. **(A)** The data are presented as mean plasma ALT (IU/L) ± SE. **(B)** RNA was isolated from livers and cDNA samples were analyzed by quantitative RT-PCR using Fmo3 mouse-specific primers. Gene expression was normalized to the housekeeping gene β-actin. Fmo3 mRNA expression are presented as mean Fold Change ± SE. One-way ANOVA was performed followed by the Dunnett's post-test. Asterisks (*) represent a statistical difference ($p < 0.05$) between vehicle-treated group and APAP-treated group and pound (#) represent a statistical difference ($p<0.05$) compared with APAP-treated wild-type mice.

Figure 3.7

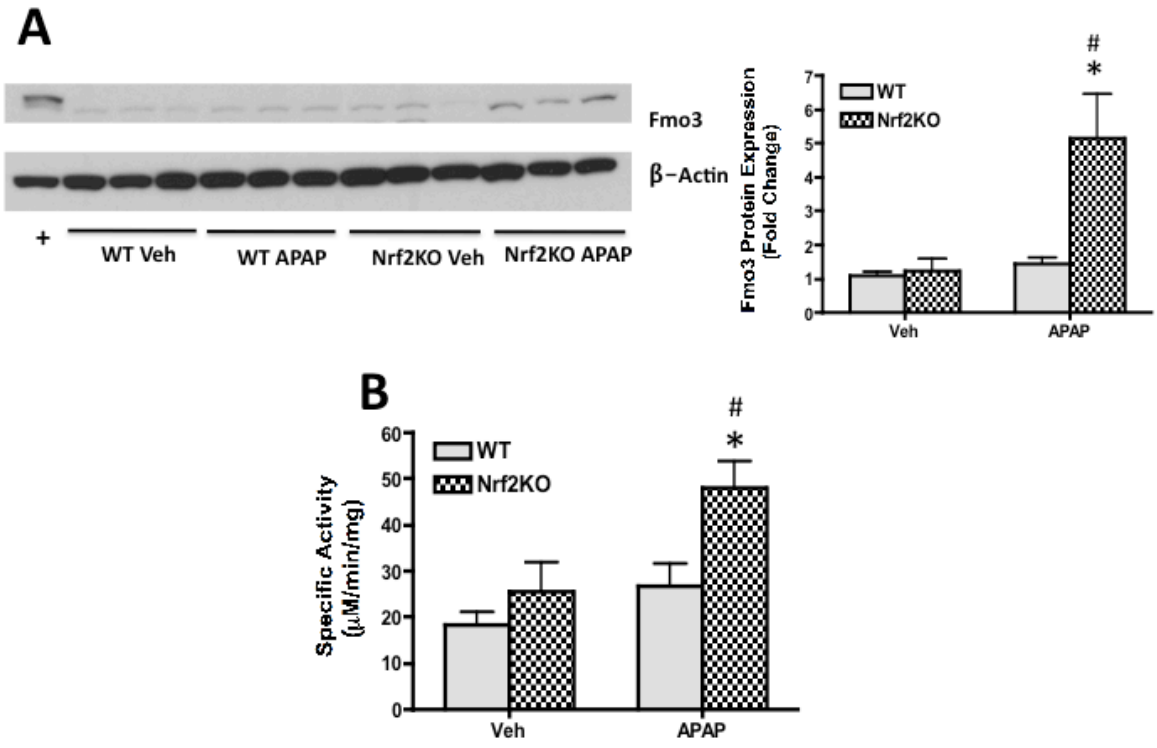
A
Fmo3
β−Actin
+
WT Veh
WT APAP
Nrf2KO Veh
Nrf2KO APAP
Fmo3 Protein Expression (Fold Change)
WT
Nrf2KO
#
*
Veh
APAP
B
Specific Activity (μM/min/mg)
WT
Nrf2KO
#
*
Veh
APAP

Figure 3.7 *Analysis of liver Fmo3 protein expression following a single dose APAP treatment in wild-type and Nrf2-knockout mice by western blotting and enzyme activity assay.* After overnight fasting, groups of wild-type and Nrf2 knockout mice received a single dose of 400 mg/kg APAP or vehicle. Livers were collected 72 h following APAP or vehicle treatments. Western blots for Fmo3 was performed using liver microsomes from control and APAP-treated mice. Equal protein loading (10 µg protein/lane) was confirmed by detection of β-actin. Microsomal proteins isolated from naïve female mouse liver were used as a positive control indicated by "**+"** sign. The data are presented as blots and as mean Fmo3 protein expression (Fold Change) ± SE **(A)**. FMO activity was measured in liver microsomes from control and APAP-treated mice using methimazole as substrate. Data are presented as mean Specific Activity (µM/min/mg) ± SE **(B)**. Asterisks (*) represent a statistical difference ($p<0.05$) between vehicle-treated group and APAP-treated group and pound (#) represent a statistical difference ($p<0.05$) compared with APAP-treated wild-type mice.

3.5 Discussion

FMO3 is a microsomal enzyme involved in the oxygenation of lipophilic substrates to more polar metabolites. Substrates include nitrogen-, sulfur- and phosphorous-containing drugs and xenobiotics, and most metabolic products of Fmo3 are considered to be non-toxic (Krueger & Williams, 2005). Although FMOs were discovered in the 1960s (Miller et al., 1960) and further purified in 1972 (Ziegler & Mitchell, 1972), it was not until 2008 that enzyme induction by xenobiotics was demonstrated (Celius et al., 2008; Celius et al., 2010). In these studies, in spite of a very large increase in Fmo3 mRNA level by AhR agonist treatment, only a modest increase in protein level and function was reported. A gene array analysis performed in our laboratory also demonstrated *Fmo3* gene induction in the mouse model of APAP autoprotection (O'Connor et al., 2014). In this APAP autoprotection mouse model, we show a significant increase in Fmo3 protein expression and function (Rudraiah et al., 2014). Constitutive Fmo3 expression in a female mouse liver is localized in the areas surrounding the periportal region (Janmohamed et al., 2004; Rudraiah et al., 2014). Following APAP exposure, the Fmo3 protein expression in APAP autoprotected livers is observed in the centrilobular regions where APAP-induced damage and/or hepatocellular compensatory proliferation is detected. Furthermore, we show that the enhanced expression of Fmo3 confers resistance against APAP-induced hepatotoxicity in mice (Rudraiah et al., 2014).

In the present study, the effect of various other hepatotoxicants on *Fmo3* gene expression in male C57BL/6J mouse liver was examined. A unifying theme for all hepatotoxicants used in our study is the oxidative stress. These models of oxidative stress used are very well studied with respect to activation of Nrf2-Keap1 regulatory pathway. This has been repeatedly demonstrated in our laboratory and in the literature (Aleksunes et al., 2005; Aleksunes et al., 2006; Aleksunes et al., 2006; Bauer et al., 2000; Chiu et al., 2002; Goldring et al., 2004; Liu et al., 2013; Randle et al., 2008; Tanaka et al., 2009). Thus, we were confident that the treatments selected result in oxidative stress and therefore the need for measuring markers of oxidative stress for each experimental group of hepatotoxicity was not deemed necessary.

Coincidentally, all of the hepatotoxicants selected produce cholestasis, with the exception of AlOH (Donepudi et al., 2012; Tanaka et al., 2009; Weerachayaphorn et al., 2012; Yamazaki et al., 2013). Furthermore, perturbation of bile acid homeostasis has been demonstrated to be an early event in the pathogenesis of drug induced liver injury (Yamazaki et al., 2013). To determine whether accumulation of bile acids is a signaling event regulating Fmo3, we measured total hepatic and plasma bile acid levels. Consistent with the literature, ANIT and BDL increased plasma and hepatic bile acid concentrations. A high CCl_4 dose did not significantly alter liver bile acid levels, but significantly increased plasma bile acid concentration. APAP

tended to increase both hepatic and plasma bile acid concentrations, but this is not statistically significant.

In general, ANIT and BDL-mediated damage significantly increased liver Fmo3 mRNA expression. While CCl_4-mediated liver injury significantly decreased Fmo3 mRNA expression, no change in expression is evidenced with AlOH. Fmo3 mRNA expression in response to ANIT treatment precedes serum and hepatic bile acid accumulation and the maximal *Fmo3* expression (both mRNA and protein) parallels the mild hepatocellular damage observed. This observation argues against the concept that hepatic bile acid accumulation is a pre-requisite for *Fmo3* gene expression changes in the ANIT model. With BDL, unlike ANIT, Fmo3 mRNA induction is associated with higher serum and hepatic bile acid levels, but protein level does not change. Since tissues were analyzed 10 days after BDL, we do not have a sense of what the temporal relationship is between hepatic bile acid accumulation and elevated Fmo3 mRNA induction. This relationship deserves further attention based on the discussion of FXR signaling that can be found below.

Overt ANIT-induced hepatocellular damage at 24 and 48 h decreased *Fmo3* gene expression and the decease is statistically significant at 48 h compared to the 12 h ANIT-treated group. This observation with respect to the relationship between plasma ALT level and *Fmo3* gene expression is consistent with our results with APAP hepatotoxicity. We have demonstrated in our APAP autoprotection mouse model that the APAP (400 mg/kg)

pretreated group as well as the autoprotected group (APAP pretreatment: 400 mg/kg, APAP challenge: 600 mg/kg) exhibit average plasma ALT values of about 250 IU/L and Fmo3 protein induction. The group that receives a toxic APAP dose of 600 mg/kg exhibits much greater average plasma ALT activity of about 1600 IU/L, but no *Fmo3* gene induction (Rudraiah et al., 2014).

One key feature that is consistent with APAP-, BDL- and ANIT-induced liver injury and enhanced *Fmo3* gene expression is the magnitude in plasma ALT elevations. Mild ALT elevation is the common feature for all three models where Fmo3 mRNA induction is observed. Although BDL is a chronic injury model, it is well known that the ALT values do not correlate well with the severity of liver damage particularly during fibrotic hepatocellular necrosis (Kallai et al., 1964). A similar clinical feature is also seen in cases of primary biliary cirrhosis (BDL models primary biliary cirrhosis in humans) (Hohenester et al., 2009). The lack of Fmo3 protein detection during BDL may be due to signal dilution by fibrotic liver tissue. It is also possible that under oxidative stress conditions some proteins involved in translation are oxidized *in vivo* inhibiting translation (Shenton et al., 2006). To add to this complexity, in spite of lower plasma ALT activity at 24 h (low dose CCl_4), and 48 h (both high and low dose CCl_4) with CCl_4, there is down-regulation of *Fmo3* gene expression. In AlOH-treated livers, lower plasma ALT activity did not show any change in *Fmo3* gene expression. This is suggestive of an unknown underlying mechanism unique to APAP, ANIT, and BDL, which is contributing to *Fmo3* mRNA induction. Studies are necessary to investigate the regional distribution

of Fmo3 protein expression during ANIT- and BDL-induced liver injury to determine whether the protein expression in these models is localized to the portal vein, where ANIT- and BDL-induced hepatotoxicity is confined. Collectively, these data suggest that there is a threshold for degree of hepatic injury that results in increased Fmo3 mRNA and protein expression. More specifically, these data suggest that acute moderate or mild hepatotoxicity is optional for Fmo3 induction, while chronic, severe hepatotoxicity is not.

As discussed before, all models of hepatic injury used in the current study result in hepatic oxidative stress and activate the Nrf2-Keap1 regulatory pathway. Importantly, CRE analysis of differentially expressed genes in our APAP autoprotection study supported an induction of the Nrf2 pathway (O'Connor et al., 2014). Additionally, Celius et al. showed that the 5'-flanking region of the mouse *Fmo3* contains multiple copies of the ARE (Celius et al., 2008). Promoter analysis of mouse *Fmo3* promoter (7 kb length) using MatInspector software (Genomatix, Munich, Germany), also showed an ARE at about 3 kb from the transcription start site (data not shown). We also found two other binding sites for Bach1, at 600 bp and 2 kb from the *Fmo3* transcription start site (data not shown). Bach1 is a regulatory mediator of Nrf2, in that it is a transcription repressor. Bach1 heterodimerizes with small Maf proteins in the absence of cellular stress and represses gene expression. In the presence of oxidative stress, Bach1 is released from the Maf proteins and is replaced by Nrf2 (Kaspar et al., 2009). Thus, using APAP as a model toxicant for Nrf2 activation, *Fmo3* gene expression was evaluated in Nrf2 KO

mice. Compared to APAP-treated wild-type mice, Nrf2 KO mice exhibit persistent and significant hepatocellular damage 72 h after APAP administration. Nrf2 KO mice are not only more susceptible to APAP-induced hepatocellular necrosis, but also fail to recover from injury as rapidly as the WT mice. This is consistent with the literature that describes Nrf2 as a master regulator of many cytoprotective genes involved in APAP-induced hepatotoxicity (Aleksunes et al., 2005; Aleksunes et al., 2006; Bauer et al., 2000; Chiu et al., 2002; Goldring et al., 2004). Finally, *Fmo3* gene induction by APAP treatment in Nrf2 null mice suggests that the transcriptional regulation of Fmo3 does not involve this transcription factor. The persistent mild hepatocellular injury and oxidative stress in Nrf2 KO mice most likely activates other signaling mechanisms involved in *Fmo3* gene induction.

Future studies will investigate the role of other nuclear receptors in *Fmo3* gene induction. Particularly, farnesoid X receptor (FXR) role in *Fmo3* gene induction during APAP hepatotoxicity is worth investigating. FXR is one of the major bile acid sensors in the liver (Chiang, 2002) and plays a protective role during cholestasis development. Recently, it is shown that activation of FXR induces Fmo3 protein function (Bennett et al., 2013). Activation of FXR also provides protection against APAP-induced hepatotoxicity (Lee et al., 2010). In addition, we discovered three binding sites for farnesoid X receptor-response element (FXRE) at about 1.6, 2.1 and 3.3 kb from the transcription start site on the mouse *Fmo3* promoter (data not shown). Although, Pregnane X receptor (PXR) is also a bile acid sensor, no

binding sites for PXR were found on promoter analysis and furthermore, PXR activation sensitizes APAP-induced hepatotoxicity (Cheng et al., 2009; Guo et al., 2004).

In conclusion, this study comprehensively characterizes for the first time temporal changes in *Fmo3* gene expression during different conditions known to impart hepatic oxidative stress. In particular, we show that toxic ANIT and BDL significantly alter Fmo3 mRNA expression, but only Fmo3 protein with ANIT. The reason for this discrepancy is not yet clear or easy to rationalize. It is possible that *Fmo3* is also protective during other chemical-induced liver injury including ANIT. Even though the exact mechanism of *Fmo3* gene expression or its role in protecting against toxicant-induced liver injury is not yet clear, the observed toxicity threshold for *Fmo3* gene expression is intriguing. This work advances the lack of knowledge with regard to the inducibility of *Fmo3* and its potential protective role in drug-induced liver injury.

CHAPTER 4

Establishment and Characterization of HepaRG Cell Line Over-Expressing Human Flavin-containing Monooxygenase-3 (FMO3)

4.1 Abstract

Flavin-containing monooxygenase (FMO) is a drug metabolizing enzyme system similar to cytochrome P450 (CYP). FMO and CYP exhibit similar cellular localization and substrate specificity, but a different catalytic cycle. FMOs were considered to be non-inducible by xenobiotics, but recently we demonstrated liver *Fmo3* gene induction and protein expression during APAP hepatotoxicity. The role of FMO3 in APAP-induced hepatotoxicity is not known. The goal of the present study was to investigate *FMO3* gene expression, and its role in APAP-induced cytotoxicity *in vitro* using HepaRG cells. HepaRG cells have been recently used as a human *in vitro* model for studying mechanisms of APAP hepatotoxicity. In this study, exposure of HepaRG cells to APAP resulted in a significant increase in *FMO3* gene expression as we see *in vivo*. To determine the functional significance of *FMO3* induction during APAP toxicity, we developed a HepaRG cell line over-expressing human FMO3 (hFMO3-HepaRG). Clonal selection from a heterogeneous population of hFMO3-HepaRG cells resulted in two homogenous cell lines. Expression of FMO3 in these clones was confirmed by qRT-PCR, western blotting and by a catalytic activity assay. Notably, the

hFMO3-HepaRG clones had a faster rate of differentiation that was dependent on the expression level of FMO3 compared to EV controls. Consistent with a faster rate of differentiation in these clones, rifampicin-induced CYP3A4 expression was also greater. In agreement with our postulated role for FMO3 as genetic determinant of APAP toxicity, the low hFMO3-HepaRG clone exhibits greater tolerance to APAP-induced (1, 5, 10 and 15 mM) cytotoxicity. In the high hFMO3-HepaRG clone, LDH leakage is significantly lower only at 1 and 5 mM APAP, while at a higher APAP concentrations, LDH leakage is significantly greater than in empty vector controls. Taken together, our results suggest that changes in *FMO3* gene expression not only alter HepaRG cell phenotype, evidenced by an expression level-dependent greater rate of cell differentiation, but also alter susceptibility to APAP-induced cytotoxicity.

4.2 Introduction

Acetaminophen is one of the most commonly used over-the-counter analgesic and antipyretic agent in the U.S. and Great Britain. It was first described more than a century ago. However, APAP-poisoning and APAP-hepatotoxicity was first recognized in 1960s in Great Britain (Davidson & Eastham, 1966) and later in the U.S. (McJunkin et al., 1976). APAP usage increased after aspirin was implicated in over 80 % of Reye's syndrome cases in children. As APAP usage increased, the incidence of APAP-induced hepatotoxicity also increased. In a retrospective study from 1994 to 1996, APAP-induced hepatotoxicity comprised 20 % of all cases of acute liver failure (ALF) in the U.S. (Schiodt et al., 1999). These numbers increased over time and by the early 2000s, nearly 50 % of all ALF cases were due to APAP use and misuse. APAP toxicity is still a very prominent cause of liver toxicity, accounting for more that 50 % of all ALF from all etiologies (Larson et al., 2005; Lee, 2010). The potential for drug-related morbidity and mortality, and the popularity of this drug, make it a significant human health problem.

Until recently, the consensus was that Flavin-containing monooxygesnases (FMOs) were not inducible (Cashman & Zhang, 2002; Krueger & Williams, 2005). However, recently Celius et al. show that activation of the Aryl hydrocarbon (Ah) receptor by 2,3,7,8-tetrachlorodibenzo-p-dioxin (TCDD) induces Fmo3 mRNA in mice, with marginal changes detected in protein levels (Celius et al., 2008; Celius et al.,

2010). Previous work in our laboratory has also documented induction of *Fmo3* gene expression in an APAP autoprotection mouse model (mice pretreated with APAP acquires resistance to APAP re-exposure) (O'Connor et al., 2014; Rudraiah et al., 2014). Furthermore, we also demonstrated an association between *Fmo3* expression and protection against APAP-induced hepatotoxicity (Rudraiah et al., 2014). More specifically, female mice express much greater Fmo3 protein levels in liver compared to their male counterparts. In fact, Fmo3 protein expression in normal male mouse liver is undetectable by immunochemical techniques (Rudraiah et al., 2014). Coincidentally, female mice are highly resistant to APAP hepatotoxicity (Dai et al., 2006). Taking advantage of this sex-dependent difference in liver *Fmo3* expression in C57BL/6J mice, we demonstrated that administration of the FMO inhibitor methimazole (MMI) renders female mice susceptible to APAP-induced hepatotoxicity (Rudraiah et al., 2014). Results from FMO3-over-expressing human hepatocyte cell line (HC-04) also supports the conclusion that Fmo3 is important for development of resistance to APAP-induced hepatotoxicity.

The human liver, similar to our APAP autoprotection mouse model, can adapt to APAP-induced hepatotoxicity (Shayiq et al., 1999; Watkins et al., 2006). In these studies, individuals developed tolerance to hepatotoxicity following repeated exposure to supratherapeutic doses of APAP. Although the clinical data suggest that the human liver can adapt to APAP-induced hepatotoxicity similar to that seen in our APAP autoprotection mouse model,

the mechanism for this adaptation is not known. Unlike C57BL/6J mouse liver where Fmo3 expression is negligible, FMO3 is the predominant FMO enzyme in the adult human liver with levels comparable to CYP3A4 (Koukouritaki et al., 2002). Furthermore, inducibility of FMO3 in the human liver has not been reported.

The HepaRG cell line, derived from a hepatoma in a female patient, is a recently developed *in vitro* system for studying hepatotoxicants. HepaRG cells are bipotent progenitors, that differentiate into hepatocyte-like cells and biliary epithelial-like cells (Cerec et al., 2007; Parent et al., 2004). HepaRG expresses a more normal spectrum of drug metabolizing enzymes similar to primary human hepatocytes and human liver tissues, unlike other hepatoma cell lines such as HepG2 (Hart et al., 2010). HepG2 cells express very low cytochrome P450 (CYP) levels compared to primary human hepatocytes or human liver, particularly those involved in APAP metabolism. McGill et al. have demonstrated that many of the mechanistic features of APAP-induced hepatotoxicity in mouse hepatocytes and HepaRG cells are very similar. In addition, APAP-induced cytotoxicity as well as key mechanistic events occurring in HepaRG cells are consistent to that seen in mouse hepatocytes (McGill et al., 2011). Thus, the goal of the current study was to investigate *FMO3* gene expression in HepaRG cells and to determine the functional significance of *FMO3* over-expression during APAP-induced cytotoxicity.

4.3 Materials and Methods

Chemicals

All chemicals were obtained from Sigma-Aldrich (St Louis, MO) and were of reagent grade or better.

Cell Culture and Treatment

HepaRG cells, growth supplement and differentiation medium supplement were obtained from Biopredic International (Saint-Gregoire, France). Cells were maintained in Williams E medium supplemented with 1X glutamax, 0.05 mM riboflavin, growth or differentiation supplement and 1 % antibiotic-antimycotic (100 units/mL penicillin G sodium, 100 µg/mL streptomycin sulfate, and 0.25 µg/mL amphotericin B) in a 5 % CO_2 and humidified environment (95 % relative humidity) at 37°C. HepaRG cell line differentiation was performed according to manufacturer's protocol and is presented as a flowchart in Figure 4.1. Briefly, HepaRG cells were grown at high density in growth medium for 14 d. Cell differentiation was induced by maintaining cells in the differentiation medium for an additional 14 to 21 d. The medium was renewed every 3 d. The cells were maintained for up to four weeks after differentiation for use.

For all treatments, HepaRG cells were seeded at $4x10^5$ cells/well in a 24-well plate. For rifampicin treatment, cells were cultured in induction medium (Biopredic International) containing 10 µM rifampicin (diluted from 1000X rifampicin stock in DMSO) for 24 h. Cells were harvested in TRIzol

reagent for RNA isolation. For APAP treatment, culture media was replaced with tox medium (Biopredic International, Saint-Gregoire, France) containing APAP (concentrations ranging from 1 mM to 15 mM). Cells were harvested for measuring LDH leakage, RNA- or microsomal-protein isolation 24 h later. For MMI treatment, cells were incubated in tox medium containing 1 mM MMI for 30 min at 37 °C. Following incubation with MMI, culture medium containing 5 mM APAP was added to wells. Cytotoxicity was measured using the LDH assay kit, 24 h later. All experiments were performed in triplicates and repeated at least three times.

Preparation of Microsomal Fractions for Western Blot Analysis

Microsomes were isolated from cells as described previously (Rudraiah et al., 2014). Protein concentration was determined by the method of Lowry using Bio-Rad protein assay reagents (Bio-Rad Laboratories, Hercules, CA). Microsomal proteins (10 µg) were electrophoretically resolved using 10 % polyacrylamide gels and transferred onto PVDF-Plus membrane (Micron Separations, Westboro, MA). A rabbit anti-human FMO3 primary antibody (BD Gentest, NJ) at a 1:500 dilution was used to detect FMO3, with β-Actin as loading control. Blots were then incubated with horseradish peroxidase (HRP) conjugated secondary antibodies against rabbit IgG (Sigma-Aldrich, St Louis, MO). Protein-antibody complexes were detected using a chemiluminescent kit (Thermo Scientific, IL) with visualization using GeneMate blue autoradiography film (Bioexpress, Kaysville, UT).

RNA Isolation and Quantitative Real-Time Polymerase Chain Reaction (qRT-PCR)

TRIzol reagent (Life Technologies, Carlsbad, CA) was used to extract total RNA from cells and cDNA was made using the M-MLV RT kit (Invitrogen, Carlsbad, CA). mRNA expression was quantified by the ΔΔCT method and normalized to the housekeeping gene, β-actin. Primer pairs were synthesized by Integrated DNA Technologies (Coralville, IA), and the primer sequences are presented in Table 1. Amplification was performed using an Applied Biosystems 7500 Fast Real-Time PCR System. Amplification was carried out in a 20 µL reaction volume containing 8 µL of diluted cDNA, Fast SYBR Green PCR Master Mix (Applied Biosystems, Foster City, CA) and 1 µM of each primer.

Lentiviral Vector Construction, Transduction and Clonal Selection

The FMO3-T2A-luc lentiviral transfer vector was constructed as described previously (Rudraiah et al., 2014). The replication-defective virus was generated in HEK 293T cells and concentrated as previously described (Rudraiah et al., 2014). HepaRG cells were seeded to confluency prior to transduction in HepaRG growth medium in a 24 well plate. The cells were then infected with a series of volumes of untitered concentrate (40 µL, 20 µL, and 10 µL per well) for three days. Prior to, during, and after viral transduction, cells were maintained in HepaRG growth medium containing 0.05 mM riboflavin. Media was changed every 3 days. Clonal selection from

heterogeneous hFMO3-HepaRG cells was performed by the method of dilution. Differentiation of selected clones was performed according to manufacturer's protocol described previously in this section.

Enzyme Assay

FMO3 enzyme activity assay was performed using methimazole (MMI) as substrate as described previously (Rudraiah et al., 2014). Briefly, MMI metabolism was determined spectrophotometrically by measuring the rate of MMI S-oxygenation via the reaction of the oxidized product with nitro-5-thiobenzoate (TNB) to generate 5,5'-dithiobis(2-nitrobenzoate) (DTNB). The incubation mixture consisted of NADPH generating system and 100 to 150 µg/mL microsomal protein in sodium phosphate buffer (pH 9.0). Reactions were initiated by the addition of different amounts of MMI. The range of MMI concentrations were between 1.25 and 800 µM. Specific activity (µM/min/mg) was determined using the molar extinction coefficient of NADPH (28.2 $mM^{-1}cm^{-1}$).

LDH Leakage

Percent lactate dehydrogenase (LDH) leakage was determined via the Tox-7 kit (Sigma-Aldrich, St. Louis, MO) as a measure of cytotoxicity following APAP treatment. The assay was performed according to manufacturer's instructions.

FMO3 Knockdown by shRNA

FMO3 short hairpin RNA (FMO3 shRNA) (sc-72256-SH) and scrambled shRNA (sc-108060) plasmids were obtained from Santa Cruz Biotechnology. Differentiated EV-HepaRG and hFMO3-HepaRG clones were plated at 40 to 80 % confluency 24 h prior to tansfection. FMO3 shRNA and scrambled shRNA plasmid transfection was performed using TransIT-TKO® Transfection Reagent (Mirus, Madison, WI) according to manufacturer's instructions. Following transfection, cells were harvested at 72 h to isolate RNA and protein. Stable shRNA knockdown of FMO3 was verified by qRT-PCR and western blot analysis for FMO3 mRNA and protein expression, respectively. All experiments were performed in triplicates and repeated at least three times. Representative results are reported.

Statistical Analysis

Results are expressed as mean ± standard error (SE). Data were analyzed using the Student's t-test or ANOVA followed by a post-hoc test. While Student's t-test was used to compare means of two different treatment groups, ANOVA was used to compare the means of more than two means of different treatment groups that are normally distributed with a common variance. All statistical analysis was performed using GraphPad Prism version 4.00 for Macintosh (GraphPad Software, Inc., San Diego, CA). Differences were considered significant at $p<0.05$.

Table 4.1. Primer Sequences for Quantitative RT-PCR

Gene	Primer Sequences
ABCC2 (MRP2)	Forward: 5'- TGG TTA TGG AGG CTG CAT CT -3'
	Reverse: 5'- CAT ACA GGC CCT GAA GAG GA -3'
ABCC3 (MRP3)	Forward: 5'- GAC CCA CAG GTA GAT GCA GG -3'
	Reverse: 5'- AGC TCG GCT CCA AGT TCT G -3'
ABCC4 (MRP4)	Forward: 5'- CCT TGC AAC TCC TCT CCA AG -3'
	Reverse: 5'- ATC TGC TCA CGC GTG TTC TT -3'
CYP1A2	Forward: 5'- CTT CGT AAA CCA GTG GCA GG -3'
	Reverse: 5'- AGG GCT TGT TAA TGG CAG TG -3'
CYP2E1	Forward: 5'- GAC CAC CAG CAC AAC TCT GA -3'
	Reverse: 5'- CCC AAT CAC CCT GTC AAT TT -3'
CYP3A4	Forward: 5'- TTT TGT CCT ACC ATA AGG GCT TT -3'
	Reverse: 5'- CAC AGG CTG TTG ACC ATC AT -3'
FMO3	Forward: 5'- TTG TAA ATG CTA GCC CTG CC -3'
	Reverse: 5'- CTG TCT GGA AGA GGG GCT G -3'
GCLC	Forward: 5'- CAA GGA CGT TCT CAA GTG GG -3'
	Reverse: 5'- CTT TCT CCC CAG ACA GGA CC -3'
GSTM1	Forward: 5'- CTG AAG GAC TTC ATC TCC CG -3'
	Reverse: 5'- CCC AGA CAG CCA TCT TTG AG -3'
UGT1A1	Forward: 5'- GTT GGT GGA ATC AAC TGC CT -3'
	Reverse: 5'- TTG ATC CCA AAG AGA AAA CCA -3'

4.4 Results

CYP3A4 Transcript Constitutive and Inducible Expression Profiles in HepaRG Cells

To examine the constitutive and inducible CYP3A4 mRNA expression in HepaRG cells, undifferentiated (early and late) and differentiated, HepaRG cells were treated with 10 μM rifampicin or vehicle for 24 h. CYP3A4 mRNA levels were quantified by qRT-PCR. The results in Figure 4.2 show that CYP3A4 mRNA levels with vehicle treatment increased by 2.8±0.5-and 6.3±0.8-fold, in late-undifferentiated and differentiated HepaRG cells, respectively, compared to the early-undifferentiated HepaRG cells. Following treatment with rifampicin, CYP3A4 mRNA expression increased by 12.5±1.1-, 56.6±2.3-, and 172.4±8.9-fold in early-undifferentiated, late-undifferentiated and differentiated HepaRG cells, respectively, in comparison with vehicle treated early-undifferentiated HepaRG cells.

FMO3 Gene Expression Following APAP Treatment in HepaRG Cells

To evaluate the *FMO3* gene expression after APAP treatment in HepaRG cells, differentiated HepaRG cells were treated with 1, 2.5 or 5 mM APAP or vehicle for 24, 48 and 72 h. APAP-induced cytotoxicity was measured by measuring percent LDH leakage into the culture media. The results are shown in Figure 4.3A. The percent LDH leakage into the medium did not change significantly with 1 mM APAP treatment at 24, 48 or 72 h. While percent LDH release with 2.5 mM APAP increased significantly at 24

and 48 h by 7.5±0.2 and 8.7±0.1 %, respectively, the values are not statistically significant at 72 h compared to respective control treatment. At all time-points tested (24, 48 and 72 h), 5 mM APAP treatment significantly increased the amount of LDH release in HepaRG cells to 8.5±0.3, 14.6±0.2, and 20.7±0.7 %, respectively. Then, the temporal FMO3 transcript expression after APAP treatment was evaluated. FMO3 mRNA expression in HepaRG cells exposed to APAP is presented in Figure 4.3B. FMO3 mRNA levels increased significantly by 2±0.35-, 2.1±0.3-, and 2±0.34- fold change in response to 1, 2.5 and 5 mM APAP, respectively, at 24 h. While FMO3 mRNA transcript levels peaked with 1 mM APAP treatment at 48 h by 3±0.4-fold change, the levels are not statistically significant at 72 h. No change is FMO3 mRNA expression is seen with all three doses at 72 h. To investigate if the increase in FMO3 transcripts translates into protein, we performed western blotting. Representative blots and densitometric analysis of blots are shown in Figure 4.3C. FMO3 protein is abundantly expressed in HepaRG cells (vehicle controls). Following treatment with 5 mM APAP, FMO3 protein levels increased significantly by 1.5±0.05- and 1.4±0.1-fold change at 24 and 48 h, respectively, compared to vehicle control. FMO3 protein levels decreased significantly at 72 h with 1, 2.5 and 5 mM APAP treatment compared to vehicle control. These data demonstrate that a single dose APAP treatment results in a significant increase in FMO3 protein levels in the human hepatoma cell line, HepaRG cells.

Establishment of Human Hepatoma Cell Line (HepaRG) Over-expressing Human FMO3 (hFMO3-HepaRG)

We developed a HepaRG cell line over-expressing human FMO3 to evaluate the functional significance of FMO3 over-expression during APAP-induced cytotoxicity. The FMO3 expression vector we used previously (Rudraiah et al., 2014) to over-express FMO3 in the human hepatocyte cell line (HC-04) was used again to over-express FMO3 in HepaRG cells. The expression vector is a bicistronic vector driven by the ubiquitin-C promoter, which allowed co-expression of the FMO3 and luciferase (LUC) genes in transduced HepaRG cells. Twelve clones were picked from a heterogenous population of hFMO3-HepaRG cells. Out of twelve clones selected, two clones were maintained for further studies. The clones expressed a 152±13- and 1031±12.6-fold change in luciferase activity, compared to the empty vector control (EV-HepaRG) (Figure 4.4A). For convenience, these two hFMO3-HepaRG clones are termed the Low-hFMO3-HepaRG and High-hFMO3-HepaRG cell line, respectively. FMO3 mRNA expression is shown in Figure 4.4B. FMO3 mRNA levels increased by 6.5±0.8- and 25±0.9-fold change in Low- and High-hFMO3-HepaRG cell line, respectively, compared with EV control. FMO3 protein expression was confirmed by performing western blotting and from FMO3 enzyme activity assay using microsomal fractions isolated from EV and both FMO3-over-expressing HepaRG clones. Representative blots, densitometric analysis of western blot and the specific activity of over-expressed FMO3 protein are shown in Figure 4.4C, 4.4D and

4.4E, respectively. Fmo3 protein levels increased by 3.2±0.1- and 5±0.04-fold in Low-, and High-FMO3 expressing HepaRG cells, respectively. Consistent with western blotting results, the specific activity of over-expressed FMO3 protein also increased to 98±1.5, and 150±8.7 µM/min/mg in Low-, and High-FMO3 expressing HepaRG cells, respectively, compared to EV-HepaRG control (64.4±5.2 µM/min/mg).

Phenotypic Characteristics of hFMO3-HepaRG Cells in Culture

Representative phase-contrast micrographs of hFMO3-HepaRG Cells in culture are shown in Figure 4.5. hFMO3-HepaRG cells exhibit a strikingly faster rate of differentiation (formation of colonies of granular epithelial cells) compared to empty vector control cells. This is evident by the appearance of colonies of granular epithelial cells in the High-hFMO3-HepaRG clone as early as 14 d while cells are still in growth medium. (Figure 4.5C). Empty vector and Low-hFMO3-HepaRG also differentiate but at slower rates. At all stages of differentiation, there is a consistent, expression level-dependent increase in rate of differentiation of hFMO3-HepaRG cells.

Transcript Expression of Transporters, Bioactivation- and Detoxification-Enzymes for APAP in hFMO3-HepaRG Cells

Untreated hFMO3-HepaRG cell lines were characterized with respect to the expression of genes critical in APAP bioactivation, transporters and detoxification pathways by qRT-PCR. Results are shown in Figure 4.6. No significant change in CYP1A2 expression is seen in both hFMO3-HepaRG

cell lines compared to EV controls. However, CYP2E1 mRNA levels increased by 5.3±0.1- and 14.2±0.2-fold change in Low- and High-hFMO3-HepaRG cell line, respectively. Among all bioactivation gene expression tested, the increase in CYP3A4 mRNA is highest by a fold change of 11±0.4 and 53±2.2 in Low- and High-hFMO3-HepaRG cell line, respectively, compared to EV control. The expression of phase II enzyme, UDP glucuronosyltransferase 1 family, polypeptide A1 (UGT1A1) also increased significantly by 2.7±0.3-fold change in High-FMO3 expressing clone while no change in expression was evidenced in the Low-FMO3 expressing clone. The expression of Glutamate-cysteine ligase (GCLC) and glutathione S-transferase μ1 (GSTM1) showed a decreasing trend in both clones. This decrease is statistically significant only with GCLC in the High-FMO3 expressing HepaRG cells. While the expression of ATP-binding cassette, sub-family C/multidrug resistance-associated protein (ABCC/MRP) particularly MRP3 and MRP4 tended to decrease with increasing FMO3 expression, this was not statistically significant. MRP2 expression on the other hand increased significantly in high-FMO3 expressing clone by 3.3±0.14-fold change compared to EV control.

CYP3A4 Transcript Constitutive and Inducible Expression Profiles in hFMO3-HepaRG Cells

To determine the CYP3A4 transcript constitutive and inducible expression in hFMO3-HepaRG cells, undifferentiated (early and late) and differentiated hFMO3-HepaRG cells were treated with 10 μM rifampicin or

vehicle for 24 h. CYP3A4 mRNA levels were quantified by qRT-PCR. mRNA levels are presented as graphs (4.7A and 4.7B) and tabulated in Figure 4.7C. The results in Figure 4.7A show CYP3A4 constitutive mRNA levels at undifferentiated (early and late) and differentiated stages. CYP3A4 mRNA expression is significantly higher in High-hFMO3-HepaRG cells at both late-undifferentiated and differentiated stages. Following treatment with rifampicin, CYP3A4 mRNA expression further increases significantly by 140.7±22- and 884.9±48.1-fold change in late-undifferentiated and differentiated in High-hFMO3-HepaRG cells, respectively, compared to respective EV-HepaRG controls (Figure 4.7B). These results are consistent with the faster rate of differentiation phenotype observed in hFMO3-HepaRG cell lines. Collectively, these data suggest that there is a correlation between FMO3 expression and differentiation in HepaRG cells that over-express human FMO3 protein and function.

Effect of FMO3 Over-expression on APAP-induced Cytotoxicity in HepaRG Cells

The basal LDH leakage in vehicle treated High-hFMO3-HepaRG clone is significantly lower (6 %) than the EV-HepaRG cells (15 %) (Figure 4.8A). In Figure 4.8B, the basal LDH leakage in significantly lower in both the Low- and the High-hFMO3-HepaRG clones (13 % and 6 %) compared to EV controls (20 %). This suggests that FMO3 over-expression contributes to a characteristic cellular ability to resist stress.

To evaluate the functional significance of *FMO3* over-expression during APAP-induced cytotoxicity, EV-HepaRG and hFMO3-HepaRG cells were treated with 1, 5, 10 and 15 mM APAP for 24 h. The percent LDH leakage into the media in response to these four concentrations of APAP in Low-FMO3 expressing HepaRG cells is significantly lower (13, 16, 23 and 24 %) compared to empty vector control (18, 22, 27 and 28 %). The percent LDH leakage in High-FMO3 expressing cells following 1 and 5 mM APAP treatment is significantly lower (8 and 11 %) than in EV cells, while higher LDH values (33 %) are seen at 15 mM APAP than in EV cells treated with the same concentration of APAP (Figure 4.8A). Taken together, these data suggest that over-expression of FMO3 protects against APAP-induced cytotoxicity in the Low-hFMO3-HepaRG clone. By contrast, High-hFMO3-HepaRG cells are protected against lower APAP concentrations, but APAP cytotoxicity is aggravated at higher APAP concentrations with high FMO3 expression.

The amount of LDH leakage (%) into the media does not change with only MMI treatment, compared with vehicle treated EV- and hFMO3-HepaRG cell lines. The percent LDH leakage in response to 5 mM APAP treatment increased significantly to 25 % in EV-HepaRG cells compared with vehicle treated EV-HepaRG cells (20 %). While no change in LDH leakage was observed in Low-hFMO3-HepaRG cells in response to APAP, percent LDH leakage increased in High-hFMO3-HepaRG cells to 11 % compared with vehicle treated High-hFMO3-HepaRG cells (8 %). The percent LDH leakage

in both Low- and High-hFMO3-HepaRG clones after APAP is significantly lower compared to APAP treated EV controls (Figure 4.8B). Following pretreatment with 1 mM MMI, APAP-induced cytotoxicity increased to 17 % in Low-FMO3 expressing cells and to 16 % in High-FMO3 expressing clone compared to only APAP-treated Low- and High-hFMO3-HepaRG clones. No change in LDH leakage is observed in MMI pretreated, APAP-treated EV cells compared with only APAP-treated EV cells. This data suggests that inhibition of FMO3 activity by MMI in Low-, and High-FMO3 expressing clones resulted in rescue of sensitivity to APAP only in Low-FMO3 expressing cell line compared to EV controls.

Effect of Short Hairpin RNA Interference (FMO3-shRNA) on FMO3 mRNA and Protein Expression in EV and FMO3 Over-expressing HepaRG Cell Lines

To knockdown FMO3 gene expression in EV, Low-, and High-FMO3 expressing HepaRG cells, differentiated clones were transfected with FMO3-shRNA or scrambled-shRNA for 72 h. qRT-PCR and western blot analysis of FMO3 was performed 72 h after transfection (Figure 4.9). FMO3 mRNA expression decreased significantly to 0.25-, 0.5- and 0.67-fold change which represents a 75, 46.2 and 33.7 % decrease, respectively, in EV-, Low- and High-hFMO3-HepaRG cells, compared to their respective scrambled-shRNA transfected cells (Figure 4.9A). Representative western blots are shown in Figure 4.9B and densitometric analysis of western blot is shown in Figure 4.9C. FMO3 protein expression in EV-HepaRG cells following FMO3-shRNA transfection decreased significantly to 0.18-fold change which represents a

82.4 % decrease, compared to scrambled-shRNA. In Low- and High-hFMO3-HepaRG clones, FMO3 protein expression also decreased significantly to 0.25- and 0.44-fold change, which represents a 74.8 and 56.3 % decrease, respectively, compared to scrambled-shRNA transfected controls (Figure 4.9C). These data shows that the FMO3 knockdown using shRNA interference in hFMO3-HepaRG and EV-HepaRG clones was successful.

Effect of FMO3 Knockdown on APAP-induced Cytotoxicity in hFMO3-HepaRG Cells

To determine whether FMO3 knockdown in hFMO3-HepaRG cells restores their susceptibility to APAP-induced cytotoxicity, FMO3-shRNA and scrambled-shRNA transfected cells were treated with 5 mM APAP for 24 h. In response to 5 mM APAP treatment, the percent LDH leakage into the medium increased significantly to 33 % in EV-HepaRG cells compared with control treated EV-HepaRG cells (26 %) (Figure 4.10). APAP treatment also increased percent LDH leakage in Low- and High-hFMO3-HepaRG clones to 31 and 30 %, respectively, compared to vehicle treated controls (25 % in Low- and 23 % in High-hFMO3-HepaRG cells). Even though the percent LDH leakage increased in hFMO3-HepaRG clones, the values were significantly lower only in the High-hFMO3 expressing clone compared with 5 mM APAP treated EV-HepaRG cells. Although, the cytotoxicity trend in response to APAP treatment is similar to that seen in Figure 4.8A, the overall percent LDH leakage is higher due to sub-confluent number of differentiated cells used in this study.

Transfection of scrambled-shRNA or FMO3-shRNA further increased the percent LDH leakage in all three EV- and hFMO3-HepaRG cell lines. No significant change in LDH leakage in scrambled-shRNA transfected, APAP treated cells is observed in comparison with scrambled-shRNA transfected cells. Furthermore, percent LDH leakage in FMO3-shRNA transfected cells exposed to APAP increased in Low- and High-hFMO3 HepaRG cells compared to scrambled shRNA transfected APAP treated cells. Together these data suggests that FMO3 knockdown in Low- and High-hFMO3-HepaRG cells restores their susceptibility to APAP-induced cytotoxicity.

Figure 4.1

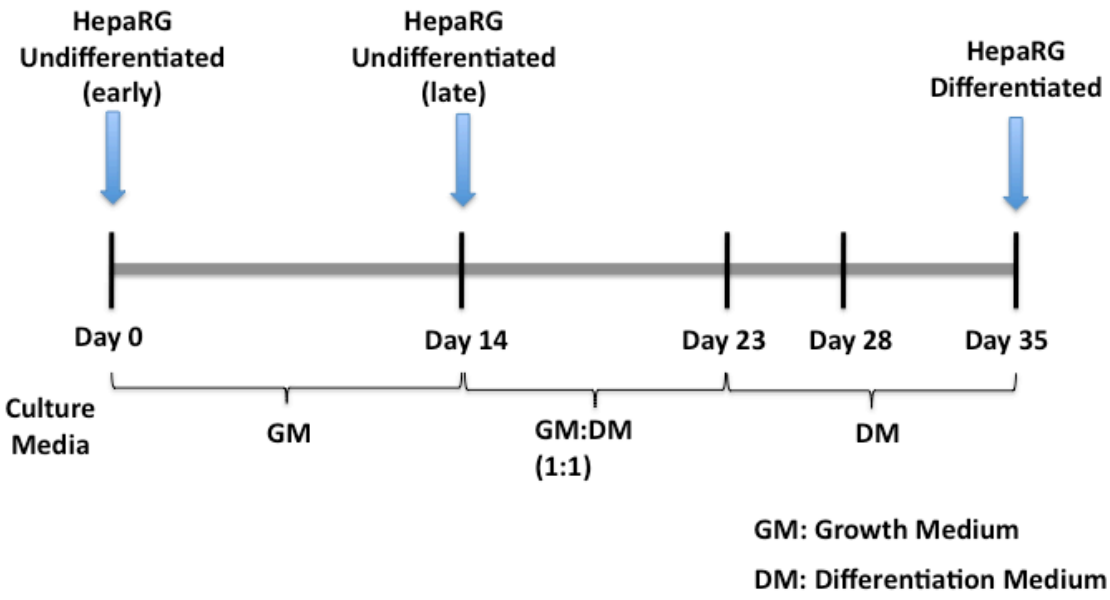
HepaRG Undifferentiated (early)
HepaRG Undifferentiated (late)
HepaRG Differentiated
Day 0
Day 14
Day 23
Day 28
Day 35
Culture Media
GM
GM:DM (1:1)
DM
GM: Growth Medium
DM: Differentiation Medium

Figure 4.1 *HepaRG cell line differentiation protocol flowchart.* Undifferentiated HepaRG cells are maintained in growth medium from Day 0 (HepaRG Undifferentiated early) to Day 14 (HepaRG Undifferentiated late). On Day 0, HepaRG cells appear elongated with clear cytoplasm. During proliferation period cells appear as a homogenous cell population with an epithelial phenotype showing no regular structural organization. When the cells reach confluency, they undergo progressive morphological changes acquiring a granular cytoplasm. From Day 15 to Day 23, cells are maintained in differentiation medium diluted by half with growth medium. From day 24 onwards, cells are maintained in only differentiation medium. Between Day 28 and Day 35, cells appear differentiated into two subpopulations (HepaRG Differentiated): hepatocyte-like cells and biliary epithelial-like cells.

Figure 4.2

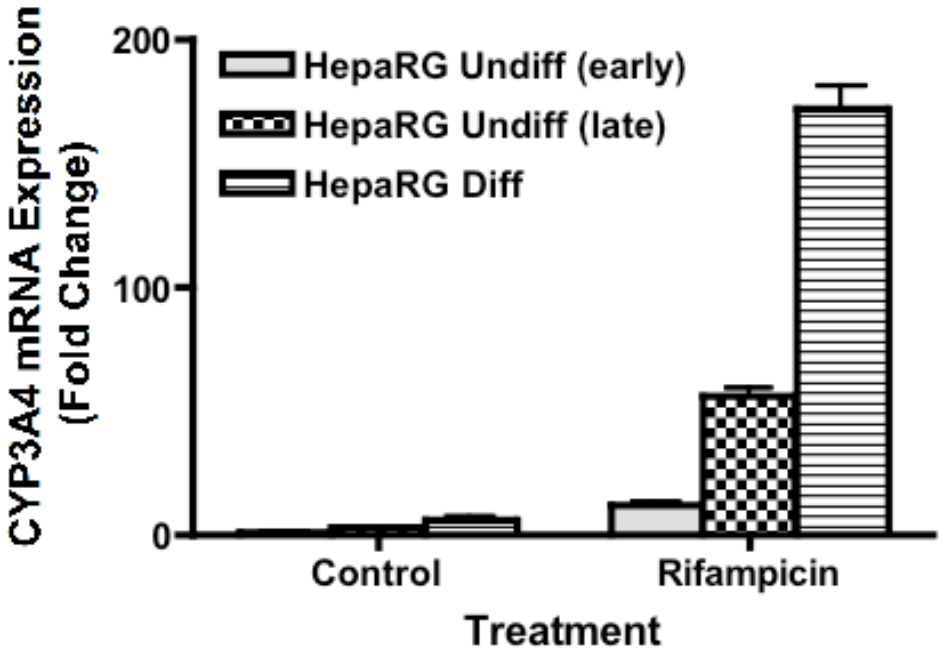
CYP3A4 mRNA Expression
(Fold Change)
200
100
0
HepaRG Undiff (early)
HepaRG Undiff (late)
HepaRG Diff
Control
Rifampicin
Treatment

Figure 4.2 *Quantitative RT-PCR analysis of CYP3A4 transcripts following Rifampicin treatment in undifferentiated (early and late) and differentiated HepaRG cells.* RNA was isolated from cells treated with rifampicin (10μM) or vehicle for 24 h. mRNA expression was measured by qRT-PCR using human primers specific for CYP3A4. Gene expression was normalized to the housekeeping gene β-Actin. CYP3A4 mRNA expression is presented as mean Fold Change ± SE. Two-way ANOVA was performed followed by the Bonferroni's post-test. Asterisks (*) represent a statistical difference ($p < 0.05$) between control and rifampicin treatment.

Figure 4.3

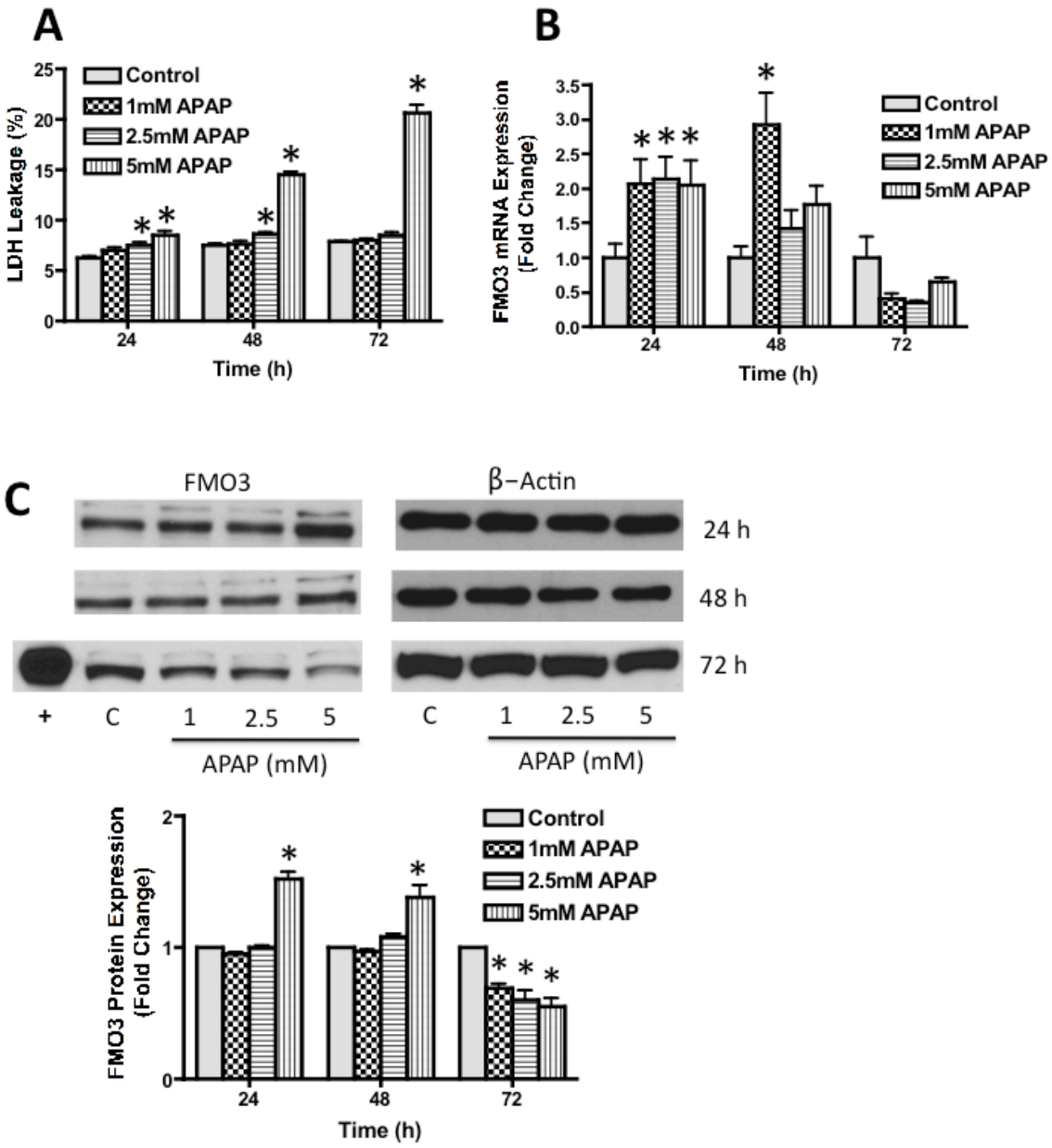
A
LDH Leakage (%)
Control
1mM APAP
2.5mM APAP
5mM APAP
Time (h)
B
FMO3 mRNA Expression (Fold Change)
Time (h)
C
FMO3
β-Actin
24 h
48 h
72 h
+
C
1
2.5
5
APAP (mM)
FMO3 Protein Expression (Fold Change)
Time (h)

Figure 4.3 *Effect of APAP treatment on cytotoxicity and FMO3 gene expression in HepaRG cells.* Differentiated HepaRG cells were treated with 1, 2.5, and 5 mM APAP or control. At 24, 48, and 72h after treatment, percent LDH leakage into the medium was measured using a commercial kit. The data are presented as mean LDH leakage (%) ± SE (A). RNA was isolated from cells at 24, 48 and 72 h after APAP treatment or vehicle. FMO3 mRNA expression was measured by qRT-PCR using human-specific FMO3 primers. Gene expression was normalized to the housekeeping gene β-Actin. FMO3 mRNA expression is shown as mean Fold Change ± SE (B). Western blot for FMO3 was performed using 10 µg microsomal protein isolated from HepaRG cells treated with APAP or vehicle. Rabbit anti-human FMO3 primary antibody was used to detect FMO3 protein expression. Equal protein loading was confirmed by detection of β-actin. The data are presented as blots as well as mean FMO3 protein expression (Fold Change) ± SE. Two-way ANOVA was performed followed by the Bonferroni's post-test. Asterisks (*) represent a statistical difference ($p < 0.05$) between control and APAP treatment.

Figure 4.4

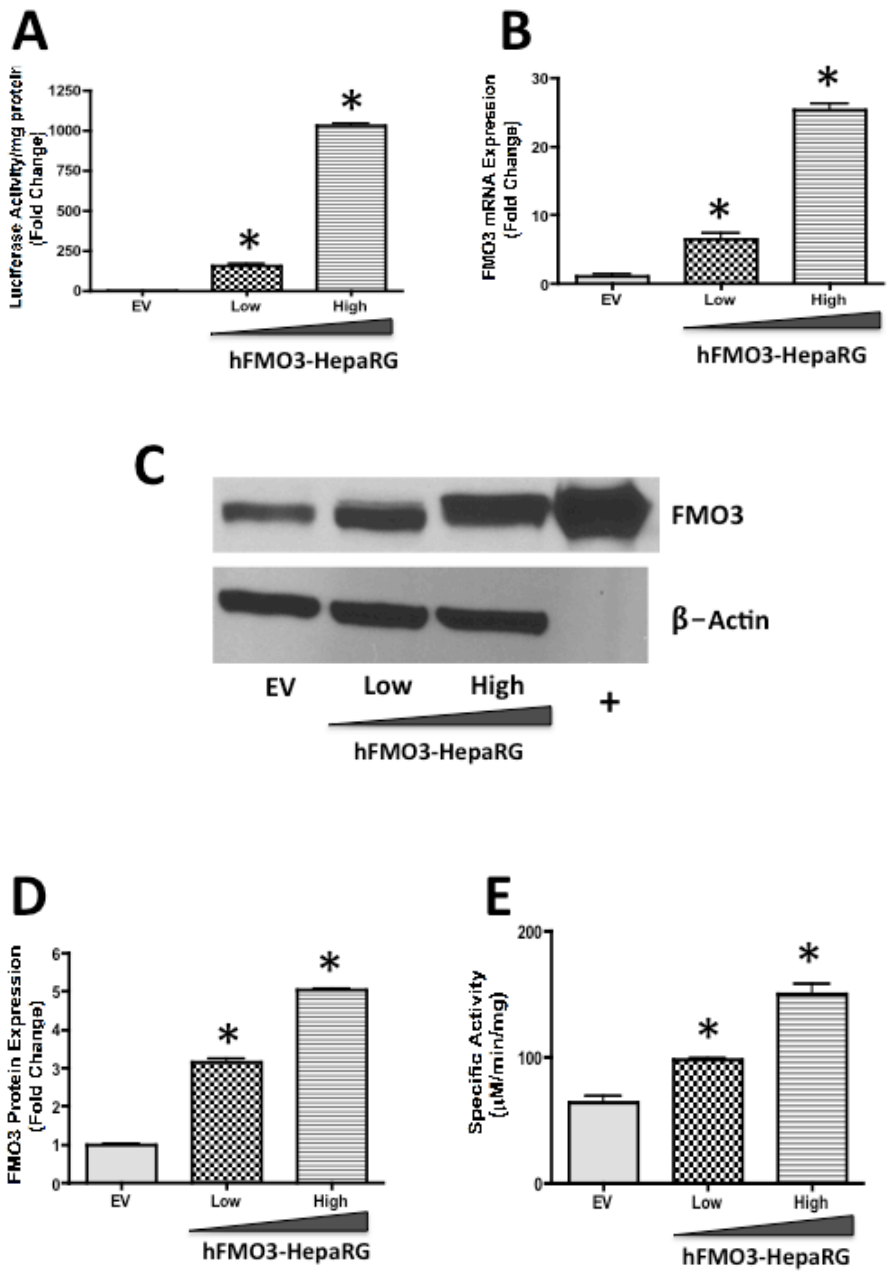
A
Luciferase Activity/mg protein (Fold Change)
1250
1000
750
500
250
0
EV
Low
High
hFMO3-HepaRG
B
FMO3 mRNA Expression (Fold Change)
30
20
10
0
EV
Low
High
hFMO3-HepaRG
C
FMO3
β−Actin
EV
Low
High
+
hFMO3-HepaRG
D
FMO3 Protein Expression (Fold Change)
6
5
4
3
2
1
0
EV
Low
High
hFMO3-HepaRG
E
Specific Activity (μM/min/mg)
200
100
0
EV
Low
High
hFMO3-HepaRG

Figure 4.4 *Establishment of HepaRG cells over-expressing human FMO3 (hFMO3-HepaRG).* Lentiviral vector construction and transduction are described in *Materials and Methods*. Luciferase activity was measured to determine the efficiency of transduction in hFMO3-HepaRG clones **(A)**. Luciferase activity is presented as mean luciferase activity/mg protein (Fold Change) ± SE. FMO3 mRNA expression in EV and FMO3 over-expressing HepaRG clones. The data are presented as mean Fold Change ± SE **(B).** Western blot for FMO3 in EV and hFMO3-HepaRG clones. Rabbit anti-human FMO3 primary antibody was used to detect FMO3 protein expression. The data are presented as blots **(C)** as well as mean FMO3 protein expression (Fold Change) ± SE **(D).** Microsomes isolated from EV and hFMO3 over-expressing clones were used to measure FMO3 activity using methimazole as substrate. Data are presented as mean Specific Activity (µM/min/mg) ± SE. One-way ANOVA was performed followed by the Dunnett's post-test. Asterisks (*) represent a statistical difference ($p < 0.05$) compared to EV controls.

Figure 4.5

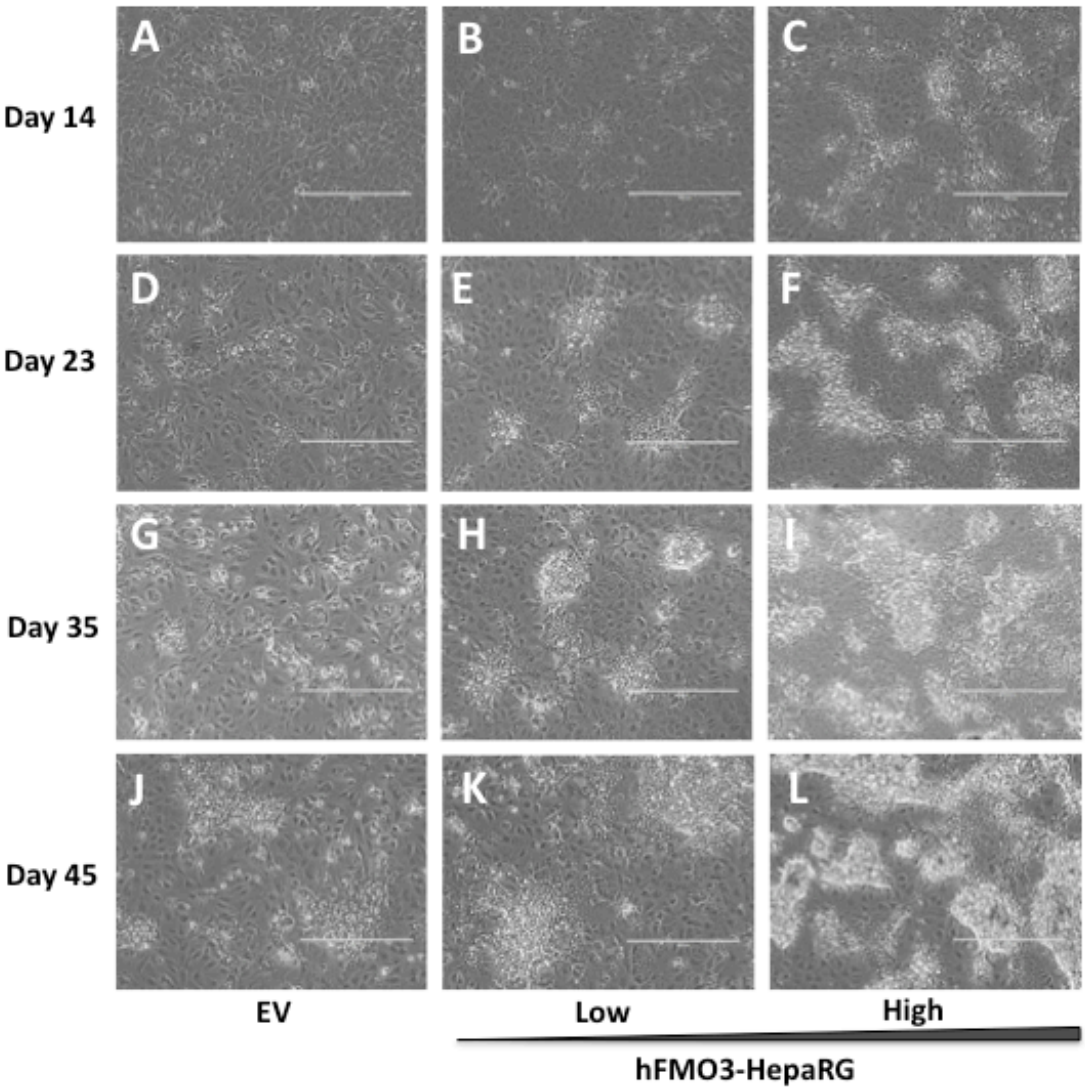
A
B
C
D
E
F
G
H
I
J
K
L
Day 14
Day 23
Day 35
Day 45
EV
Low
High
hFMO3-HepaRG

Figure 4.5 *Phase-contrast micrographs of HepaRG cells over-expressing human FMO3 (hFMO3-HepaRG).* Empty vector and hFMO3 over-expressing HepaRG clones were grown and differentiated as described in *Materials and Methods* and Figure 1. Representative micrographs on Day 14 (A, B, C), Day 23 (D, E, F), Day 35 (G, H, I) and Day 45 (J, K, L) are shown. Scale bar: 400 µm.

Figure 4.6

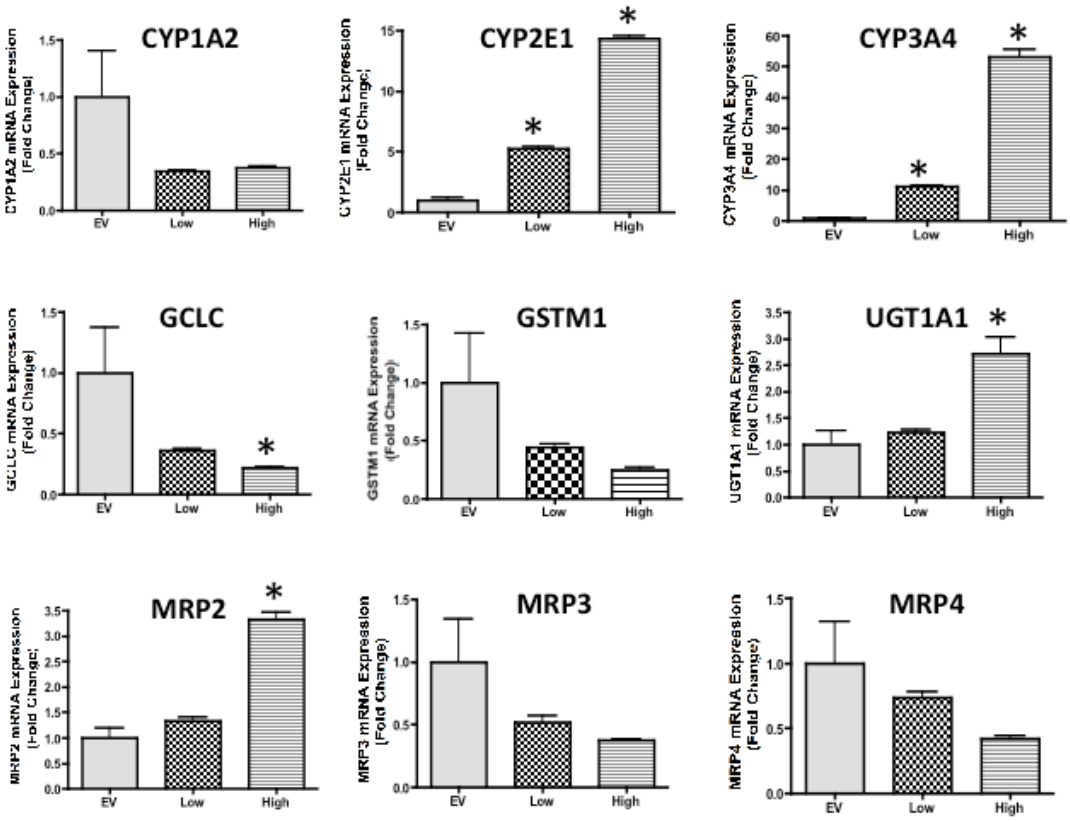
CYP1A2
CYP1A2 mRNA Expression (Fold Change)
EV
Low
High
CYP2E1
CYP2E1 mRNA Expression (Fold Change)
CYP3A4
CYP3A4 mRNA Expression (Fold Change)
GCLC
GCLC mRNA Expression (Fold Change)
GSTM1
GSTM1 mRNA Expression (Fold Change)
UGT1A1
UGT1A1 mRNA Expression (Fold Change)
MRP2
MRP2 mRNA Expression (Fold Change)
MRP3
MRP3 mRNA Expression (Fold Change)
MRP4
MRP4 mRNA Expression (Fold Change)

Figure 4.6 *Expression profiles of genes involved in acetaminophen bioactivation, detoxification, and transport in HepaRG cells over-expressing human FMO3 (hFMO3-HepaRG).* RNA isolated from untreated empty vector- and hFMO3-HepaRG clones was reverse transcribed to cDNA. The cDNA samples were analyzed by qRT-PCR using human-specific primers and the gene expression was normalized to the housekeeping gene β-Actin. Gene expression of acetaminophen bioactivating enzymes (CYP1A2, CYP2E1, and CYP3A4), detoxifying enzyme (UGT1A1), glutathione homeostasis enzymes (GCLC and GSTM1), and efflux transporters (MRP2, MRP3 and MRP4) were analyzed. mRNA expression are presented as mean Fold Change ± SE. One-way ANOVA was performed followed by the Dunnett's post-test. Asterisks (*) represent a statistical difference ($p < 0.05$) compared to EV controls.

Figure 4.7

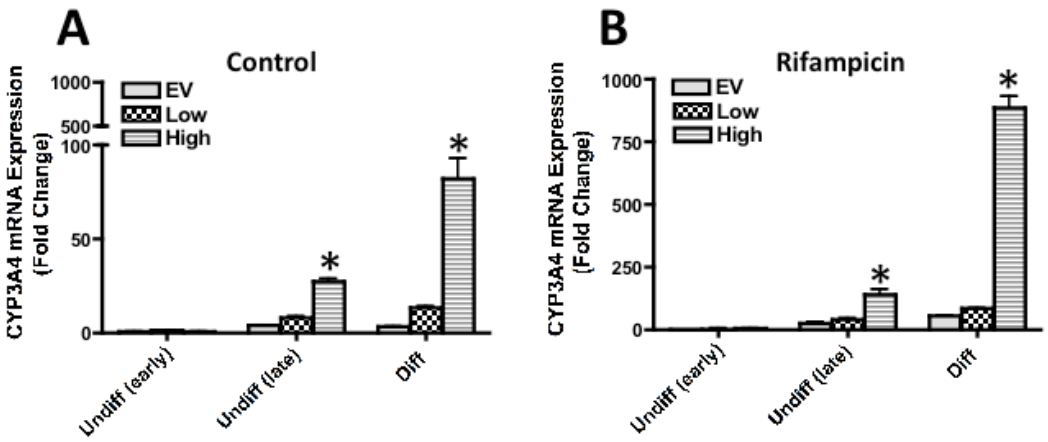

C **CYP3A4 mRNA Constitutive and Inducible Expression Profiles in hFMO3-HepaRG Cells.** The data are presented as mean fold change ± SE compared with early undifferntiated EV-HepaRG cells. Asterisks (*) represent a significant difference compared to respective EV controls.

	Control						Rifampicin					
	EV		Low		High		EV		Low		High	
	Mean	SE	Mean	SE	Mean	SE	Mean	SE	Mean	SE	Mean	SE
Undifferentiated (early)	1.0	0.1	1.16	0.2	0.92	0.1	2.2	0.2	2.79	0.1	3.4	0.37
Undifferentiated (late)	4.18	0.2	7.85	1.1	27.2*	1.5	24.5	6.6	40.6	6.9	140.7*	22.0
Differentiated	3.25	0.1	13.54	0.7	82.0*	10.7	55.3	0.63	85.14	2.4	884.9*	48.1

Figure 4.7 *Relative CYP3A4 mRNA expression following Rifampicin treatment in empty vector and hFMO3-HepaRG clones.* RNA was extracted from cells following rifampicin (10 μM) treatment or control, and cDNA was prepared using a commercial MMLV-RT kit. The cDNA samples were analyzed for CYP3A4 mRNA levels by quantitative RT-PCR. *CYP3A4* gene expression was normalized to housekeeping gene β-Actin. mRNA expression after control (A) and rifampicin (B) treatment are presented as mean Fold Change ± SE. CYP3A4 mRNA expression profiles in hFMO3-HepaRG Cells is shown in Table (C). Two-way ANOVA was performed followed by the Bonferroni's post-test. Asterisks (*) represent a statistical difference ($p < 0.05$) from respective EV-HepaRG cells.

Figure 4.8

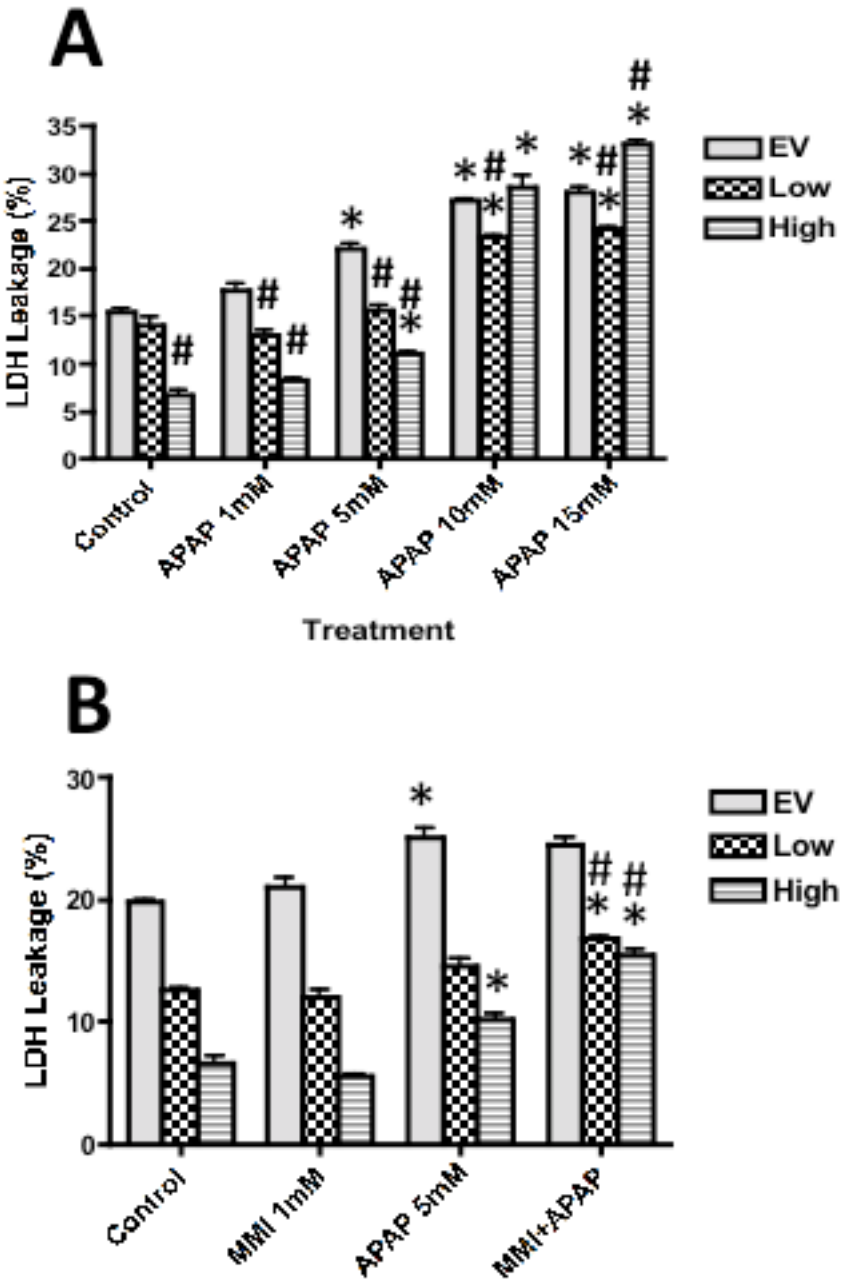
A
LDH Leakage (%)
35
30
25
20
15
10
5
0
EV
Low
High
Control
APAP 1mM
APAP 5mM
APAP 10mM
APAP 15mM
Treatment
B
LDH Leakage (%)
30
20
10
0
EV
Low
High
Control
MMI 1mM
APAP 5mM
MMI+APAP

Figure 4.8 *Significance of FMO3 over-expression During APAP-induced cytotoxicity in HepaRG cells.* Empty vector, Low-, and High-FMO3 expressing clones were treated with APAP concentrations from 1 mM to 15 mM. Percent LDH leakage into the medium was measured 24 h later, using a commercial kit. The data are presented as mean LDH leakage (%) ± SE (A). Two-way ANOVA was performed followed by the Bonferroni's post-test. Asterisks (*) represent a significant difference ($p < 0.05$) compared to respective vehicle control group and pound (#) represent a significant change ($p<0.05$) compared to respective EV controls. (B) To inhibit FMO3, EV, Low-, and High-FMO3 expressing clones were incubated with MMI (1 mM) for 30 min before APAP (15 mM) treatment. Percent LDH leakage into the medium was measured 24 h after APAP treatment. The data are presented as mean LDH leakage (%) ± SE. Asterisks (*) represent a significant difference ($p < 0.05$) compared to the respective vehicle treated clone, and pound (#) represent a significant difference ($p<0.05$) compared to respective 5 mM APAP treated clone.

Figure 4.9

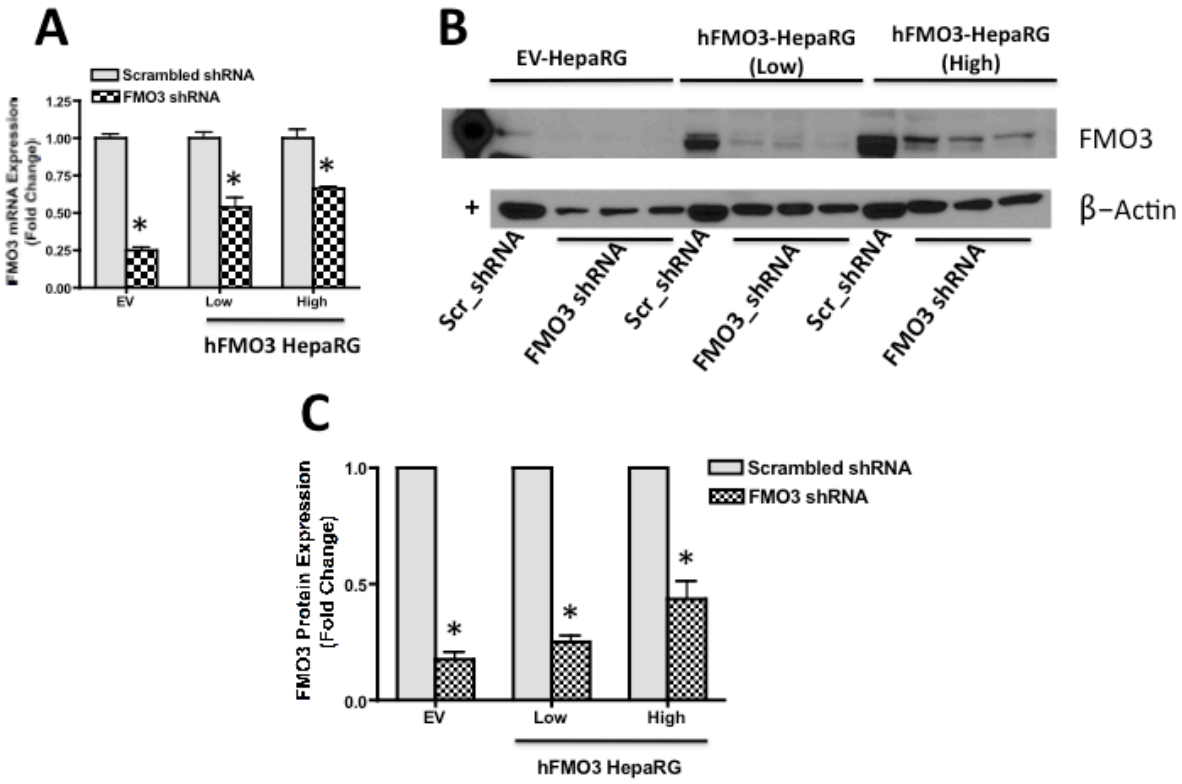
A
Scrambled shRNA
FMO3 shRNA
FMO3 mRNA Expression (Fold Change)
1.25
1.00
0.75
0.50
0.25
0.00
EV
Low
High
hFMO3 HepaRG
B
EV-HepaRG
hFMO3-HepaRG (Low)
hFMO3-HepaRG (High)
FMO3
β−Actin
+
Scr_shRNA
FMO3 shRNA
Scr_shRNA
FMO3_shRNA
Scr_shRNA
FMO3 shRNA
C
Scrambled shRNA
FMO3 shRNA
FMO3 Protein Expression (Fold Change)
1.0
0.5
0.0
EV
Low
High
hFMO3 HepaRG

Figure 4.9 *FMO3 mRNA and protein expression after short hairpin RNA interference in EV and FMO3 over-expressing HepaRG clones.* qRT-PCR analysis of FMO3 transcripts 72 h after FMO3-shRNA or scrambled-shRNA transfection in EV, Low-, and High-FMO3 expressing clones. The data are presented as mean Fold Change ± SE (A). Western blots for FMO3 were performed using microsomes isolated from scrambled- or FMO3-shRNA transfected EV and FMO3 over-expressing HepaRG clones. Recombinant human FMO3 protein was used as a positive control indicated by "+" sign. The data are presented as blots (B) and as mean FMO3 protein expression (Fold Change) ± SE (C). Two-way ANOVA was performed followed by the Bonferroni's post-test. Asterisks (*) represent a significant decrease compared to scrambled-shRNA transfected control.

Figure 4.10

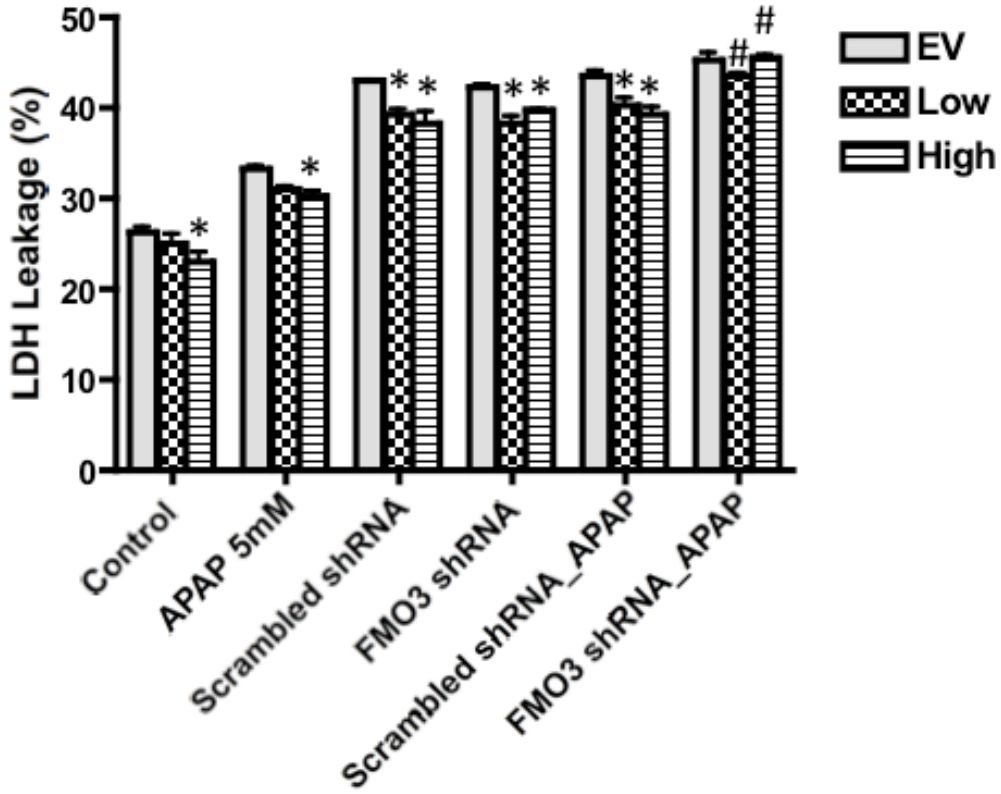
LDH Leakage (%)
50
40
30
20
10
0
EV
Low
High
Control
APAP 5mM
Scrambled shRNA
FMO3 shRNA
Scrambled shRNA_APAP
FMO3 shRNA_APAP

Figure 4.10 *Effect of FMO3 knockdown on APAP-induced cytotoxicity in FMO3 over-expressing HepaRG clones.* Empty vector, Low-, and High-FMO3 expressing cell lines were transfected with scrambled- or FMO3-shRNA for 72 h. Cells were treated with 5 mM APAP for 24 h. Percent LDH leakage into the medium was measured. The data are presented as mean LDH leakage (%) ± SE. Two-way ANOVA was performed followed by the Bonferroni's post-test. Asterisks (*) represent a significant decrease ($p < 0.05$) compared to respective EV-HepaRG cells and pound (#) represent a significant increase compared to respective APAP treated scrambled sh-RNA transfected clone.

4.5 Discussion

Primary human hepatocytes are the most pertinent model for studying xenobiotic metabolism and toxicity, including APAP-induced hepatotoxicity. However, they have major drawbacks in that the availability of these cells is limited, isolation procedures are complicated, they are expensive and due to inter-individual variability, the drug response can vary significantly from one batch of hepatocytes to the next (Madan et al., 2003). The lifespan of primary human hepatocytes is short and they undergo changes in CYP expression levels (primarily loss) over time in culture. To overcome these limitations, immortalized liver-derived cell lines were introduced as an alternative model for studying *in vitro* metabolism and cytotoxicity (Gerets et al., 2012). Because of their unlimited availability and phenotypic stability, hepatoma cell lines like HepG2 cells have been used extensively in toxicity studies. They express very low CYP levels compared to primary human hepatocytes or human liver, especially those isoforms that are involved in the metabolism of APAP (Rodriguez-Antona et al., 2002). Their low metabolic capacity makes them useful for toxicity testing of parent molecules and less suitable for metabolite toxicity testing. HepaRG, a human hepatoma cell line, is a recently developed cellular model that expresses a more normal spectrum of drug metabolizing enzymes. The mechanistic features of APAP-induced hepatotoxicity in HepaRG cells are similar to that reported for mouse hepatocytes and mouse liver *in vivo* (McGill et al., 2011). Recently we demonstrated FMO3 gene induction in an acetaminophen resistance mouse

model termed APAP autoprotection. Although the phenomenon of APAP autoprotection is also seen in patients exposed to supratherapeutic doses of APAP, the mechanism is not known. Thus, the goal of the present study was to investigate *FMO3* gene induction in HepaRG cells, an *in vitro* model of human hepatocytes much closer to the *in vivo* situation, and to also determine the functional significance of *FMO3* over-expression during APAP-induced cytotoxicity.

Primary human hepatocytes express high cytochrome P450 (CYP) levels and exhibit higher responsiveness to CYP inducers, such as phenobarbital, beta-naphthoflavone and rifampicin. Constitutive and inducible CYP3A4 mRNA expression in HepaRG cells is widely used to assess metabolic and/or differentiation status (Aninat et al., 2006; Gerets et al., 2012; Hart et al., 2010). Thus, HepaRG cell's responsiveness to rifampicin was evaluated at different growth stages. At confluence, as well as, with addition of differentiation medium, HepaRG cells differentiate into hepatocyte- and biliary epithelial-like cells (Gripon et al., 2002; Hart et al., 2010). Consistent with the literature, HepaRG cells in culture progressively differentiate which is evident from their responsiveness to rifampicin on Day 14 and Day 35. Then, differentiated HepaRG cells were exposed to APAP concentrations ranging from 1 to 5 mM. While 1 mM APAP treatment did not significantly increase LDH release from cells at any of the time-points tested, 2.5 mM APAP increased LDH leakage at 24 and 48 h. By 72 h, no difference in LDH leakage was detected compared to vehicle treated controls. This is suggestive of mild

cellular injury caused by 2.5 mM APAP that resolves by 72 h. On the contrary, the cellular injury by 5 mM APAP is progressive and does not resolve by 72 h. FMO3 mRNA levels increase at 24 h with all three doses of APAP and at 48 h, the increase is statistically significant only with 1 mM APAP. Even though mRNA increase is seen with 1 and 2.5 mM APAP, the FMO3 protein expression does not change. On the contrary, 5 mM APAP results in significant increase in FMO3 protein levels at 24 and 48 h, but the levels are significantly lower at 72 h. This observation with respect to the relationship between degree of toxicity and *FMO3* gene expression, where *FMO3* gene expression decreases during overt toxicity and mild toxicity induces *FMO3* gene expression, is consistent with our previous results *in vivo* with various hepatoxicants in mice (Rudraiah et al., 2014; Rudraiah et al., 2014).

The decrease in FMO3 protein expression at 72 h may be due to production of H_2O_2. Even though FMOs form a relatively stable hydroperoxyflavin intermediate and does not contribute to production of H_2O_2, during absence of NADPH, peroxyflavin can decompose to hydrogen peroxide resulting in significant loss of enzyme activity (Cashman, 1999). Collectively, it is notable that FMO3 gene expression is inducible by APAP-induced cytotoxicity in HepaRG cells. Although the change in FMO3 protein expression is only by a fold-change of 1.5, the constitutive FMO3 protein expression in HepaRG cells is very high (comparable to CYP3A4 expression). A fold-change of 1.5, can be very large and physiologically significant.

To further investigate the importance of FMO3 over-expression during APAP-induced cytotoxicity, we successfully established an over-expression system. The FMO3 over-expressing HepaRG cell lines exhibit a striking expression level-dependent faster rate of differentiation compared to empty vector control cells. To examine any possible difference in gene expression profiles that might contribute to APAP-induced cytotoxicity, genes involved in acetaminophen-bioactivation, -detoxification, and efflux transporters were screened. Interestingly, an FMO3 level-dependent increase in expression of CYP2E1, CYP3A4, UGT1A1 and MRP2 genes and a decrease in GCLC, are seen. Most striking are the gene expression changes for CYPs, particularly CYP3A4. Cashman et al. reported a concomitant increase in FMO3, FMO4 and CYP2E1 functional activity in rats on total parenteral nutrition and choline (Cashman et al., 2004), but a correlation or interdependence between the two was not investigated. Currently there are no reports in the literature that show a correlation with FMO3 gene expression and CYP activity. The mechanism of such a regulation is also not known and warrants further investigation.

To examine whether the observed phenotype of faster differentiation in hFMO3-HepaRG cells is consistent with its responsiveness to rifampicin treatment, FMO3-over-expressing HepaRG cells were exposed to rifampicin and CYP3A4 mRNA levels were quantified. Consistent with the observed phenotype of greater differentiation state, CYP3A4 induction is significantly higher in FMO3-over-expressing cell lines compared to empty vector control. This suggests that the HepaRG cells over-expressing FMO3 are

differentiating at a faster rate compared to control cell line and that they respond more robustly to enzyme induction treatment. The mechanism by which FMO3 over-expression is driving cellular differentiation is not known.

Furthermore, the percent LDH leakage into the media in Low-hFMO3-HepaRG cells in response to APAP treatment is significantly lower compared to empty vector control. In High-hFMO3-HepaRG cells, the amount of LDH leakage by APAP is significantly lower at lower APAP concentrations, but at higher APAP concentrations, the LDH leakage is significantly greater. This trend where low FMO3-over-expression being protective and high FMO3-over-expression combined with toxic APAP dose being more toxic is also seen with FMO3-over-expressing hepatocyte cell line (HC-04) (Rudraiah et al., 2014). Taken together, these data suggest that over-expression of FMO3 significantly alters susceptibility to APAP-induced cytotoxicity. It should also be noted that the High-hFMO3-HepaRG cells express significantly higher CYPs that metabolize APAP. The toxicity noticed may be due to over production of toxic metabolite NAPQI or due to production of H_2O_2. Examining gene expression and metabolite profiles using transcriptomics and metabolomic approaches in these cell lines could help identify signaling molecules and pathways involved in cellular differentiation driven by FMO3.

FMO3 inhibition by MMI has been demonstrated in our lab (Rudraiah et al., 2014). Inhibition of FMO3 activity by MMI resulted in rescue of sensitivity to APAP toxicity. However, since MMI is not a specific FMO3 inhibitor, we used RNA interference to knockdown over-expressed FMO3 in

FMO3-over-expressing cell lines. Transfection of sh-FMO3 resulted in a significant decrease in FMO3 protein expression in EV- and FMO3-over-expressing cell lines. These transfection experiments and APAP treatment were performed in a 50 to 60 % cell confluent conditions but APAP dose response in Figure 8 was performed at a high density (100 % confluent conditions). Because of the lower confluency as well as toxicity resulting from transfection procedure itself, cells exhibit higher basal LDH leakage into the media compared to experiments performed using 100 % confluent conditions. Although the knockdown of FMO3 in hFMO3-HepaRG cells did restore the susceptibility to APAP-induced cytotoxicity exhibited by the EV cells with normal FMO3 levels, the scrambled-RNA transfected cells exhibit higher toxicity compared to only APAP treated EV- and hFMO3-HepaRG cell lines. Finally, FMO3 knockdown in hFMO3-HepaRG cells were capable of differentiating at a rate similar to non-knockdown hFMO3-HepaRG clones (data not shown). Furthermore, western blotting of differentiated knockdown-hFMO3-HepaRG cells, failed to show low *FMO3* expression compared to differentiated scrambled-shRNA transfected hFMO3-HepaRG cells (data not shown). Although FMO3 knockdown was successful, the lack of a selection marker in the sh-FMO3 plasmid prevented us to control the cells repopulating the plate after knockdown. Development of a knockdown clone can address this problem.

In summary, we show *FMO3* gene induction by APAP-induced cytotoxicity in HepaRG cells. This is the first report demonstrating xenobiotic

mediated *FMO3* gene induction in a human hepatoma cell line. Even though the mechanism of induction or the role of FMO3 in APAP-induced hepatotoxicity/cytotoxicity is not clearly known, there are two potential hypotheses for its potential role during toxicant exposure. One involving a role for cyteamine in maintaining the cellular thiol:disulphide potential in a cell (Ziegler et al., 1979) and the other is the possible regulation of immune cells by an FMO3 metabolite (Bennett et al., 2013; Z. Wang et al., 2011). Strikingly, data presented in this manuscript demonstrates a third novel dimension to FMO3 function during toxicant exposure. Our data shows that FMO3 may be involved in driving cellular differentiation. Although this calls for further investigation, the potential role of FMO3 in cellular proliferation and differentiation is consistent with the considerable lag time in gene and protein induction seen in our mouse model of APAP autoprotection (Rudraiah et al., 2014), where protein peaks at 72 h after a single dose APAP treatment. This time frame is consistent with stages of repair and regeneration with APAP toxicity.

CHAPTER 5

Human Hepatic Flavin-containing Monooxygenase-3 (FMO3) Gene Expression is Not Regulated by Nuclear Factor, Erythroid 2- Like 2 (NRF2/NFE2L2) Under Oxidative Stress Conditions

5.1 Abstract

The flavin-containing monooxygenases (FMOs) are important for the oxidation of a variety of endogenous compounds and xenobiotics. The hepatic expression of *FMO3* is highly variable and until recently, it was thought to be uninducible. In this study, human *FMO3* gene regulation by the oxidative stress transcription factor, nuclear factor (erythroid-derived 2)-like 2 (NRF2) was examined. Constitutive *FMO3* gene expression is repressed in HepG2 cells, thus this cell can be a good model for *FMO3* gene regulation studies. Over-expression of NRF2 in HepG2 cells increased NRF2 target gene expression, heme oxygenase-1 (*HMOX1*) and NAD(P)H:quinone oxidoreductase-1 (*NQO1*), but did not alter *FMO3* gene expression. Co-transfection studies with NRF2 or its cytosolic regulatory protein, Kelch-like ECH-associated protein 1 (KEAP1), expression vectors, along with FMO3 promoter luciferase reporter constructs of various lengths (5 Kb or 6 Kb), did not change FMO3 reporter gene activity significantly. Furthermore, treatment with tert-butyl hydroperoxide (tBHP) or tert-butyl hydroquinone (tBHQ) did not alter FMO3 reporter construct activity. In summary, *in vitro* results suggest

that the transcriptional regulation of FMO3 might not involve the NRF2-KEAP1 regulatory pathway.

5.2 Introduction

Flavin-containing monooxygenases (FMOs) are enzymes that catalyze oxidation of a variety of nitrogen-, sulphur- and phosphorous-containing xenobiotics to their respective oxides. In human liver, constitutive *FMO3* expression and developmental expression patterns have been extensively studied (Klick & Hines, 2007; Klick et al., 2008; Shimizu et al., 2008). Briefly, Klick and Hines demonstrated that binding of transcription factors such as nuclear factor Y (NFY), upstream stimulatory factor 1 (USF1), YYI and an unidentified GC box to the regulatory domains upstream of the transcription start site are important for regulating constitutive *FMO3* transcription (Klick & Hines, 2007). The pre-B-cell leukemia factor 2 (Pbx2) as a heterodimer with an unidentified homeobox (Hox) isoform contributes to *FMO3* developmental- and tissue-specific regulation (Klick & Hines, 2007). Another factor, CCAAT enhancer-binding protein β (C/EBPβ), binding more distal to the transcription start site, is important for the *FMO3* developmental expression pattern (Klick et al., 2008). Finally, Shimuzu et al. (2008) reported that HNF-4 and NF-Y modulates *FMO3* gene expression in the Japanese population. Because xenobiotic-induced *FMO3* gene expression was not identified, transcriptional regulation during toxicant exposure is not well characterized.

Acetaminophen (APAP)-induced hepatotoxicity results in *Fmo3* over-expression in mice (Rudraiah et al., 2014). Additionally, we also showed that toxic alpha-naphthyl isothiocyanate (ANIT) treatment and bile duct ligation (BDL) induced *Fmo3* gene expression (Rudraiah et al., 2014). Because all

hepatotoxicants that induce *Fmo3* also induce oxidative stress, the goal of the current study was to investigate whether oxidative stress transcription factor nuclear factor (erythroid-derived 2)-like 2 (NRF2) might regulate *FMO3* gene expression. *FMO3* Constitutive expression is repressed in HepG2 cells making this cell line useful for studying *FMO3* regulation using recombinant *FMO3* promoter-directed reporter constructs. Thus, all *in vitro* studies were performed in HepG2 cells. Reporter constructs containing *FMO3* promoter sequences of various lengths (5 Kb or 6 Kb) directing luciferase expression were used in the current study. Co-transfection studies with *FMO3* promoter luciferase reporter constructs and NRF2 or its cytosolic retainer Kelch-like ECH-associated protein 1 (KEAP1) did not significantly alter luciferase reporter gene activity. Subsequent promoter analysis using MatInspector software (Genomatix, Munich, Germany), did not identify any antioxidant response element (ARE) sites on the reporter constructs used in the current study. These results suggest that the transcriptional regulation of *FMO3* might not involve NRF2-KEAP1 regulatory pathway.

5.3 Material and Methods

Chemicals

Tert-butyl hydroperoxide and tert-butyl hydroquinone were purchased from Sigma-Aldrich (St Louis, MO). All other reagents were of reagent grade or better and commercially available.

Cell Culture and Transient Transfection Reporter Gene Assay

HepG2 cells were maintained in Dulbecco's Modified Eagle's Medium (DMEM) supplemented with 10 mM glucose, 10 % fetal bovine serum and 1 % antibiotic-antimycotic (100 units/mL penicillin G sodium, 100 µg/mL streptomycin sulfate, and 0.25 µg/mL amphotericin B) in a 5 % CO_2 and humidified environment (95 % relative humidity) at 37°C. Expression plasmids containing variable lengths of FMO3 promoter sequences (5905bp:pRNH970 or 4908bp:pRNH1013) directing luciferase expression were prepared using a Genome Walker Kit (BD Biosciences) as described previously (Klick & Hines, 2007). Expression plasmid p3XFLAG-myc-CMV-26 (EV26) was obtained from Sigma-Aldrich (St Louis, MO). NRF2 or KEAP1 ORF (Open Biosystems, Waltham, MA) was cloned into EV26. For transient transfection, HepG2 cells were seeded in a 12-well plate at approximately 30 % confluence. The following day, transient transfection (NRF2 or KEAP1 expression plasmids prepared in our lab) or co-transfections (*FMO3* promoter luciferase reporter constructs and transcription factor expression plasmids) was performed using Lipofectamine (Invitrogen) according to the manufacturer's manual. Cells were harvested for RNA isolation or to determine luciferase activity using the luciferase assay system (Promega) according to the manufacturer's protocol. For tert-butyl hydroperoxide (tBHP) and tert-butyl hydroquinone (tBHQ) treatment culture media (complete DMEM) was replaced with media containing 100 µM tBHP or 100 µM tBHQ 6 h after transfection. Cells were harvested 42 h after treatment to determine luciferase activity. If not otherwise indicated, the amount of lipofectamine used was 2.5 µL/well, the amount of

transfected plasmids was 0.3 µg/well for transcription factors and 0.5 µg/well for reporter genes.

RNA Isolation and Quantitative Real-Time Polymerase Chain Reaction (qRT-PCR)

TRIzol reagent (Life Technologies, Carlsbad, CA) was used to extract total RNA from cells transiently transfected with expression plasmids containing NRF2 or KEAP1. cDNA was prepared using the M-MLV RT kit (Invitrogen, Carlsbad, CA). NRF2, KEAP1, HMOX1, NQO1 and FMO3 mRNA expression was quantified by the ΔΔCT method and normalized to the housekeeping gene, β-actin. Primer pairs were synthesized by Integrated DNA Technologies (Coralville, IA) and are presented in Table 1. Amplification was performed using an Applied Biosystems 7500 Fast Real-Time PCR System. Amplification was carried out in a 20 µL reaction volume containing 8 µL diluted cDNA, Fast SYBR Green PCR Master Mix (Applied Biosystems, Foster City, CA) and 1 µM of each primer.

Isolation of Nuclear Fraction from HepG2 Cells

HepG2 cells were plated at $8x10^5$ cells per dish in a 60 mm dish overnight. The following day, cells were treated with 100 µM tBHP in serum free DMEM for 2 h. After 2 h, cells were removed from the incubator, scraped and collected in 1 mL cold PBS and transferred into microcentrifuge tubes. The cell suspension was then centrifuged at 12000 g for 1 min to collect the cells. Cell pellets were resuspended in 400 µL cold hypotonic buffer [10 mM

HEPES, pH 7.9, 1.5 mM MgCl2, 10 mM KCl, 0.5 mM DTT and 0.2 mM phenylmethylsulfonylfluoride (PMSF)] and incubated for 20 min on ice, vortexed for 10s and then centrifuged at 1000 g for 10 min at 4°C. The resulting pellet was again resuspended in hypertonic buffer (20 mM HEPES, pH 7.9, 1.5 mM MgCl2, 420 mM NaCl, 0.2 mM EDTA, 0.5 mM DTT, 25 % glycerol and 0.2 mM PMSF) and incubated on ice for 20 min for high-salt extraction. Samples were vortexed for 10s and centrifuged at 1000 g for 10 min. The supernatant fraction containing nuclear proteins was measured for protein concentration.

Western Blot Analysis

For western blot analysis of NRF2, 40 µg nuclear protein was mixed with Laemmli's buffer, incubated at 90°C for 10 min, and electrophoretically resolved using 10 % SDS polyacrylamide gels and transblotted onto PVDF-Plus membrane (Micron Separations, Westboro, MA). A custom rabbit anti-Human NRF2 primary antibody (Cell Signaling Technology, Inc. Danvers, MA) was used to detect NRF2 with TFIIB as a loading control. Blots were then incubated with HRP conjugated secondary antibodies against rabbit IgG (Sigma-Aldrich, St Louis, MO). Protein-antibody complexes were detected using a chemiluminescent kit (Thermo Scientific, IL) with visualization using GeneMate blue autoradiography film (Bioexpress, Kaysville, UT).

LDH Leakage

Percent lactate dehydrogenase (LDH) leakage was determined via the Tox-7 kit (Sigma-Aldrich, St. Louis, MO) as a measure of cytotoxicity following tBHP treatment. The assay was performed according to manufacturer's instructions.

Statistical Analysis

Results are expressed as mean ± standard error (SE). Data were analyzed using the student's t-test, one-way ANOVA with Dunnett's post-hoc test or two-way ANOVA followed by the Bonferroni's post-hoc test. All statistical analysis was performed using GraphPad Prism version 4.00 for Macintosh (GraphPad Software, Inc., San Diego, CA). A p value of <0.05 was considered statistically significant.

Table 5.1 Primer Sequences for Quantitative RT-PCR

Gene	Primer Sequences
FMO3	Forward: 5'- TTG TAA ATG CTA GCC CTG CC -3'
	Reverse: 5'- CTG TCT GGA AGA GGG GCT G -3'
HMOX1	Forward: 5'- GCC AGC AAC AAA GTG CAA G -3'
	Reverse: 5'- GAG TGT AAG GAC CCA TCG GA -3'
KEAP1	Forward: 5'- TGA CAA GCT TAT GCA GCC AGA TCC CAG G -3'
	Reverse: 5'- GTG AGG ATC CTC AAC AGG TAC AGT TCT GCT GGT -3'
NQO1	Forward: 5'- GGA CTG CAC CAG AGC CAT -3'
	Reverse: 5'- TCC TTT CTT CTT CAA AGC CG -3'
NRF2	Forward: 5'- GCT CAT ACT CTT TCC GTC GC -3'
	Reverse: 5'- ATC ATG ATG GAC TTG GAG CTG -3'

5.4 Results

NRF2 and KEAP1 Over-expression Did Not Significantly Alter FMO3 mRNA Expression in HepG2 Cells

To examine the possible role of the NRF2-KEAP1 regulatory pathway in controlling *FMO3* gene expression, FMO3 mRNA levels were quantified in cells over-expressing NRF2 or its cytosolic regulatory protein, KEAP1. The results in Figure 5.1 show that transfection with the NRF2 expression vector results in a 2.7±0.2-fold change in NRF2 mRNA levels compared to empty vector-transfected cells. Transfection with KEAP1 expression vector results in a 1.4±0.15-fold change in KEAP1 mRNA levels compared to empty vector controls. Over-expression of NRF2 results in significantly higher expression of the NRF2 target genes, NQO1 and HMOX1, by 3.1±0.7-fold and 3.4±0.4-fold, respectively, compared to the empty vector. No significant change in FMO3 mRNA expression is observed with NRF2 over-expression. In addition, no significant change in NQO1, HMOX1 and FMO3 mRNA expression is seen with KEAP1 over-expression (Figure 5.1).

A Subtoxic Dose of tBHP Results in NRF2 Nuclear Translocation and Expression of NRF2 Target Genes in HepG2 Cells

In response to a 100 μM tBHP treatment for 24 h, the percent LDH leakage from HepG2 cells did not change (Figure 5.2A). Treatment with a subtoxic dose of tBHP (100 μM) for 2 h results in an increase in NRF2 nuclear localization (Figure 5.2B). The increased nuclear localization of NRF2 is

associated with significant increases in the expression of the NRF2 target genes, HMOX1 and NQO1 by 1.8±0.3- and 1.7±0.06-fold, respectively, compared to vehicle treated controls (Figure 5.2C and 5.2D).

Effect of NRF2 or KEAP1 Over-expression on FMO3-directed Reporter Gene Activity

To determine whether the transcription factor, NRF2, activates *FMO3* gene expression, co-transfection studies with NRF2 or KEAP1 expression vectors and FMO3 promoter luciferase reporter constructs (pRNH1013 and pRNH970) were performed. Co-transfection of reporter genes with NRF2 or KEAP1 did not significantly alter FMO3-directed reporter gene activity (Figure 5.3A). Furthermore, NRF2 or KEAP1 over-expression studies also were carried out using a subtoxic dose of the pro-oxidant and Nrf2 activator, tBHP. Results are shown in Figure 5.3B. No significant change in reporter gene activity is seen with KEAP1 co-transfection. However, tBHP treatment combined with NRF2 expression plasmid and *FMO3* promoter luciferase reporter construct co-transfection, significantly decreased luciferase activity.

Effect of Pro-oxidant-induced NRF2-KEAP1 Regulatory Pathway Activation on FMO3-directed Reporter Gene Activity

FMO3 promoter luciferase reporter constructs (pRNH1013 & pRNH970) or empty vector were transiently expressed in HepG2 cells and exposed to tBHP or tBHQ. No significant change in reporter gene activity is observed after treatment (Figure 5.4).

Figure 5.1

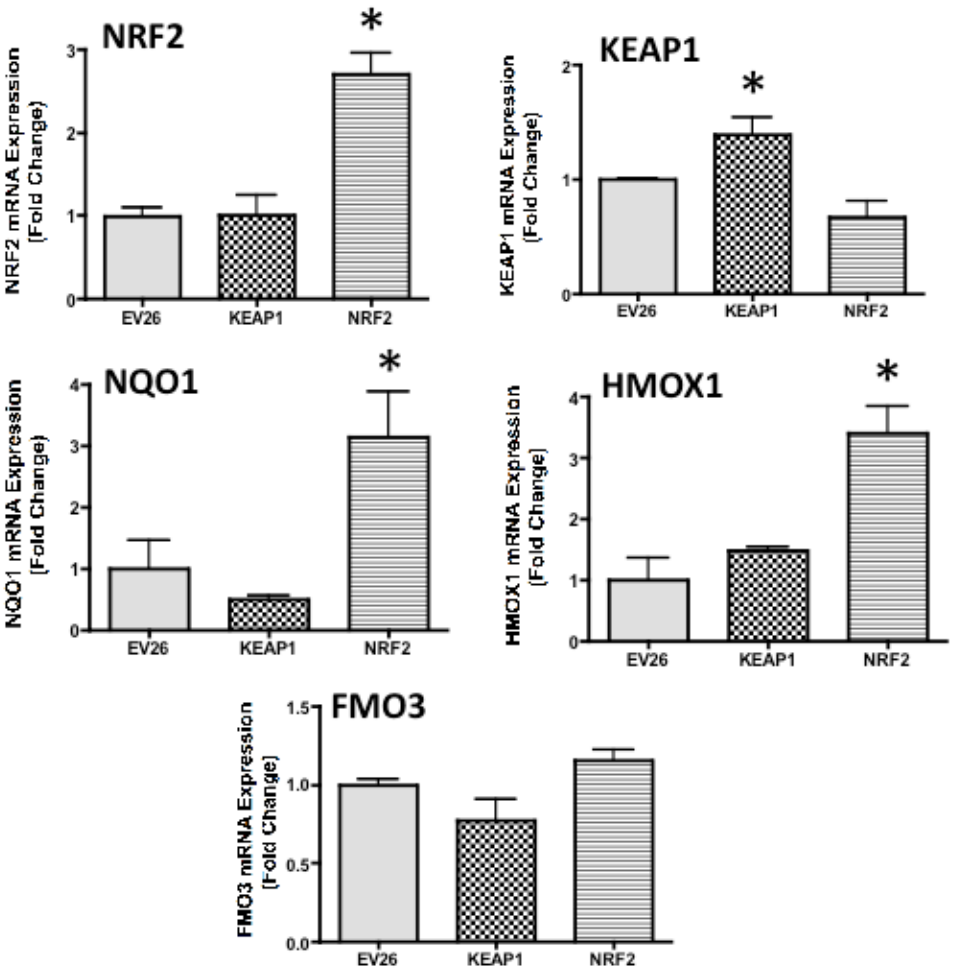
NRF2
NRF2 mRNA Expression (Fold Change)
EV26
KEAP1
NRF2
KEAP1
KEAP1 mRNA Expression (Fold Change)
NQO1
NQO1 mRNA Expression (Fold Change)
HMOX1
HMOX1 mRNA Expression (Fold Change)
FMO3
FMO3 mRNA Expression (Fold Change)

Figure 5.1 *Effect of NRF2 and KEAP1 over-expression on FMO3 mRNA levels in HepG2 cells.* The oxidative stress responsive transcription factor, NRF2, or its cytosolic regulatory protein, KEAP1, were transiently expressed in HepG2 cells. RNA was isolated from cells 48 h after transfection. cDNA was made using a commercial MMLV-RT kit and the cDNA samples were analyzed by quantitative RT-PCR using human NRF2, KEAP1, NQO1, HMOX1 and FMO3 specific primers. mRNA levels were normalized to the housekeeping gene, β-Actin. NRF2, KEAP1, HMOX1, NQO1 and FMO3 mRNA expression are presented as mean fold change ± SE. Each experiment was done in triplicate and repeated at least three times, and representative experimental results are shown. One-way ANOVA followed by Dunnett's post-hoc test was used for data analysis. Asterisks (*) represent a statistical difference ($p < 0.05$) from empty vector (EV26) transfected group.

Figure 5.2

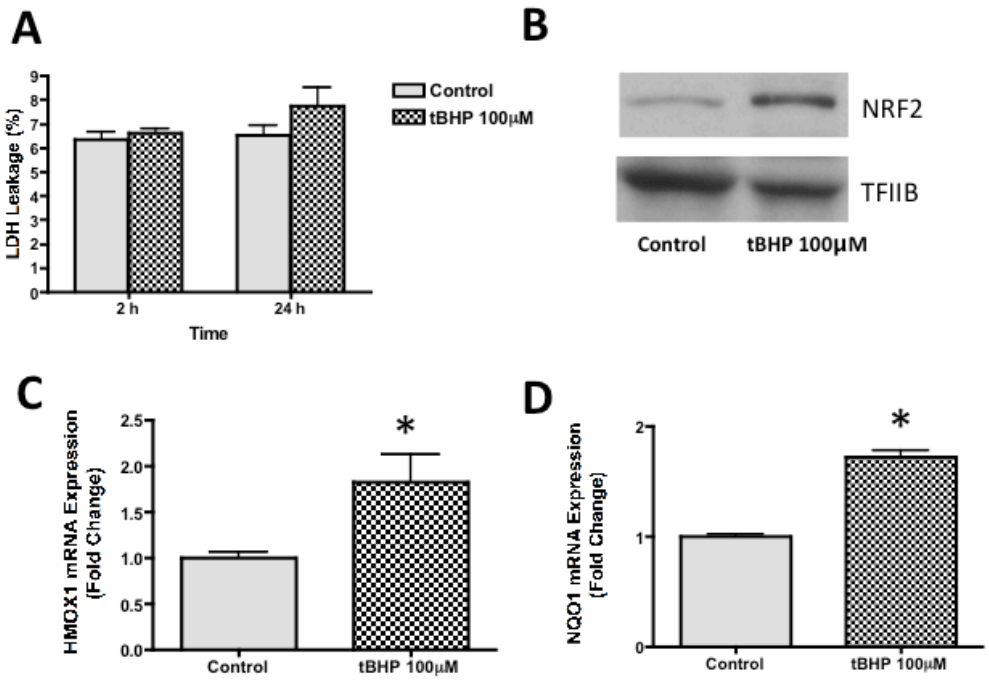
A
LDH Leakage (%)
Control
tBHP 100µM
2 h
24 h
Time
B
NRF2
TFIIB
Control
tBHP 100µM
C
HMOX1 mRNA Expression (Fold Change)
*
Control
tBHP 100µM
D
NQO1 mRNA Expression (Fold Change)
*
Control
tBHP 100µM

Figure 5.2 *Effect of tBHP treatment on cytotoxicity and NRF2-KEAP1 regulatory pathway in HepG2 cells.* **(A)** HepG2 cells were treated with tBHP (100 µM) or vehicle for 2 h. Cytotoxicity with 100 µM tBHP was measured by measuring LDH activity in the medium 2 and 24 h after treatment. The data are presented as LDH leakage (%) ± SE. **(B)** Western blots for NRF2 were performed using nuclear fractions from tBHP- and vehicle-treated HepG2 cells. RNA was isolated from HepG2 cells 24 h after treatment with tBHP. cDNA samples were analyzed by quantitative RT-PCR for NRF2 target genes HMOX1 **(C)** and NQO1 **(D)**. Gene expression was normalized to the housekeeping gene β-Actin. NQO1 and HMOX1 mRNA expression are presented as mean fold change ± SE. Each experiment was done in triplicate and repeated at least three times, and representative experimental results are shown. Student's t-test was used for data analysis. Asterisks (*) represent a statistical difference ($p < 0.05$) from control treated group.

Figure 5.3

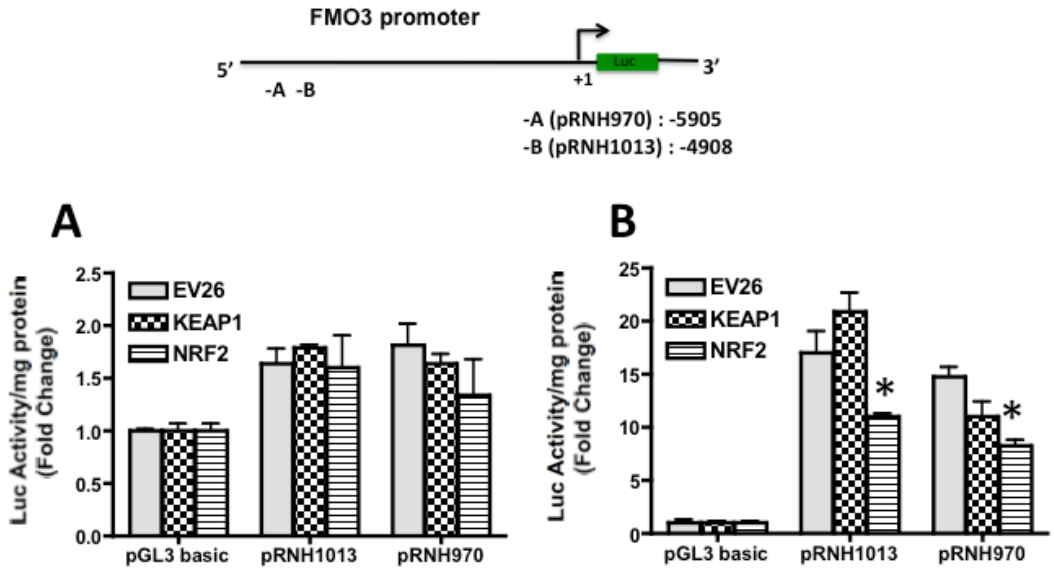
FMO3 promoter
5′
3′
Luc
+1
-A -B
-A (pRNH970) : -5905
-B (pRNH1013) : -4908
A
B
Luc Activity/mg protein (Fold Change)
EV26
KEAP1
NRF2
pGL3 basic
pRNH1013
pRNH970
*
*

Figure 5.3 *Effect of NRF2 or KEAP1 over-expression on FMO3-directed reporter gene activity.* Transcription factor, NRF2, or its cytosolic regulatory protein, KEAP1, were transiently co-expressed with the FMO3 promoter luciferase reporter constructs 5kb-length (pRNH1013), 6kb-length (pRNH970) or the parent plasmid, pGL3 basic, in HepG2 cells. **(A)** Luciferase activity was measured 48 h after transfection, using a commercial kit. Luciferase activity was normalized to total protein and data are presented as mean fold change ± SE. **(B)** HepG2 cells were treated with the pro-oxidant, tBHP (100 µM), or vehicle 24 h after transfection for 6 h. Luciferase activity was measured 42 h after tBHP treatment. Luciferase activity was normalized to total protein and presented as mean fold change ± SE. Each experiment was done in triplicate and repeated at least three times, and representative experimental results are shown. Two-way ANOVA was performed followed by the Bonferroni's post-test. Asterisks (*) represent a statistical difference ($p < 0.05$) from the respective empty vector (EV26) transfected group.

Figure 5.4

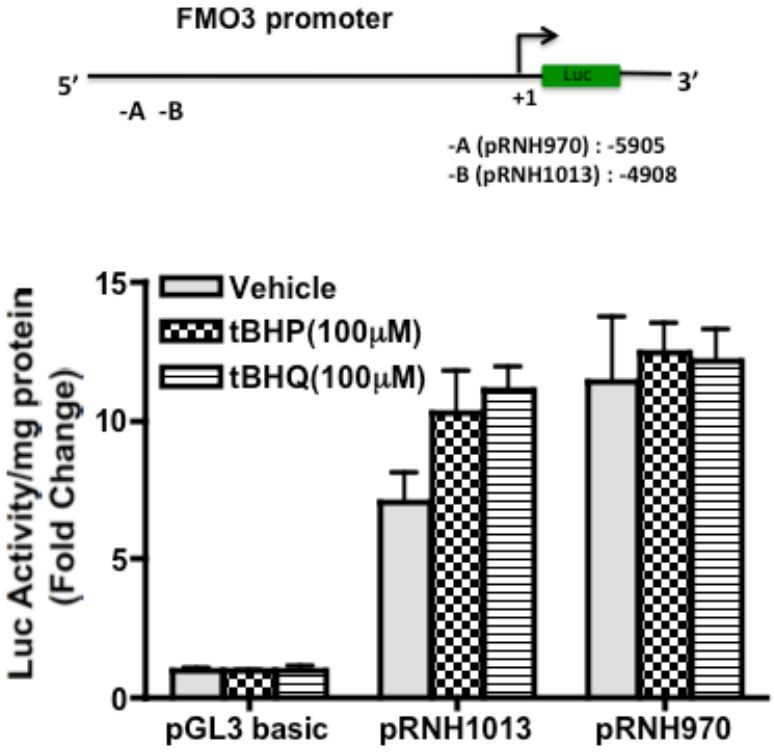
FMO3 promoter
5'
3'
Luc
+1
-A -B
-A (pRNH970) : -5905
-B (pRNH1013) : -4908
Luc Activity/mg protein
(Fold Change)
15
10
5
0
Vehicle
tBHP(100μM)
tBHQ(100μM)
pGL3 basic
pRNH1013
pRNH970

Figure 5.4 *Effect of tBHP and tBHQ on FMO3-directed reporter gene activity.* FMO3 promoter luciferase reporter constructs (pRNH1013 & pRNH970) or the parent plasmid, pGL3 basic were transiently transfected into HepG2 cells. The transfected cells were treated with the pro-oxidant tBHP (100 µM), tBHQ (100 µM) or vehicle 48 h after transfection for 6 h. Luciferase activity was measured 42 h following treatment with tBHP or tBHQ. Luciferase activity was normalized to total protein and presented as mean fold change ± SE. Each experiment was done in triplicate and repeated at least three times, and representative experimental results are shown. Two-way ANOVA was performed followed by the Bonferroni's post-test. Statistical comparisons revealed no significant differences among the data sets.

5.5 Discussion

Mammalian FMOs have long been considered non-inducible by xenobiotics (Cashman & Zhang, 2002; Krueger & Williams, 2005). Thus, the transcriptional regulation of FMO involving stress activated transcription factors has not been studied. Recently, Celius et al. (2008, 2010) showed that activation of the Aryl hydrocarbon (Ah) receptor by 2,3,7,8-tetrachlorodibenzo-p-dioxin (TCDD) induced Fmo3 mRNA expression in mice. The authors also showed that increased Fmo3 mRNA levels in response to 3-methylcholanthrene (3MC) and benzo(a)pyrene (BaP) treatment, but not by TCDD, in Hepa-1 cells was mediated by p53 binding to a response element in the *Fmo3* promoter region (Celius et al., 2010). A gene array analysis performed in our laboratory also identified increased *Fmo3* gene expression after APAP treatment (O'Connor et al., 2014). We have also demonstrated enhanced *Fmo3* gene expression after treatment with other hepatotoxicants such as alpha-naphthyl isothiocyanate and after bile duct ligation (Rudraiah et al., 2014; Rudraiah et al., 2014). Given that all three of these latter treatments results in oxidative stress, the goal of the present study was to determine whether *FMO3* regulation under oxidative stress conditions might involve NRF2-KEAP1 regulatory pathway activation, which is known to mediate many oxidative-stress induced changes in gene expression.

Over-expression of NRF2 induced expression of its known target genes, HMOX1 and NQO1 (Aleksunes et al., 2006; Aleksunes & Manautou, 2007; Aleksunes et al., 2008). With over-expression of KEAP1 we anticipated

seeing a significant decrease in HMOX1 and NQO1 expression, but no such changes were observed. HMOX1 has also been shown to be regulated by hypoxia-inducible factor-1α (HIF-1α) and JNK-1 (Yeligar et al., 2010). Similarly, AhR has been shown to regulate NQO1 (Wang et al., 2013; Yeligar et al., 2010). It is possible that during over-expression of KEAP1, transcription factors other than Nrf2 play a role in maintaining expression of HMOX1 and NQO1. Over-expression of NRF2 or KEAP1 did not significantly alter *FMO3* gene expression, suggesting that *FMO3* gene regulation does not involve NRF2-KEAP1. However, Klick et al. demonstrated that treatment of HepG2 cells with 5-aza-2'-deoxycytidine (DNA methyl transferase inhibitor) resulted in detectable FMO3 expression, consistent with DNA methylation being a major mechanism repressing HepG2 FMO3 expression (Klick et al., 2008). The DNA methylation-mediated suppression of HepG2 *FMO3* may well have prevented any NRF2-mediated effects on this gene.

To further investigate possible NRF2-mediated *FMO3* gene regulation, co-transfection studies using two FMO3 promoter luciferase reporter constructs (pRNH1013 and pRNH970) were performed. Co-transfection of NRF2 or KEAP1 expression vectors along with the FMO3 reporter constructs did not significantly alter reporter gene activity. However, co-transfection of the NRF2 expression vector and the FMO3 reporter constructs, in addition to activation of NRF2 nuclear translocation by a treatment with a subtoxic dose of tBHP, did reduce reporter gene activity significantly. Although, this is suggestive of a potential NRF2 suppressive effect on *FMO3* gene

transcription, a 6 kb promoter analysis using MatInspector software (Genomatix, Munich, Germany), did not identify any antioxidant response element (ARE) site on *FMO3* promoter. The decrease in reporter gene activity might be due to an indirect mechanism during oxidative stress conditions that may or may not involve NRF2. The one other major possibility worth evaluating is the activator protein-1 mediated regulation of *FMO3*. Oxidative stress is known to alter signaling through c-Jun N-terminal Kinase (JNK) and related pathways, thus activating AP-1 (Elsby et al., 2003; Enomoto et al., 2001; Li & Jaiswal, 1992). In addition, promoter analysis discovered four binding sites for AP-1 at about 0.7, 0.9, 4.9 and 5.7 kb from the transcription start site on the human *FMO3* promoter (data not shown).

FMO3 reporter construct over-expression along with NRF2 activation by tBHP or tBHQ treatment also failed to alter reporter gene activity. The tBHP dose used in this study increased NRF2 nuclear translocation and expression of the known NRF2 target genes, HMOX1 and NQO1. Collectively, these data suggest that *FMO3* transcriptional regulation does not involve the NRF2-KEAP1 signaling pathway.

CHAPTER 6

Summary

Flavin-containing monooxygenase-3 (Fmo3) is a drug-metabolizing enzyme involved in oxygenation of a wide variety of endogenous substances and xenobiotics (Krueger & Williams, 2005). The importance of mammalian FMO in xenobiotic metabolism is known, but its physiological function(s) are poorly understood. Among all FMOs in humans, FMO3 is most studied because mutant alleles contribute to a disease known as trimethylaminuria or fish-odor syndrome. Until recently, *Fmo3* gene inducibility by xenobiotics was not known. Recent studies with Ah receptor agonists demonstrated increased *Fmo3* gene expression in mice livers (Celius et al., 2008; Celius et al., 2010). A gene array analysis performed previously in our laboratory also demonstrated increases in liver *Fmo3* gene expression in the mouse model of APAP autoprotection (O'Connor et al., 2014). Given the prevalence of APAP-hepatotoxicity and the human health impact associated with the misuse of this popular over-the-counter and prescription medication, a further understanding of the mechanism(s) involved in such protection and the identification of new genetic determinants of APAP toxicity is of considerable significance. The work presented in this dissertation examines *Fmo3* gene expression and regulation during oxidative stress conditions. Our studies provide the first comprehensive analysis of Fmo3 gene and protein expression changes, as well as catalytic enzyme activity, in response to treatment with a xenobiotic.

The functional significance of *Fmo3* over-expression to APAP toxicity was also investigated employing both *in vitro* and *in vivo* methods.

In **Chapter 2**, we examined *Fmo3* mRNA and protein expression during APAP-induced liver injury. The significance of *FMO3* over-expression was also investigated to establish a causal relationship between the *Fmo3* gene expression and APAP hepatotoxicity. It is demonstrated in **Chapter 2** that Fmo3 mRNA expression in response to a single dose of APAP is accompanied by marginal increases in Fmo3 protein expression and catalytic activity. In contrast to what was observed with a single mildly hepatotoxic dose of APAP, both liver Fmo3 mRNA and protein expression are significantly higher in mice treated with the APAP autoprotection regimen (pre- and post-APAP treatment). *Fmo3* gene expression alteration was further confirmed by examining protein expression by western blotting, immunohistochemistry as well as enzymatic assay. Consistent with the protein expression analysis by western blotting, Fmo3 catalytic activity and centrilobular zonal expression are also significantly greater in the APAP autoprotection group. One of the most striking finding in this study is the highly confined distribution of the Fmo3 protein around the central vein after APAP in the APAP autoprotected livers. Together, these studies suggest that the regulation of *Fmo3* gene expression (transcriptional and/or translational) is different under the conditions of treatment with a single APAP dose versus an autoprotection treatment regimen.

The functional significance of *Fmo3* over-expression during APAP hepatotoxicity was evaluated both *in vivo* and *in vitro*. Female mice express higher basal *Fmo3* levels in liver than male mice (Cherrington et al., 1998; Hines, 2006; Janmohamed et al., 2004), and are much more resistant to APAP hepatotoxicity compared to males (Dai et al., 2006). MMI inhibition of Fmo3 renders female mice highly susceptible to APAP-induced hepatotoxicity without altering the magnitude of liver injury produced by APAP in male mice. Results from hepatocyte cell line (HC-04) over-expressing FMO3 demonstrate that enhanced expression of FMO3 confers resistance against APAP-induced cytotoxicity. Together, our studies in **Chapter 2** indicate that *Fmo3* gene is inducible following hepatotoxic APAP treatment in mice and that FMO3 over-expression is protective against APAP-induced cytotoxicity in cultured liver cells. These data provide the foundation for subsequent studies aimed at unveiling the function(s) that make Fmo3 a novel genetic determinant of APAP toxicity.

The purpose of the next set of studies presented in **Chapter 3** was to investigate *Fmo3* gene induction in other mouse models of hepatic injury. Hepatotoxicants used in this study include ANIT, CCl_4 and AlOH. In addition, BDL was used as our fourth model since it is a widely accepted surgical intervention producing cholestatic liver injury. Since a common feature of all these forms of liver injury is oxidative stress, the potential role of the transcription factor Nrf2 in altering *Fmo3* gene expression was also examined. We show that toxic ANIT and BDL significantly alter Fmo3 mRNA

expression. CCl_4-mediated liver injury significantly decreased Fmo3 mRNA expression and no change in expression is evidenced with AlOH. We also observed a toxicity threshold for *Fmo3* gene expression in APAP, ANIT and BDL livers. Mild to moderate injury in all three models appears to be optimal for Fmo3 mRNA induction, while no change and/or reduction in Fmo3 expression is seen with more pronounced injury. While both cholestasis models, toxic ANIT and BDL, significantly alter Fmo3 mRNA expression, Fmo3 protein increase is observed only with ANIT. It is possible that under more pronounced oxidative stress conditions (as seen in cases of greater magnitude of hepatotoxicity) some proteins involved in gene translation are oxidized *in vivo* inhibiting translation (Shenton et al., 2006). The possibility of translational inhibition during BDL should not be overlooked.

In addition, *Fmo3* gene induction is still observed in Nrf2 knockout mice in response to APAP treatment, indicating that the transcriptional regulation of *Fmo3* does not involve Nrf2 signaling. It is also possible that the hepatocellular injury that persists at 72 h in Nrf2 KO mice most likely activates other signaling mechanisms mediating *Fmo3* gene induction. To determine whether accumulation of bile acids is a signaling event regulating Fmo3, total hepatic and plasma bile acid levels were measured with all hepatotoxicants. Consistent with the literature, ANIT and BDL increased plasma and hepatic bile acid concentrations. A high CCl_4 dose did not significantly alter liver bile acid levels, but significantly increased plasma bile acid concentration. APAP tended to increase both hepatic and plasma bile acid concentrations, but this

is not statistically significant. No change in plasma and hepatic bile acid levels were observed with AlOH treatment. Because, ANIT, BDL and APAP that induced *Fmo3* gene expression also increased hepatic and plasma bile acid levels, future studies to address the mouse liver *Fmo3* gene regulation should investigate the role of nuclear receptor farnesoid X receptor (FXR) in *Fmo3* gene induction. FXR is one of the major bile acid sensors in the liver (Chiang, 2002) and plays a protective role during cholestasis development. Recently, it has also been shown that activation of FXR induces Fmo3 protein function in mice (Bennett et al., 2013). Furthermore, activation of FXR can protect against APAP-induced hepatotoxicity (Lee et al., 2010). In support of all this, we discovered using Matinspector three binding sites for farnesoid X receptor-response element (FXRE) on the mouse *Fmo3* promoter.

Similar to our APAP autoprotection mouse model, human liver can adapt to APAP-induced hepatotoxicity (Shayiq et al., 1999; Watkins et al., 2006). Thus, the goal of **Chapter 4** was to investigate *FMO3* gene induction in a human hepatoma cell line, HepaRG cells. HepaRG cell line is a recently developed cellular model that expresses a more normal spectrum of drug metabolizing enzymes comparable to human hepatocytes. The mechanistic features of APAP-induced hepatotoxicity in HepaRG cells are similar to that reported for mouse primary hepatocytes and mouse liver *in vivo* (McGill et al., 2011). Experiments in **Chapter 4** demonstrate *FMO3* gene induction during APAP-induced cytotoxicity. This is the first report showing induction of *FMO3* by a xenobiotic treatment in human hepatocytes.

Furthermore, to study the functional significance of *FMO3* over-expression during APAP-induced cytotoxicity, HepaRG cells over-expressing FMO3, as an alternative *in vitro* system, were developed. As described previously in this dissertation (**Chapter 2**), we had already established the hepatocyte cell line HC-04 over-expressing human FMO3 (hFMO3-HC-04). HepaRG cells differ from HC-04 cells in that the constitutive FMO3 expression is very high, which is comparable to adult human liver. FMO3 over-expression in HepaRG cells was assumed to model FMO3 over-expression during APAP treatment in human liver/hepatocytes. Consistent with results from hFMO3-HC-04 cells, the results from hFMO3-HepaRG cells also show that FMO3 over-expression alters susceptibility to APAP-induced hepatotoxicity. Most importantly and highly intriguing, our data with the HepaRG cells show that FMO3 may play an important role in cellular differentiation. The potential role for FMO3 in cellular differentiation is consistent with the latent profile of Fmo3 protein expression changes we observed *in vivo* in our APAP autoprotection mouse model (**Chapter 2**). It remains to be determined the mechanism underlying the faster rate of cell differentiation driven by FMO3 over-expression in HepaRG cells. Future studies that could aid in not only characterizing the functions of Fmo3 that make it a genetic determinant of APAP hepatotoxicity, but also its potential role in speeding cell differentiation are planned employing transcriptomics, proteomics and possibly RNA-seq approaches. The goal of these proposed

studies is to identify signaling pathway(s) and cellular events associated with FMO3 function that may be relevant to the main findings of this dissertation.

Toxic APAP, ANIT and BDL induce *Fmo3* gene expression in mice. A common event for all hepatotoxicants that induce *Fmo3* in mice is oxidative stress, and activation of Nrf2-Keap1 regulatory pathway. NRF2 target gene NQO1 induction is also reported in human liver samples obtained from patients during transplantation following APAP overdose (Aleksunes et al., 2006). The results in **Chapter 3** with Nrf2 null mice show that *Fmo3* is not regulated by transcription factor Nrf2 but *FMO3* gene regulation and promoter sequences differ between humans and mice. Thus, the experiments in **Chapter 5** were aimed to investigate whether NRF2 regulates human *FMO3* gene expression. Constitutive *FMO3* expression is repressed in HepG2 cells (Klick et al., 2008). Thus, HepG2 cells were used for all experiments in this study. Co-transfection studies with FMO3 promoter luciferase reporter constructs (5 kb or 6 kb) and NRF2 or its cytosolic retainer Kelch-like ECH-associated protein 1 (KEAP1) did not significantly alter luciferase reporter gene activity. Subsequent promoter analysis using Matinspector did not identify any antioxidant response element (ARE) sites on reporter constructs used in the current study. Based on these results we concluded that the transcriptional regulation of *FMO3* might not involve NRF2-KEAP1 regulatory pathway.

Although, investigating FMO3-driven HepaRG differentiation is a potential subject of future innovative research, the possible involvement of

FMO in maintaining cellular thiol:disulphide ratios deserves consideration also and should not be overlooked. The relationship between cellular thiol:disulphide ratios and the regulation of metabolic reactions is very well documented (Barron, 1953). Cysteamine is a substrate for FMO3 oxygenation and oxygenation of cysteamine during APAP hepatotoxicity may serve to help control the overall thiol:disulphide redox state of the cell. This in turn may modulate cellular metabolism and/or activate signal transduction pathway leading to altered susceptibility to APAP (or protection). Thus, strengthening cellular defenses and heightened toxicant tolerability. It is also possible that oxygenation of cysteamine to cystamine by Fmo3 and transport out of the cell also may represent a detoxication mechanism and/or protective event, because cysteamine is toxic to cells at concentrations as low as 39 μM through the transition metal-dependent formation of hydrogen peroxide (Jeitner & Lawrence, 2001). To investigate whether oxygenation of cysteamine to cystamine by Fmo3 is important during APAP hepatotoxicity, follow-up studies will measure the total hepatic cysteamine and cystamine concentrations in the mouse model of APAP autoprotection. Together, this work not only supports the usefulness, but also validates the use of transcriptomic analysis for identifying genetic determinants of diseases and adverse reactions to chemicals (e.g. chemical-induced hepatotoxicity). Both the *in vitro* and *in vivo* approaches used in this study represent valuable tools for investigating the involvement of *FMO3* during APAP-induced hepatic injury.

REFERENCES

Aleksunes, L. M., Campion, S. N., Goedken, M. J., & Manautou, J. E. (2008). Acquired resistance to acetaminophen hepatotoxicity is associated with induction of multidrug resistance-associated protein 4 (Mrp4) in proliferating hepatocytes. *Toxicological Sciences : An Official Journal of the Society of Toxicology, 104*(2), 261-273.

Aleksunes, L. M., Goedken, M., & Manautou, J. E. (2006). Up-regulation of NAD(P)H quinone oxidoreductase 1 during human liver injury. *World Journal of Gastroenterology : WJG, 12*(12), 1937-1940.

Aleksunes, L. M., & Manautou, J. E. (2007). Emerging role of Nrf2 in protecting against hepatic and gastrointestinal disease. *Toxicologic Pathology, 35*(4), 459-473.

Aleksunes, L. M., Scheffer, G. L., Jakowski, A. B., Pruimboom-Brees, I. M., & Manautou, J. E. (2006). Coordinated expression of multidrug resistance-associated proteins (mrps) in mouse liver during toxicant-induced injury. *Toxicological Sciences : An Official Journal of the Society of Toxicology, 89*(2), 370-379.

Aleksunes, L. M., Slitt, A. L., Maher, J. M., Augustine, L. M., Goedken, M. J., Chan, J. Y., et al. (2008). Induction of Mrp3 and Mrp4 transporters during acetaminophen hepatotoxicity is dependent on Nrf2. *Toxicology and Applied Pharmacology, 226*(1), 74-83.

Aleksunes, L. M., Slitt, A. L., Maher, J. M., Dieter, M. Z., Knight, T. R., Goedken, M., et al. (2006). Nuclear factor-E2-related factor 2 expression in liver is critical for induction of NAD(P)H:Quinone oxidoreductase 1 during cholestasis. *Cell Stress & Chaperones, 11*(4), 356-363.

Aleksunes, L. M., Slitt, A. M., Cherrington, N. J., Thibodeau, M. S., Klaassen, C. D., & Manautou, J. E. (2005). Differential expression of mouse hepatic

transporter genes in response to acetaminophen and carbon tetrachloride. *Toxicological Sciences : An Official Journal of the Society of Toxicology, 83*(1), 44-52.

Aninat, C., Piton, A., Glaise, D., Le Charpentier, T., Langouet, S., Morel, F., et al. (2006). Expression of cytochromes P450, conjugating enzymes and nuclear receptors in human hepatoma HepaRG cells. *Drug Metabolism and Disposition: The Biological Fate of Chemicals, 34*(1), 75-83.

Attar, M., Dong, D., Ling, K. H., & Tang-Liu, D. D. (2003). Cytochrome P450 2C8 and flavin-containing monooxygenases are involved in the metabolism of tazarotenic acid in humans. *Drug Metabolism and Disposition: The Biological Fate of Chemicals, 31*(4), 476-481.

Badr, M. Z. (1991). Periportal hepatotoxicity due to allyl alcohol: A myriad of proposed mechanisms. *Journal of Biochemical Toxicology, 6*(1), 1-5.

Bajt, M. L., Knight, T. R., Lemasters, J. J., & Jaeschke, H. (2004). Acetaminophen-induced oxidant stress and cell injury in cultured mouse hepatocytes: Protection by N-acetyl cysteine. *Toxicological Sciences : An Official Journal of the Society of Toxicology, 80*(2), 343-349.

Barnes, S. N., Aleksunes, L. M., Augustine, L., Scheffer, G. L., Goedken, M. J., Jakowski, A. B., et al. (2007). Induction of hepatobiliary efflux transporters in acetaminophen-induced acute liver failure cases. *Drug Metabolism and Disposition: The Biological Fate of Chemicals, 35*(10), 1963-1969.

Barron, E. S. (1953). The importance of sulfhydryl groups in biology and medicine. *Texas Reports on Biology and Medicine, 11*(4), 653-670.

Bataille, A. M., & Manautou, J. E. (2012). Nrf2: A potential target for new therapeutics in liver disease. *Clinical Pharmacology and Therapeutics, 92*(3), 340-348.

Bauer, I., Vollmar, B., Jaeschke, H., Rensing, H., Kraemer, T., Larsen, R., et al. (2000). Transcriptional activation of heme oxygenase-1 and its functional significance in acetaminophen-induced hepatitis and hepatocellular injury in the rat. *Journal of Hepatology, 33*(3), 395-406.

Bennett, B. J., de Aguiar Vallim, T. Q., Wang, Z., Shih, D. M., Meng, Y., Gregory, J., et al. (2013). Trimethylamine-N-oxide, a metabolite associated with atherosclerosis, exhibits complex genetic and dietary regulation. *Cell Metabolism, 17*(1), 49-60.

Brunelle, A., Bi, Y. A., Lin, J., Russell, B., Luy, L., Berkman, C., et al. (1997). Characterization of two human flavin-containing monooxygenase (form 3) enzymes expressed in escherichia coli as maltose binding protein fusions. *Drug Metabolism and Disposition: The Biological Fate of Chemicals, 25*(8), 1001-1007.

Burcham, P. C., & Fontaine, F. (2001). Extensive protein carbonylation precedes acrolein-mediated cell death in mouse hepatocytes. *Journal of Biochemical and Molecular Toxicology, 15*(6), 309-316.

Campion, S. N., Johnson, R., Aleksunes, L. M., Goedken, M. J., van Rooijen, N., Scheffer, G. L., et al. (2008). Hepatic Mrp4 induction following acetaminophen exposure is dependent on kupffer cell function. *American Journal of Physiology.Gastrointestinal and Liver Physiology, 295*(2), G294-304.

Campion, S. N., Tatis-Rios, C., Augustine, L. M., Goedken, M. J., van Rooijen, N., Cherrington, N. J., et al. (2009). Effect of allyl alcohol on hepatic transporter expression: Zonal patterns of expression and role of kupffer cell function. *Toxicology and Applied Pharmacology, 236*(1), 49-58.

Capizzo, F., & Roberts, R. J. (1971). -Naphthylisothiocyanate (ANIT)-induced hepatotoxicity and disposition in various species. *Toxicology and Applied Pharmacology, 19*(2), 176-187.

Cashman, J. R. (1995). Structural and catalytic properties of the mammalian flavin-containing monooxygenase. *Chemical Research in Toxicology, 8*(2), 166-181.

Cashman, J. R. (1999). In vitro metabolism: FMO and related oxygenations. In T. F. Woolf (Ed.), *Handbook of drug metabolism* (pp. 477). New york: Marcel Dekker, Inc.

Cashman, J. R. (2005). Some distinctions between flavin-containing and cytochrome P450 monooxygenases. *Biochemical and Biophysical Research Communications, 338*(1), 599-604.

Cashman, J. R., & Hanzlik, R. P. (1981). Microsomal oxidation of thiobenzamide. A photometric assay for the flavin-containing monooxygenase. *Biochemical and Biophysical Research Communications, 98*(1), 147-153.

Cashman, J. R., Lattard, V., & Lin, J. (2004). Effect of total parenteral nutrition and choline on hepatic flavin-containing and cytochrome P-450 monooxygenase activity in rats. *Drug Metabolism and Disposition: The Biological Fate of Chemicals, 32*(2), 222-229.

Cashman, J. R., & Williams, D. E. (1990). Enantioselective S-oxygenation of 2-aryl-1,3-dithiolanes by rabbit lung enzyme preparations. *Molecular Pharmacology, 37*(2), 333-339.

Cashman, J. R., & Zhang, J. (2002). Interindividual differences of human flavin-containing monooxygenase 3: Genetic polymorphisms and functional variation. *Drug Metabolism and Disposition: The Biological Fate of Chemicals, 30*(10), 1043-1052.

Cashman, J. R., & Zhang, J. (2006). Human flavin-containing monooxygenases. *Annual Review of Pharmacology and Toxicology, 46*, 65-100.

Celius, T., Pansoy, A., Matthews, J., Okey, A. B., Henderson, M. C., Krueger, S. K., et al. (2010). Flavin-containing monooxygenase-3: Induction by 3-methylcholanthrene and complex regulation by xenobiotic chemicals in hepatoma cells and mouse liver. *Toxicology and Applied Pharmacology, 247*(1), 60-69.

Celius, T., Roblin, S., Harper, P. A., Matthews, J., Boutros, P. C., Pohjanvirta, R., et al. (2008). Aryl hydrocarbon receptor-dependent induction of flavin-containing monooxygenase mRNAs in mouse liver. *Drug Metabolism and Disposition: The Biological Fate of Chemicals, 36*(12), 2499-2505.

Cerec, V., Glaise, D., Garnier, D., Morosan, S., Turlin, B., Drenou, B., et al. (2007). Transdifferentiation of hepatocyte-like cells from the human hepatoma HepaRG cell line through bipotent progenitor. *Hepatology (Baltimore, Md.), 45*(4), 957-967.

Chan, K., Han, X. D., & Kan, Y. W. (2001). An important function of Nrf2 in combating oxidative stress: Detoxification of acetaminophen. *Proceedings of the National Academy of Sciences of the United States of America, 98*(8), 4611-4616.

Chen, C., Hennig, G. E., & Manautou, J. E. (2003). Hepatobiliary excretion of acetaminophen glutathione conjugate and its derivatives in transport-deficient (TR-) hyperbilirubinemic rats. *Drug Metabolism and Disposition: The Biological Fate of Chemicals, 31*(6), 798-804.

Cheng, J., Ma, X., Krausz, K. W., Idle, J. R., & Gonzalez, F. J. (2009). Rifampicin-activated human pregnane X receptor and CYP3A4 induction enhance acetaminophen-induced toxicity. *Drug Metabolism and Disposition: The Biological Fate of Chemicals, 37*(8), 1611-1621.

Cherrington, N. J., Cao, Y., Cherrington, J. W., Rose, R. L., & Hodgson, E. (1998). Physiological factors affecting protein expression of flavin-containing monooxygenases 1, 3 and 5. *Xenobiotica; the Fate of Foreign Compounds in Biological Systems, 28*(7), 673-682.

Chiang, J. Y. (2002). Bile acid regulation of gene expression: Roles of nuclear hormone receptors. *Endocrine Reviews, 23*(4), 443-463.

Chiu, H., Brittingham, J. A., & Laskin, D. L. (2002). Differential induction of heme oxygenase-1 in macrophages and hepatocytes during acetaminophen-induced hepatotoxicity in the rat: Effects of hemin and biliverdin. *Toxicology and Applied Pharmacology, 181*(2), 106-115.

Cohen, S. D., Pumford, N. R., Khairallah, E. A., Boekelheide, K., Pohl, L. R., Amouzadeh, H. R., et al. (1997). Selective protein covalent binding and target organ toxicity. *Toxicology and Applied Pharmacology, 143*(1), 1-12.

Cui, Y. J., Aleksunes, L. M., Tanaka, Y., Goedken, M. J., & Klaassen, C. D. (2009). Compensatory induction of liver efflux transporters in response to ANIT-induced liver injury is impaired in FXR-null mice. *Toxicological Sciences : An Official Journal of the Society of Toxicology, 110*(1), 47-60.

Dai, G., He, L., Chou, N., & Wan, Y. J. (2006). Acetaminophen metabolism does not contribute to gender difference in its hepatotoxicity in mouse. *Toxicological Sciences : An Official Journal of the Society of Toxicology, 92*(1), 33-41.

Davidson, D. G., & Eastham, W. N. (1966). Acute liver necrosis following overdose of paracetamol. *British Medical Journal, 2*(5512), 497-499.

Dietrich, C. G., Ottenhoff, R., de Waart, D. R., & Oude Elferink, R. P. (2001). Role of MRP2 and GSH in intrahepatic cycling of toxins. *Toxicology, 167*(1), 73-81.

Dixit, A., & Roche, T. E. (1984). Spectrophotometric assay of the flavin-containing monooxygenase and changes in its activity in female mouse liver with nutritional and diurnal conditions. *Archives of Biochemistry and Biophysics, 233*(1), 50-63.

Dolphin, C. T., Cullingford, T. E., Shephard, E. A., Smith, R. L., & Phillips, I. R. (1996). Differential developmental and tissue-specific regulation of expression of the genes encoding three members of the flavin-containing monooxygenase family of man, FMO1, FMO3 and FM04. *European Journal of Biochemistry / FEBS, 235*(3), 683-689.

Donepudi, A. C., Aleksunes, L. M., Driscoll, M. V., Seeram, N. P., & Slitt, A. L. (2012). The traditional ayurvedic medicine, eugenia jambolana (jamun fruit), decreases liver inflammation, injury and fibrosis during cholestasis. *Liver International : Official Journal of the International Association for the Study of the Liver, 32*(4), 560-573.

Duffel, M. W., Graham, J. M., & Ziegler, D. M. (1981). Changes in dimethylaniline N-oxidase activity of mouse liver and kidney induced by steroid sex hormones. *Molecular Pharmacology, 19*(1), 134-139.

El-Hassan, H., Anwar, K., Macanas-Pirard, P., Crabtree, M., Chow, S. C., Johnson, V. L., et al. (2003). Involvement of mitochondria in acetaminophen-induced apoptosis and hepatic injury: Roles of cytochrome c, bax, bid, and caspases. *Toxicology and Applied Pharmacology, 191*(2), 118-129.

Elsby, R., Kitteringham, N. R., Goldring, C. E., Lovatt, C. A., Chamberlain, M., Henderson, C. J., et al. (2003). Increased constitutive c-jun N-terminal kinase signaling in mice lacking glutathione S-transferase pi. *The Journal of Biological Chemistry, 278*(25), 22243-22249.

Enomoto, A., Itoh, K., Nagayoshi, E., Haruta, J., Kimura, T., O'Connor, T., et al. (2001). High sensitivity of Nrf2 knockout mice to acetaminophen hepatotoxicity associated with decreased expression of ARE-regulated drug metabolizing enzymes and antioxidant genes. *Toxicological Sciences : An Official Journal of the Society of Toxicology, 59*(1), 169-177.

Falls, J. G., Cherrington, N. J., Clements, K. M., Philpot, R. M., Levi, P. E., Rose, R. L., et al. (1997). Molecular cloning, sequencing, and expression in escherichia coli of mouse flavin-containing monooxygenase 3 (FMO3):

Comparison with the human isoform. *Archives of Biochemistry and Biophysics, 347*(1), 9-18.

Gartung, C., Ananthanarayanan, M., Rahman, M. A., Schuele, S., Nundy, S., Soroka, C. J., et al. (1996). Down-regulation of expression and function of the rat liver Na+/bile acid cotransporter in extrahepatic cholestasis. *Gastroenterology, 110*(1), 199-209.

Geier, A., Dietrich, C. G., Voigt, S., Kim, S. K., Gerloff, T., Kullak-Ublick, G. A., et al. (2003). Effects of proinflammatory cytokines on rat organic anion transporters during toxic liver injury and cholestasis. *Hepatology (Baltimore, Md.), 38*(2), 345-354.

Geier, A., Kim, S. K., Gerloff, T., Dietrich, C. G., Lammert, F., Karpen, S. J., et al. (2002). Hepatobiliary organic anion transporters are differentially regulated in acute toxic liver injury induced by carbon tetrachloride. *Journal of Hepatology, 37*(2), 198-205.

Geier, A., Zollner, G., Dietrich, C. G., Wagner, M., Fickert, P., Denk, H., et al. (2005). Cytokine-independent repression of rodent ntcp in obstructive cholestasis. *Hepatology (Baltimore, Md.), 41*(3), 470-477.

Gerets, H. H., Tilmant, K., Gerin, B., Chanteux, H., Depelchin, B. O., Dhalluin, S., et al. (2012). Characterization of primary human hepatocytes, HepG2 cells, and HepaRG cells at the mRNA level and CYP activity in response to inducers and their predictivity for the detection of human hepatotoxins. *Cell Biology and Toxicology, 28*(2), 69-87.

Ghanem, C. I., Gomez, P. C., Arana, M. C., Perassolo, M., Ruiz, M. L., Villanueva, S. S., et al. (2004). Effect of acetaminophen on expression and activity of rat liver multidrug resistance-associated protein 2 and P-glycoprotein. *Biochemical Pharmacology, 68*(4), 791-798.

Ghanem, C. I., Ruiz, M. L., Villanueva, S. S., Luquita, M. G., Catania, V. A., Jones, B., et al. (2005). Shift from biliary to urinary elimination of acetaminophen-glucuronide in acetaminophen-pretreated rats. *The*

Journal of Pharmacology and Experimental Therapeutics, 315(3), 987-995.

Ghosh, J., Das, J., Manna, P., & Sil, P. C. (2010). Arjunolic acid, a triterpenoid saponin, prevents acetaminophen (APAP)-induced liver and hepatocyte injury via the inhibition of APAP bioactivation and JNK-mediated mitochondrial protection. *Free Radical Biology & Medicine, 48*(4), 535-553.

Goldring, C. E., Kitteringham, N. R., Elsby, R., Randle, L. E., Clement, Y. N., Williams, D. P., et al. (2004). Activation of hepatic Nrf2 in vivo by acetaminophen in CD-1 mice. *Hepatology (Baltimore, Md.), 39*(5), 1267-1276.

Gripon, P., Rumin, S., Urban, S., Le Seyec, J., Glaise, D., Cannie, I., et al. (2002). Infection of a human hepatoma cell line by hepatitis B virus. *Proceedings of the National Academy of Sciences of the United States of America, 99*(24), 15655-15660.

Gruebele, A., Zawaski, K., Kaplan, D., & Novak, R. F. (1996). Cytochrome P4502E1- and cytochrome P4502B1/2B2-catalyzed carbon tetrachloride metabolism: Effects on signal transduction as demonstrated by altered immediate-early (c-fos and c-jun) gene expression and nuclear AP-1 and NF-kappa B transcription factor levels. *Drug Metabolism and Disposition: The Biological Fate of Chemicals, 24*(1), 15-22.

Guo, G. L., Moffit, J. S., Nicol, C. J., Ward, J. M., Aleksunes, L. A., Slitt, A. L., et al. (2004). Enhanced acetaminophen toxicity by activation of the pregnane X receptor. *Toxicological Sciences : An Official Journal of the Society of Toxicology, 82*(2), 374-380.

Hart, S. N., Li, Y., Nakamoto, K., Subileau, E. A., Steen, D., & Zhong, X. B. (2010). A comparison of whole genome gene expression profiles of HepaRG cells and HepG2 cells to primary human hepatocytes and human liver tissues. *Drug Metabolism and Disposition: The Biological Fate of Chemicals, 38*(6), 988-994.

Hernandez, D., Janmohamed, A., Chandan, P., Omar, B. A., Phillips, I. R., & Shephard, E. A. (2009). Deletion of the mouse Fmo1 gene results in enhanced pharmacological behavioural responses to imipramine. *Pharmacogenetics and Genomics, 19*(4), 289-299.

Hines, R. N. (2006). Developmental and tissue-specific expression of human flavin-containing monooxygenases 1 and 3. *Expert Opinion on Drug Metabolism & Toxicology, 2*(1), 41-49.

Hines, R. N., Cashman, J. R., Philpot, R. M., Williams, D. E., & Ziegler, D. M. (1994). The mammalian flavin-containing monooxygenases: Molecular characterization and regulation of expression. *Toxicology and Applied Pharmacology, 125*(1), 1-6.

Hines, R. N., Luo, Z., Hopp, K. A., Cabacungan, E. T., Koukouritaki, S. B., & McCarver, D. G. (2003). Genetic variability at the human FMO1 locus: Significance of a basal promoter yin yang 1 element polymorphism (FMO1*6). *The Journal of Pharmacology and Experimental Therapeutics, 306*(3), 1210-1218.

Hinson, J. A., Roberts, D. W., & James, L. P. (2010). Mechanisms of acetaminophen-induced liver necrosis. *Handbook of Experimental Pharmacology, (196):369-405. doi*(196), 369-405.

Hodgson, E., Cherrington, N. J., Philpot, R. M., & Rose, R. L. (1999). Biochemical aspects of flavin-containing monooxygenases (FMOs). In E. Arinc, J. B. Schenkman & E. Hodgson (Eds.), *In molecular and applied aspects of oxidative drug metabolizing enzymes* (Nato ASI series ed., pp. 55). New york: Plenum Publishers.

Hodgson, E., Rose, R. L., Ryu, D. Y., Falls, G., Blake, B. L., & Levi, P. E. (1995). Pesticide-metabolizing enzymes. *Toxicology Letters, 82-83*, 73-81.

Hohenester, S., Oude-Elferink, R. P., & Beuers, U. (2009). Primary biliary cirrhosis. *Seminars in Immunopathology, 31*(3), 283-307.

Hunter, A. L., & Neal, R. A. (1975). Inhibition of hepatic mixed-function oxidase activity in vitro and in vivo by various thiono-sulfur-containing compounds. *Biochemical Pharmacology, 24*(23), 2199-2205.

Jaeschke, H. (1990). Glutathione disulfide formation and oxidant stress during acetaminophen-induced hepatotoxicity in mice in vivo: The protective effect of allopurinol. *The Journal of Pharmacology and Experimental Therapeutics, 255*(3), 935-941.

Jaeschke, H. (2003). Are cultured liver cells the right tool to investigate mechanisms of liver disease or hepatotoxicity? *Hepatology (Baltimore, Md.), 38*(4), 1053-1055.

Jaeschke, H., & Bajt, M. L. (2006). Intracellular signaling mechanisms of acetaminophen-induced liver cell death. *Toxicological Sciences : An Official Journal of the Society of Toxicology, 89*(1), 31-41.

Jaeschke, H., McGill, M. R., & Ramachandran, A. (2012). Oxidant stress, mitochondria, and cell death mechanisms in drug-induced liver injury: Lessons learned from acetaminophen hepatotoxicity. *Drug Metabolism Reviews, 44*(1), 88-106.

Jaeschke, H., McGill, M. R., Williams, C. D., & Ramachandran, A. (2011). Current issues with acetaminophen hepatotoxicity--a clinically relevant model to test the efficacy of natural products. *Life Sciences, 88*(17-18), 737-745.

Jaiswal, A. K. (2004). Nrf2 signaling in coordinated activation of antioxidant gene expression. *Free Radical Biology & Medicine, 36*(10), 1199-1207.

Janmohamed, A., Hernandez, D., Phillips, I. R., & Shephard, E. A. (2004). Cell-, tissue-, sex- and developmental stage-specific expression of mouse flavin-containing monooxygenases (fmos). *Biochemical Pharmacology, 68*(1), 73-83.

Jeitner, T. M., & Lawrence, D. A. (2001). Mechanisms for the cytotoxicity of cysteamine. *Toxicological Sciences : An Official Journal of the Society of Toxicology, 63*(1), 57-64.

Jollow, D. J., Mitchell, J. R., Potter, W. Z., Davis, D. C., Gillette, J. R., & Brodie, B. B. (1973). Acetaminophen-induced hepatic necrosis. II. role of covalent binding in vivo. *The Journal of Pharmacology and Experimental Therapeutics, 187*(1), 195-202.

Kallai, L., Hahn, A., Roeder, V., & Zupanic, V. (1964). Correlation between histological findings and serum transaminase values in chronic diseases of the liver. *Acta Medica Scandinavica, 175*, 49-56.

Kaspar, J. W., Niture, S. K., & Jaiswal, A. K. (2009). Nrf2:INrf2 (Keap1) signaling in oxidative stress. *Free Radical Biology & Medicine, 47*(9), 1304-1309.

Katchamart, S., & Williams, D. E. (2001). Indole-3-carbinol modulation of hepatic monooxygenases CYP1A1, CYP1A2 and FMO1 in guinea pig, mouse and rabbit. *Comparative Biochemistry and Physiology.Toxicology & Pharmacology : CBP, 129*(4), 377-384.

Kensler, T. W., Wakabayashi, N., & Biswal, S. (2007). Cell survival responses to environmental stresses via the Keap1-Nrf2-ARE pathway. *Annual Review of Pharmacology and Toxicology, 47*, 89-116.

Klick, D. E., & Hines, R. N. (2007). Mechanisms regulating human FMO3 transcription. *Drug Metabolism Reviews, 39*(2-3), 419-442.

Klick, D. E., Shadley, J. D., & Hines, R. N. (2008). Differential regulation of human hepatic flavin containing monooxygenase 3 (FMO3) by CCAAT/enhancer-binding protein beta (C/EBPbeta) liver inhibitory and liver activating proteins. *Biochemical Pharmacology, 76*(2), 268-278.

Korsmeyer, K. K., Guan, S., Yang, Z. C., Falick, A. M., Ziegler, D. M., & Cashman, J. R. (1998). N-glycosylation of pig flavin-containing monooxygenase form 1: Determination of the site of protein modification by mass spectrometry. *Chemical Research in Toxicology, 11*(10), 1145-1153.

Koukouritaki, S. B., Simpson, P., Yeung, C. K., Rettie, A. E., & Hines, R. N. (2002). Human hepatic flavin-containing monooxygenases 1 (FMO1) and 3 (FMO3) developmental expression. *Pediatric Research, 51*(2), 236-243.

Krueger, S. K., & Williams, D. E. (2005). Mammalian flavin-containing monooxygenases: Structure/function, genetic polymorphisms and role in drug metabolism. *Pharmacology & Therapeutics, 106*(3), 357-387.

Larson, A. M., Polson, J., Fontana, R. J., Davern, T. J., Lalani, E., Hynan, L. S., et al. (2005). Acetaminophen-induced acute liver failure: Results of a united states multicenter, prospective study. *Hepatology (Baltimore, Md.), 42*(6), 1364-1372.

Lee, F. Y., de Aguiar Vallim, T. Q., Chong, H. K., Zhang, Y., Liu, Y., Jones, S. A., et al. (2010). Activation of the farnesoid X receptor provides protection against acetaminophen-induced hepatic toxicity. *Molecular Endocrinology (Baltimore, Md.), 24*(8), 1626-1636.

Lee, W. M. (2010). The case for limiting acetaminophen-related deaths: Smaller doses and unbundling the opioid-acetaminophen compounds. *Clinical Pharmacology and Therapeutics, 88*(3), 289-292.

Lemoine, A., Williams, D. E., Cresteil, T., & Leroux, J. P. (1991). Hormonal regulation of microsomal flavin-containing monooxygenase: Tissue-dependent expression and substrate specificity. *Molecular Pharmacology, 40*(2), 211-217.

Li, Y., & Jaiswal, A. K. (1992). Regulation of human NAD(P)H:Quinone oxidoreductase gene. role of AP1 binding site contained within human

antioxidant response element. *The Journal of Biological Chemistry, 267*(21), 15097-15104.

Lim, P. L., Tan, W., Latchoumycandane, C., Mok, W. C., Khoo, Y. M., Lee, H. S., et al. (2007). Molecular and functional characterization of drug-metabolizing enzymes and transporter expression in the novel spontaneously immortalized human hepatocyte line HC-04. *Toxicology in Vitro : An International Journal Published in Association with BIBRA, 21*(8), 1390-1401.

Liu, J., Wu, K. C., Lu, Y. F., Ekuase, E., & Klaassen, C. D. (2013). Nrf2 protection against liver injury produced by various hepatotoxicants. *Oxidative Medicine and Cellular Longevity, 2013*, 305861.

Luo, Z., & Hines, R. N. (2001). Regulation of flavin-containing monooxygenase 1 expression by ying yang 1 and hepatic nuclear factors 1 and 4. *Molecular Pharmacology, 60*(6), 1421-1430.

Madan, A., Graham, R. A., Carroll, K. M., Mudra, D. R., Burton, L. A., Krueger, L. A., et al. (2003). Effects of prototypical microsomal enzyme inducers on cytochrome P450 expression in cultured human hepatocytes. *Drug Metabolism and Disposition: The Biological Fate of Chemicals, 31*(4), 421-431.

Maherali, N., Ahfeldt, T., Rigamonti, A., Utikal, J., Cowan, C., & Hochedlinger, K. (2008). A high-efficiency system for the generation and study of human induced pluripotent stem cells. *Cell Stem Cell, 3*(3), 340-345.

Manautou, J. E., de Waart, D. R., Kunne, C., Zelcer, N., Goedken, M., Borst, P., et al. (2005). Altered disposition of acetaminophen in mice with a disruption of the Mrp3 gene. *Hepatology (Baltimore, Md.), 42*(5), 1091-1098.

Manautou, J. E., Hoivik, D. J., Tveit, A., Hart, S. G., Khairallah, E. A., & Cohen, S. D. (1994). Clofibrate pretreatment diminishes acetaminophen's

selective covalent binding and hepatotoxicity. *Toxicology and Applied Pharmacology, 129*(2), 252-263.

McGill, M. R., Williams, C. D., Xie, Y., Ramachandran, A., & Jaeschke, H. (2012). Acetaminophen-induced liver injury in rats and mice: Comparison of protein adducts, mitochondrial dysfunction, and oxidative stress in the mechanism of toxicity. *Toxicology and Applied Pharmacology, 264*(3), 387-394.

McGill, M. R., Yan, H. M., Ramachandran, A., Murray, G. J., Rollins, D. E., & Jaeschke, H. (2011). HepaRG cells: A human model to study mechanisms of acetaminophen hepatotoxicity. *Hepatology (Baltimore, Md.), 53*(3), 974-982.

McJunkin, B., Barwick, K. W., Little, W. C., & Winfield, J. B. (1976). Fatal massive hepatic necrosis following acetaminophen overdose. *JAMA : The Journal of the American Medical Association, 236*(16), 1874-1875.

Meyers, L. L., Beierschmitt, W. P., Khairallah, E. A., & Cohen, S. D. (1988). Acetaminophen-induced inhibition of hepatic mitochondrial respiration in mice. *Toxicology and Applied Pharmacology, 93*(3), 378-387.

Miller, J. A., Cramer, J. W., & Miller, E. C. (1960). The N- and ringhydroxylation of 2-acetylaminofluorene during carcinogenesis in the rat. *Cancer Research, 20*, 950-962.

Mitchell, J. R., Jollow, D. J., Gillette, J. R., & Brodie, B. B. (1973). Drug metabolism as a cause of drug toxicity. *Drug Metabolism and Disposition: The Biological Fate of Chemicals, 1*(1), 418-423.

Mitchell, J. R., Jollow, D. J., Potter, W. Z., Davis, D. C., Gillette, J. R., & Brodie, B. B. (1973). Acetaminophen-induced hepatic necrosis. I. role of drug metabolism. *The Journal of Pharmacology and Experimental Therapeutics, 187*(1), 185-194.

Mitchell, J. R., Jollow, D. J., Potter, W. Z., Gillette, J. R., & Brodie, B. B. (1973). Acetaminophen-induced hepatic necrosis. IV. protective role of glutathione. *The Journal of Pharmacology and Experimental Therapeutics, 187*(1), 211-217.

Mizutani, T., Murakami, M., Shirai, M., Tanaka, M., & Nakanishi, K. (1999). Metabolism-dependent hepatotoxicity of methimazole in mice depleted of glutathione. *Journal of Applied Toxicology : JAT, 19*(3), 193-198.

Mizutani, T., Yoshida, K., Murakami, M., Shirai, M., & Kawazoe, S. (2000). Evidence for the involvement of N-methylthiourea, a ring cleavage metabolite, in the hepatotoxicity of methimazole in glutathione-depleted mice: Structure-toxicity and metabolic studies. *Chemical Research in Toxicology, 13*(3), 170-176.

Moffit, J. S., Koza-Taylor, P. H., Holland, R. D., Thibodeau, M. S., Beger, R. D., Lawton, M. P., et al. (2007). Differential gene expression in mouse liver associated with the hepatoprotective effect of clofibrate. *Toxicology and Applied Pharmacology, 222*(2), 169-179.

Moi, P., Chan, K., Asunis, I., Cao, A., & Kan, Y. W. (1994). Isolation of NF-E2-related factor 2 (Nrf2), a NF-E2-like basic leucine zipper transcriptional activator that binds to the tandem NF-E2/AP1 repeat of the beta-globin locus control region. *Proceedings of the National Academy of Sciences of the United States of America, 91*(21), 9926-9930.

Nace, C. G., Genter, M. B., Sayre, L. M., & Crofton, K. M. (1997). Effect of methimazole, an FMO substrate and competitive inhibitor, on the neurotoxicity of 3,3'-iminodipropionitrile in male rats. *Fundamental and Applied Toxicology : Official Journal of the Society of Toxicology, 37*(2), 131-140.

Nakatsukasa, H., Silverman, J. A., Gant, T. W., Evarts, R. P., & Thorgeirsson, S. S. (1993). Expression of multidrug resistance genes in rat liver during regeneration and after carbon tetrachloride intoxication. *Hepatology (Baltimore, Md.), 18*(5), 1202-1207.

Nelson, S. D. (1990). Molecular mechanisms of the hepatotoxicity caused by acetaminophen. *Seminars in Liver Disease, 10*(4), 267-278.

Niture, S. K., & Jaiswal, A. K. (2009). Prothymosin-alpha mediates nuclear import of the INrf2/Cul3 Rbx1 complex to degrade nuclear Nrf2. *The Journal of Biological Chemistry, 284*(20), 13856-13868.

O'Connor, M. A., Koza-Taylor, P., Campion, S. N., Aleksunes, L. M., Gu, X., Enayetallah, A. E., et al. (2014). Analysis of changes in hepatic gene expression in a murine model of tolerance to acetaminophen hepatotoxicity (autoprotection). *Toxicology and Applied Pharmacology, 274*(1), 156-167.

Ohno, Y., Ormstad, K., Ross, D., & Orrenius, S. (1985). Mechanism of allyl alcohol toxicity and protective effects of low-molecular-weight thiols studied with isolated rat hepatocytes. *Toxicology and Applied Pharmacology, 78*(2), 169-179.

Okada, K., Shoda, J., Taguchi, K., Maher, J. M., Ishizaki, K., Inoue, Y., et al. (2009). Nrf2 counteracts cholestatic liver injury via stimulation of hepatic defense systems. *Biochemical and Biophysical Research Communications, 389*(3), 431-436.

Okawa, H., Motohashi, H., Kobayashi, A., Aburatani, H., Kensler, T. W., & Yamamoto, M. (2006). Hepatocyte-specific deletion of the keap1 gene activates Nrf2 and confers potent resistance against acute drug toxicity. *Biochemical and Biophysical Research Communications, 339*(1), 79-88.

Overby, L. H., Buckpitt, A. R., Lawton, M. P., Atta-Asafo-Adjei, E., Schulze, J., & Philpot, R. M. (1995). Characterization of flavin-containing monooxygenase 5 (FMO5) cloned from human and guinea pig: Evidence that the unique catalytic properties of FMO5 are not confined to the rabbit ortholog. *Archives of Biochemistry and Biophysics, 317*(1), 275-284.

Parent, R., Marion, M. J., Furio, L., Trepo, C., & Petit, M. A. (2004). Origin and characterization of a human bipotent liver progenitor cell line. *Gastroenterology, 126*(4), 1147-1156.

Patten, C. J., Thomas, P. E., Guy, R. L., Lee, M., Gonzalez, F. J., Guengerich, F. P., et al. (1993). Cytochrome P450 enzymes involved in acetaminophen activation by rat and human liver microsomes and their kinetics. *Chemical Research in Toxicology, 6*(4), 511-518.

Potter, W. Z., Davis, D. C., Mitchell, J. R., Jollow, D. J., Gillette, J. R., & Brodie, B. B. (1973). Acetaminophen-induced hepatic necrosis. 3. cytochrome P-450-mediated covalent binding in vitro. *The Journal of Pharmacology and Experimental Therapeutics, 187*(1), 203-210.

Poulsen, L. L. (1981). Reviews in biochemical toxicology. In E. Hodgson, J. R. Bend & R. M. Philpot (Eds.), (pp. 33-49). North Holland: Elsevier Press.

Poulsen, L. L., & Ziegler, D. M. (1995). Multisubstrate flavin-containing monooxygenases: Applications of mechanism to specificity. *Chemico-Biological Interactions, 96*(1), 57-73.

Rahman, I., Kode, A., & Biswas, S. K. (2006). Assay for quantitative determination of glutathione and glutathione disulfide levels using enzymatic recycling method. *Nature Protocols, 1*(6), 3159-3165.

Randle, L. E., Goldring, C. E., Benson, C. A., Metcalfe, P. N., Kitteringham, N. R., Park, B. K., et al. (2008). Investigation of the effect of a panel of model hepatotoxins on the Nrf2-Keap1 defence response pathway in CD-1 mice. *Toxicology, 243*(3), 249-260.

Reid, W. D. (1972). Mechanism of allyl alcohol-induced hepatic necrosis. *Experientia, 28*(9), 1058-1061.

Reisman, S. A., Csanaky, I. L., Aleksunes, L. M., & Klaassen, C. D. (2009). Altered disposition of acetaminophen in Nrf2-null and Keap1-knockdown

mice. *Toxicological Sciences : An Official Journal of the Society of Toxicology, 109*(1), 31-40.

Rettie, A. E., & Fisher, M. B. (1999). Handbook of drug metabolism. In T. F. Woolf (Ed.), [Transformation enzymes: Oxidative; non-P450] (pp. 132). New York: Marcel Dekker, Inc.

Ripp, S. L., Itagaki, K., Philpot, R. M., & Elfarra, A. A. (1999). Species and sex differences in expression of flavin-containing monooxygenase form 3 in liver and kidney microsomes. *Drug Metabolism and Disposition: The Biological Fate of Chemicals, 27*(1), 46-52.

Rodriguez-Antona, C., Donato, M. T., Boobis, A., Edwards, R. J., Watts, P. S., Castell, J. V., et al. (2002). Cytochrome P450 expression in human hepatocytes and hepatoma cell lines: Molecular mechanisms that determine lower expression in cultured cells. *Xenobiotica; the Fate of Foreign Compounds in Biological Systems, 32*(6), 505-520.

Rudraiah, S., Moscovitz, J. E., Campion, S., Slittt, A. L., Aleksunes, L. M., & Manautou, J. E. (2014). Differential Fmo3 gene expression in various liver injury models involving hepatic oxidative stress in mice. *Toxicology, Communicated for Publication.*

Rudraiah, S., Rohrer, P., Gurevich, I., Goedken, M. J., Rasmussen, T., Hines, R. N., et al. (2014). Tolerance to acetaminophen hepatotoxicity in the mouse model of autoprotection is associated with induction of flavin-containing monooxygenase-3 (FMO3) in hepatocytes. *Toxicological Sciences : An Official Journal of the Society of Toxicology.*

Rushmore, T. H., Morton, M. R., & Pickett, C. B. (1991). The antioxidant responsive element. activation by oxidative stress and identification of the DNA consensus sequence required for functional activity. *The Journal of Biological Chemistry, 266*(18), 11632-11639.

Ryu, S. D., Kang, J. H., Yi, H. G., Nahm, C. H., & Park, C. S. (2004). Hepatic flavin-containing monooxygenase activity attenuated by cGMP-

independent nitric oxide-mediated mRNA destabilization. *Biochemical and Biophysical Research Communications, 324*(1), 409-416.

Schiodt, F. V., Atillasoy, E., Shakil, A. O., Schiff, E. R., Caldwell, C., Kowdley, K. V., et al. (1999). Etiology and outcome for 295 patients with acute liver failure in the united states. *Liver Transplantation and Surgery : Official Publication of the American Association for the Study of Liver Diseases and the International Liver Transplantation Society, 5*(1), 29-34.

Schmidt, G., Borsch, G., Muller, K. M., & Wegener, M. (1986). Methimazole-associated cholestatic liver injury: Case report and brief literature review. *Hepato-Gastroenterology, 33*(6), 244-246.

Shayiq, R. M., Roberts, D. W., Rothstein, K., Snawder, J. E., Benson, W., Ma, X., et al. (1999). Repeat exposure to incremental doses of acetaminophen provides protection against acetaminophen-induced lethality in mice: An explanation for high acetaminophen dosage in humans without hepatic injury. *Hepatology (Baltimore, Md.), 29*(2), 451-463.

Shenton, D., Smirnova, J. B., Selley, J. N., Carroll, K., Hubbard, S. J., Pavitt, G. D., et al. (2006). Global translational responses to oxidative stress impact upon multiple levels of protein synthesis. *The Journal of Biological Chemistry, 281*(39), 29011-29021.

Shephard, E. A., & Phillips, I. R. (2010). The potential of knockout mouse lines in defining the role of flavin-containing monooxygenases in drug metabolism. *Expert Opinion on Drug Metabolism & Toxicology, 6*(9), 1083-1094.

Shimizu, M., Murayama, N., Nagashima, S., Fujieda, M., & Yamazaki, H. (2008). Complex mechanism underlying transcriptional control of the haplotyped flavin-containing monooxygenase 3 (FMO3) gene in japanese: Different regulation between mutations in 5'-upstream distal region and common element in proximal region. *Drug Metabolism and Pharmacokinetics, 23*(1), 54-58.

Silva, V. M., Hennig, G. E., & Manautou, J. E. (2006). Cholestasis induced by model organic anions protects from acetaminophen hepatotoxicity in male CD-1 mice. *Toxicology Letters, 160*(3), 204-211.

Slitt, A. L., Allen, K., Morrone, J., Aleksunes, L. M., Chen, C., Maher, J. M., et al. (2007). Regulation of transporter expression in mouse liver, kidney, and intestine during extrahepatic cholestasis. *Biochimica Et Biophysica Acta, 1768*(3), 637-647.

Slitt, A. L., Cherrington, N. J., Maher, J. M., & Klaassen, C. D. (2003). Induction of multidrug resistance protein 3 in rat liver is associated with altered vectorial excretion of acetaminophen metabolites. *Drug Metabolism and Disposition: The Biological Fate of Chemicals, 31*(9), 1176-1186.

Sokol, R. J., Winklhofer-Roob, B. M., Devereaux, M. W., & McKim, J. M.,Jr. (1995). Generation of hydroperoxides in isolated rat hepatocytes and hepatic mitochondria exposed to hydrophobic bile acids. *Gastroenterology, 109*(4), 1249-1256.

Suh, J. K., & Robertus, J. D. (2002). Role of yeast flavin-containing monooxygenase in maintenance of thiol-disulfide redox potential. *Methods in Enzymology, 348*, 113-121.

Szymczak, A. L., Workman, C. J., Wang, Y., Vignali, K. M., Dilioglou, S., Vanin, E. F., et al. (2004). Correction of multi-gene deficiency in vivo using a single 'self-cleaving' 2A peptide-based retroviral vector. *Nature Biotechnology, 22*(5), 589-594.

Tanaka, Y., Aleksunes, L. M., Cui, Y. J., & Klaassen, C. D. (2009). ANIT-induced intrahepatic cholestasis alters hepatobiliary transporter expression via Nrf2-dependent and independent signaling. *Toxicological Sciences : An Official Journal of the Society of Toxicology, 108*(2), 247-257.

Thakore, K. N., & Mehendale, H. M. (1991). Role of hepatocellular regeneration in CCl4 autoprotection. *Toxicologic Pathology, 19*(1), 47-58.

Tom, W. M., Fong, L. Y., Woo, D. Y., Prasongwatana, V., & Boyde, T. R. (1984). Microsomal lipid peroxidation and oxidative metabolism in rat liver: Influence of vitamin A intake. *Chemico-Biological Interactions, 50*(3), 361-366.

Trauner, M., Meier, P. J., & Boyer, J. L. (1998). Molecular pathogenesis of cholestasis. *The New England Journal of Medicine, 339*(17), 1217-1227.

Wang, Q. M., Du, J. L., Duan, Z. J., Guo, S. B., Sun, X. Y., & Liu, Z. (2013). Inhibiting heme oxygenase-1 attenuates rat liver fibrosis by removing iron accumulation. *World Journal of Gastroenterology : WJG, 19*(19), 2921-2934.

Wang, Z., Klipfell, E., Bennett, B. J., Koeth, R., Levison, B. S., Dugar, B., et al. (2011). Gut flora metabolism of phosphatidylcholine promotes cardiovascular disease. *Nature, 472*(7341), 57-63.

Watkins, P. B., Kaplowitz, N., Slattery, J. T., Colonese, C. R., Colucci, S. V., Stewart, P. W., et al. (2006). Aminotransferase elevations in healthy adults receiving 4 grams of acetaminophen daily: A randomized controlled trial. *JAMA : The Journal of the American Medical Association, 296*(1), 87-93.

Weber, L. W., Boll, M., & Stampfl, A. (2003). Hepatotoxicity and mechanism of action of haloalkanes: Carbon tetrachloride as a toxicological model. *Critical Reviews in Toxicology, 33*(2), 105-136.

Weerachayaphorn, J., Mennone, A., Soroka, C. J., Harry, K., Hagey, L. R., Kensler, T. W., et al. (2012). Nuclear factor-E2-related factor 2 is a major determinant of bile acid homeostasis in the liver and intestine. *American Journal of Physiology.Gastrointestinal and Liver Physiology, 302*(9), G925-36.

Yamazaki, M., Miyake, M., Sato, H., Masutomi, N., Tsutsui, N., Adam, K. P., et al. (2013). Perturbation of bile acid homeostasis is an early pathogenesis event of drug induced liver injury in rats. *Toxicology and Applied Pharmacology, 268*(1), 79-89.

Yang, H., Ramani, K., Xia, M., Ko, K. S., Li, T. W., Oh, P., et al. (2009). Dysregulation of glutathione synthesis during cholestasis in mice: Molecular mechanisms and therapeutic implications. *Hepatology (Baltimore, Md.), 49*(6), 1982-1991.

Yeligar, S. M., Machida, K., & Kalra, V. K. (2010). Ethanol-induced HO-1 and NQO1 are differentially regulated by HIF-1alpha and Nrf2 to attenuate inflammatory cytokine expression. *The Journal of Biological Chemistry, 285*(46), 35359-35373.

Zaher, H., Buters, J. T., Ward, J. M., Bruno, M. K., Lucas, A. M., Stern, S. T., et al. (1998). Protection against acetaminophen toxicity in CYP1A2 and CYP2E1 double-null mice. *Toxicology and Applied Pharmacology, 152*(1), 193-199.

Zamek-Gliszczynski, M. J., Hoffmaster, K. A., Nezasa, K., Tallman, M. N., & Brouwer, K. L. (2006). Integration of hepatic drug transporters and phase II metabolizing enzymes: Mechanisms of hepatic excretion of sulfate, glucuronide, and glutathione metabolites. *European Journal of Pharmaceutical Sciences : Official Journal of the European Federation for Pharmaceutical Sciences, 27*(5), 447-486.

Zamek-Gliszczynski, M. J., Hoffmaster, K. A., Tian, X., Zhao, R., Polli, J. W., Humphreys, J. E., et al. (2005). Multiple mechanisms are involved in the biliary excretion of acetaminophen sulfate in the rat: Role of Mrp2 and Bcrp1. *Drug Metabolism and Disposition: The Biological Fate of Chemicals, 33*(8), 1158-1165.

Zhang, J., Cerny, M. A., Lawson, M., Mosadeghi, R., & Cashman, J. R. (2007). Functional activity of the mouse flavin-containing monooxygenase forms 1, 3, and 5. *Journal of Biochemical and Molecular Toxicology, 21*(4), 206-215.

Zheng, M., & Storz, G. (2000). Redox sensing by prokaryotic transcription factors. *Biochemical Pharmacology, 59*(1), 1-6.

Ziegler, D. M. (1988). Flavin-containing monooxygenases: Catalytic mechanism and substrate specificities. *Drug Metabolism Reviews, 19*(1), 1-32.

Ziegler, D. M. (2002). An overview of the mechanism, substrate specificities, and structure of FMOs. *Drug Metabolism Reviews, 34*(3), 503-511.

Ziegler, D. M., Duffel, M. W., & Poulsen, L. L. (1979). Studies on the nature and regulation of the cellular thio:Disulphide potential. *Ciba Foundation Symposium, (72)*(72), 191-204.

Ziegler, D. M., Jollow, D., & Cook, D. F. (1971). Properties of a purified liver microsomal mixed-function amine oxidase. In H. Kamin (Ed.), *Proceedings of the third international symposium on flavins and flavin-proteins* (pp. 507). Baltimore, London: University Park Press, Butterworth and Co Ltd.

Ziegler, D. M., & Mitchell, C. H. (1972). Microsomal oxidase. IV. properties of a mixed-function amine oxidase isolated from pig liver microsomes. *Archives of Biochemistry and Biophysics, 150*(1), 116-125.

Ziegler, D. M., & Poulsen, L. L. (1998). Catalytic mechanism of FMO-catalysed N- and S-oxidations. In N. J. Gooderham (Ed.), *Drug metabolism: Towards the next millennium* (pp. 30). Netherlands: IOS Press.

Zipper, L. M., & Mulcahy, R. T. (2002). The Keap1 BTB/POZ dimerization function is required to sequester Nrf2 in cytoplasm. *The Journal of Biological Chemistry, 277*(39), 36544-36552.